LAPPEENRANTA UNIVERSITY OF TECHNOLOGY
LUT School of Energy Systems
LUT Mechanical Engineering

Mehul Bansal

THERMAL OPTIMIZATION OF STEAM AIR COOLED CONDENSERS FOR POWER PLANTS

Supervisors: Professor Jussi Sopanen
D. Sc. Behnam Ghalamchi

ABSTRACT

Lappeenranta University of Technology
LUT School of Energy Systems
LUT Mechanical Engineering

Mehul Bansal

Thermal optimization of steam air cooled condensers for power plants

Master's thesis

2017

91 pages, 42 figures, 22 tables and 3 appendices

Supervisors: Professor Jussi Sopanen
D. Sc. Behnam Ghalamchi

Keywords: Air cooled condenser, heat transfer coefficient, pressure drop, tube bundles, condenser design, finned tubes, air and steam properties.

Cooling is a significant part of any power generation cycle. An ACC (Air Cooled Condenser) is used to condense steam vapors from the steam turbine, lower heat rejection temperature and increase the power generation efficiency. Traditional evaporative cooling towers, evaporate a fraction of the recirculating water to take away its latent heat of evaporation, thereby cooling the rest of the volume of water. Even if only a small fraction of the recirculating water is evaporated, a large amount of make-up water is required. This imposes a huge requirement of water which adds to the global water crises. Further, many projects become unfeasible due to water shortages. On the other hand ACCs are dry cooling towers that do not require any water for cooling as they dissipate the waste heat directly into the ambient air. On the contrary, ACCs have a lower thermal performance than water based cooling towers and their performance is adversely affected by local weather fluctuations. Further ACCs are known for poor performance during the peak summer months which increases the turbine back pressure, thereby decreasing the overall power output of the turbine. This leaves the designers with a very narrow margin for performance optimization with respect to their capital and running costs. In this thesis the heat transfer characteristics of ACCs are evaluated based on computer simulations and theoretical formulations. For a given set of operating conditions and parameters, it is possible to design ACCs in different types and configurations. A comprehensive thermal design software package, Aspen EDR from Aspen Technologies has been used to simulate specific property methods and models to obtain the most effective design. Further design optimization has been carried out by varying the tube and fin diameters, their numbers, number of bays and fan diameters. The knowledge and results from the thesis will help design thermally optimized ACCs. The research has be done for a cooling tower manufacturing company, North Street Cooling Towers P Ltd which is based in India, that currently does not manufacture ACCs but would like to start manufacturing them in the near future. The knowledge and results from the research will help the company to design thermally optimized ACCs which will have performance advantages over what is currently available in the mainstream market.

ACKNOWLEDGEMENT

The research project was carried out for North Street Cooling Towers P Ltd, which is a cooling tower manufacturing company based in India. The company takes a keen interest in the development of sustainable products and since ACCs (Air Cooled Condensers) do not require water for cooling, they fall perfectly in the area of interest of the company. I personally as a design and manufacturing engineer, believe that environmental sustainability should play a major part in all industrial sectors. This belief that I am contributing towards a suitable future, has been one of the major motivating factors for me to carry out his project. I thank the managing director of the company, Mr. Mukesh Bansal for proving me this opportunity to work on the project with all necessary resources.

The research work was carried out at Lappeenranta University of Technology, Finland under the guidance and supervision of Professor Jussi Sopanen and post-doctoral researcher, D. Sc. Behnam Ghalamchi. Firstly, I would like to thank my supervisor Professor Jussi Sopanen for giving me full freedom to decide the direction for the project. His practical guidance and approach has been very helpful in taking this project forward. My second supervisor D. Sc. Behnam Ghalamchi has taken a keen interest in the project. His highly valuable and helpful comments, and suggestion were indispensable in completing the project within the required time frame. Both my supervisors have always been always available to give support for this project which I highly appreciate.

I would also like to thank my family especially my parents back home for their continuous support and encouragement throughout my studies. I hold special gratitude to my mother for teaching me personal and professional work ethics which have been very important for my career. My friends in Lappeenranta made my student life immensely enjoyable and memorable. They have positively contributed in my all-round personal development in all spheres of life.

Mehul Bansal

Mehul Bansal

Lappeenranta 16.03.2017

TABLE OF CONTENTS

LIST OF SYMBOLS AND ABBREVIATIONS

A	Surface area of the condenser
A_{face}	Total face area of all the bundles
A_{fins}	Fin surface area
A_i	Internal surface area of tubes
A_{min}	Minimum flow area
A_{prime}	Prime surface area
A_r	Area ratio
A_{total}	Total surface area of the finned tubes per meter length
$C_{p\ air}$	Specific capacity at constant pressure of air
$C_{p\ cond}$	Specific heat at constant pressure of the condensate
D_R	Outer diameter of root tube
D_f	Fin outside diameter
D_{fan}	Fan diameter
D_i	Inner diameter of root tube
F	Correction factor
f	Darcy friction factor
f_{fr}	Friction factor
$G_{tube\ side}$	Tube-side stream mass flux
$G_{air\ side}$	Air-side mass flux
g_c	Unit conversion factor
g_n	Acceleration due to gravity
H	Fin height
$h_{air\ side}$	Air-side heat transfer coefficient
h_e	Specific enthalpy of evaporation for steam
$h_{tube\ side}$	Tube-side heat transfer coefficient
j_R	j-factor for round tubes
k	Thermal conductivity of metal
k_{air}	Air thermal conductivity
k_{cond}	Thermal conductivity of the condensate

L	Tube length
l	Fin spacing
L_T	Length of finned tubes exposed to the air flow
m	Fin parameter
$\dot{m}_{air}$	Outside air mass flow rate
$\dot{m}_{cond}$	Condensate mass flow rate
$\dot{m}_{fluid}$	Tube-side fluid mass flow rate
$\dot{m}_{max}$	Maximum mass velocity
N_T	Number of tubes in a row
N_{fan}	Number of fans
N_r	Number of rows
n_f	Fin frequency per meter length
n_p	Number of passes
n_t	Number of tubes
P	Thermal effectiveness of air
$Pr_{air\ side}$	Air-side Prandtl number
Pr_{cond}	Condensate Prandtl number
P_t	Transverse pitch
Q	Heat load
$\dot{q}_{cond}$	Rate of heat transfer during condensation
$\dot{q}_{\Delta t}$	Amount of heat exchanged during a temperature drop
$\dot{q}_{total}$	Total rate of heat transfer
R	Ratio of effectiveness
R_D	Total fouling resistance
R_{D0}	Air-side fouling resistance
R_{Di}	Tube-side fouling resistance
$Re_{air\ side}$	Air-side Reynold's number
Re_{cond}	Local condensate Reynold's number
Re_{eff}	Effective Reynold's number
$Re_{tube\ side}$	Reynold's number for tube-side fluid
r_1	Fin inner radius or tube outer radius
r_2	Fin outer radius

r_{2c}	Corrected fin radius
S	Fin thickness
s	Specific gravity
S_{min}	Minimum flow area
T_{cond}	Condensing temperature
T_{in}	Inlet temperature of the tube-side stream
T_{out}	Outlet temperature of the tube-side stream
t_{in}	Inlet temperature of the air-side stream
t_{out}	Outlet temperature of the air-side stream
U	Overall heat transfer coefficient
U_D	Design overall heat transfer coefficient
U_c	Clean overall heat transfer coefficient
U_{req}	Overall required heat transfer coefficient
V_{fan}	Velocity of air leaving the fan
$\dot{V}_{fan}$	Volumetric flow rate per fan
V_{face}	Standard face velocity for axial flow fans
$V_{face,\ act}$	Actual face velocity
V_{max}	Maximum air velocity in tube bundles
V_{steam}	Tube-side fluid (steam) velocity
W	Width of the tube bundles
$\dot{W}_{fan}$	Fan break down power
α_c^*	Dimensionless local heat transfer coefficient for turbulent region
α_{fan}	Kinetic energy correction factor for air leaving the fan
α_r	Number of velocity heads for tube-side pressure losses
$\Delta P_{air\ side}$	Total air-side pressure drop
$\Delta P_{f-air\ side}$	Air-side pressure drop due friction
$\Delta P_{f-tube\ side}$	Tube-side pressure drop due to fluid friction inside the tubes
$\Delta P_{r-tube\ side}$	Tube-side pressure drop due to tube entrance and exit losses
$\Delta P_{total-fan}$	Total pressure change across the fan
$\Delta P_{tube\ side}$	Total tube-side pressure drop
ΔT_{lm}	Logarithmic mean temperature difference

ΔT_m	Mean temperature difference
Δt	Change in temperature
μ_{air}	Dynamic viscosity of air
μ_{cond}	Dynamic viscosity of the condensate
μ_{steam}	Dynamic viscosity of steam
$\mu_{w\ steam}$	Dynamic viscosity of steam at average wall temperature
η_f	Fin efficiency
η_{fan}	Total fan efficiency
η_w	Weighed efficiency
ρ_{air}	Air density
ρ_{cond}	Condensate density
ρ_{fan}	Density of air leaving the fan
ρ_{std}	Standard air density
ρ_{steam}	Steam density
τ_{cond}	Local condensate flow rate
$\emptyset$	Viscosity correction factor
ψ	Effective fin height

ACC	Air cooled condenser
ACHE	Air cooled heat exchanger
ASME	American Society of Mechanical Engineers
BWG	Birmingham wire gauge
EDR	Exchanger design and rating
FSP	Fan static pressure
ID	Inner diameter
ITD	Inlet temperature difference
MTD	Mean temperature difference
OD	Outer diameter

1 INTRODUCTION

Cooling is a significant part of any power generation cycle. A cooling tower is used to condense steam vapors from the steam turbine, lower heat rejection temperature and increase the power generation efficiency. For the thesis, the research is carried out on ACCs (Air Cooled Condensers) for steam power plants.

In the past the hydrosphere has been used as a heat sump where, cold water from river, lakes or ocean has been used for cooling purposes. Hot process water used to be directly discharged back into the water bodies, which has detrimental environmental effects. As per new regulations around the world, industries now cannot return heater water into the water bodies Therefore every industry has to have a cooling tower. (Kröger 2004, p. 1.)

Traditional evaporative cooling towers, evaporate a fraction of the recirculating water to take away its latent heat of evaporation, thereby cooling the rest of the volume of water. Even if only about 2 to 4% of the recirculating water is evaporated, a large amount of make-up water is required. Typically about 30 m^3/hr of make-up water is required per MWe of the installed capacity. This imposes a huge requirement of water which adds to the global water crises. Further, many projects become unfeasible due to water shortages. (Mendrinos, Kontoleontos and Karytsas 2006, p. 1.)

ACCs on the other hand do not require any water for cooling as the ambient air is used as a heat sump. As a result ACCs eliminate the need for blowdown disposals, water- freezing problems in cold conditions, water vapor plumes and governmental water pollution restrictions (Larinoff, Moles and Reichhelm 1978, p. 2). On the down side, ACCs require higher capital costs, larger areal foot prints and offer lower cooling efficiencies than their wet cooling tower counterparts. Further for a given set of operating conditions and parameters, it is possible to design ACCs in different types (rectangular, A-frame and V-frame). For these reasons, thermal optimization of ACCs becomes a bit more challenging and powerful simulations tools are required. An isometric view of an A-frame ACC is shown in Figure 1. The figure shows a single bay unit with one fan.

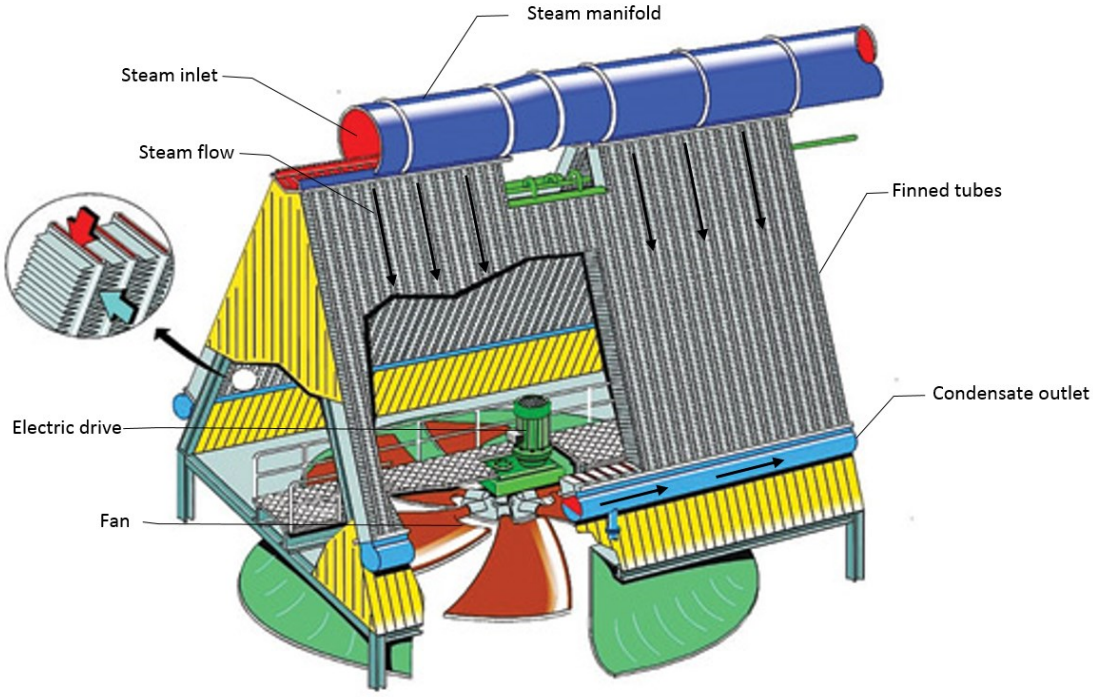

Figure 1. Isometric view of an A-frame ACC (Wurtz 2008).

The purpose of a turbine steam condenser is to condenser the outlet turbine steam into water but at the highest possible temperature. This helps in energy saving because the condensate then can be re-boiled in the boiler to produce high quality steam with a high energy density.

Although, ACCs incur higher capital and running costs, this may not be always the case when taken into account the costs related to providing suitable water. This in many cases offsets all the costs of the prior, over the expected lifecycle of the system. Further to this in most arid and semi-arid regions, heat dissipation into the ambient air is the only option available. (Kröger 2004, p. 12.)

This thesis looks at using computer based simulation tools for the optimization of heat transfer characteristics in ACCs. The results from computer simulations are then verified through theoretical formulations.

1.1 Motivation for the thesis

Since ACCs do not require water for cooling, they can be used in areas with water shortages without exhausting the local water sources. The research project has been carried out for

North Street Cooling Towers P Ltd, a cooling tower manufacturing company based in India. Since, the company takes a great interest in developing sustainable technologies, the development of thermally optimized ACCs fall perfectly into their area of interest. As a researcher, I personally take a keen interest in sustainable development and aim to develop and design product with a minimal ecological footprint.

The research is aimed at evaluating the heat transfer characteristics of ACCs based on computer simulations. For a given set of operating conditions and parameters, it is possible to design ACCs in different types (rectangular, A-frame, V-frame). A comprehensive software package, Aspen EDR is used to simulate property packages and calculation models, specific to the application. Further based on a number of suitable design outputs from the software, design optimization is performed which is verified through theoretical formulations. Such optimization techniques are currently not being used in the mainstream industry and therefore, research is required in this area. The knowledge and results from the research will help the company to design thermally optimized ACCs which will have performance advantages over what is currently available in the mainstream market.

1.2 Objectives

The aim of the project is to obtain a thermally optimized ACC design for a power plant, based on the process parameters given by North Street Cooling Towers P Ltd. The design simulations are performed on Aspen EDR. The final design is optimized for both capital and running costs. Design optimization is achieved by varying the most important input design parameters including the tube and fin diameter and their numbers. The design obtained from the software is then validated through theoretical formulations. The project also aims at understanding the theoretical background of ACCs with respect to their various types and configurations. Then it looks at the theoretical design principles and condenser design methodologies.

1.3 Delimitations

ACCs are a particular type of ACHEs (Air Cooled Heat Exchangers). ACHEs are a broader classification of heat exchangers that use ambient air as a cooling medium. They can be constructed in various configurations depending on their application. They can be used for a broader range of applications and industries, including the electronics industry, vehicles,

air conditioning, chemical plants and refrigeration (Kröger 2004, p. 2). ACCs on the other hand are only used for the condensation of a vapour stream. This projects focuses only on ACCs even though the basic operating principle and mechanical design remains the same as ACHEs.

In the report, design challenges faced with the presence of non-condensable gasses in the incoming steam have been reported briefly. Since the process data obtained from the company does not have any non-condensable gases, no provisions for their elimination have been provided in the final ACC design.

2 THERMAL DESIGN PRINCIPLES OF AIR COOLED CONDENSERS

Most ACCs when used for steam turbines in power plants, function as vacuum condensers, that is, their operating pressure is lower than the atmospheric pressure. This is because, a steam turbine uses a pressure difference between its entry and exit ports. Having a vacuum at the exit port of the turbine increases its efficiency. The exit steam from a turbine can only be reused in two ways. One way is to use compressors to compress the steam and pass it through super heaters before feeding it back to the turbine. Compressing steam would take a large amount of energy and therefore the power plant will not be efficient. An effective way to reuse the steam is to condense it into a liquid at the highest possible temperature that is, isothermally condense, using a condenser. Isothermal condensation takes place when there is no temperature drop but a phase change from vapor to liquid takes place. A typical power plant turbine is shown in Figure 2 where the outlet steam is reused within the system and therefore passed through an ACC for condensation.

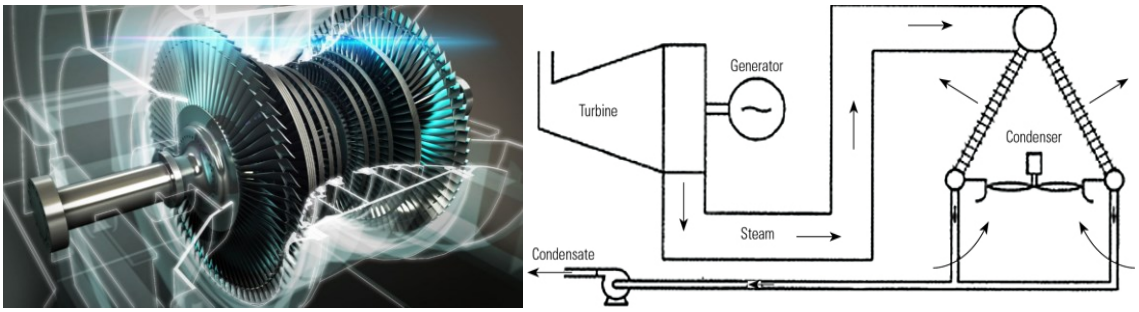

Figure 2. Power plant steam turbine (Benchmark Power International 2016), Steam air cooled condensing system (Kröger 2004, p. 16).

2.1 Operating principle

An ACC transfers the process heat form the working fluid into the ambient air stream through extended heat transfer surfaces (finned tubes) as shown in Figure 3. Since air has a heat transfer coefficient much lower than that of water, the temperature difference between the outlet stream and the ambient air temperature (approach) in case of ACCs must be 10 to 12^{o}C to get an economical design. On the other hand in case of wet cooling towers, this temperature difference can only be 3 to 4^{o}C (Mukherjee 2007 p. 12).

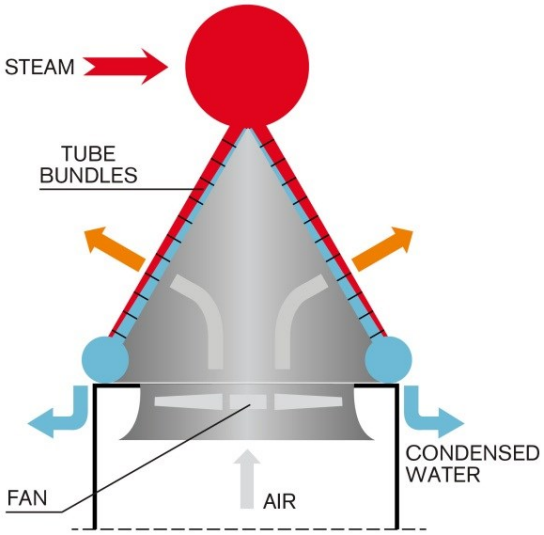

Figure 3. Heat flow in an ACC (Hamon 2017).

Generally an ACC consists of a number of bays which form a unit. Multiple bay configurations are shown in Figure 4. Each bay is serviced by an axial flow fan, driven by an electric fan via a gear reducer (gear box). On each side of the bay, there are a series of tube bundles. Each tube bundle consists of a number of finned tubes as shown in Figure 5, which offer extended surfaces for heat transfer. The outlet steam from the steam turbine, flows into the steam manifold located on top of the tube bundles and enters the finned tubes through the inlet headers. The fan delivers a flow of air which passes through the tube bundles and takes away the latent heat of condensation from the steam flowing through the tubes. The condensate flows down with gravity and is let out through the outlet header of the tube bundles.

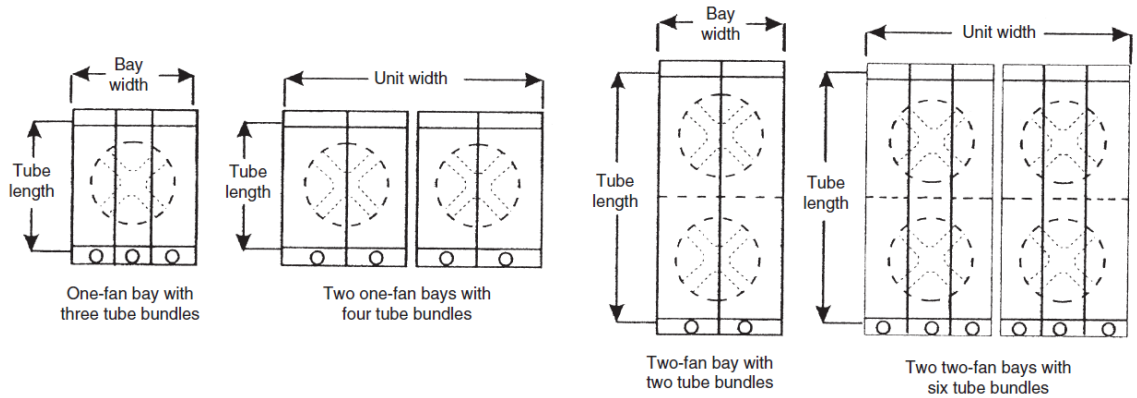

Figure 4. Fan bay configurations in air cooled heat exchangers (Serth and Lestina 2014, p. 514).

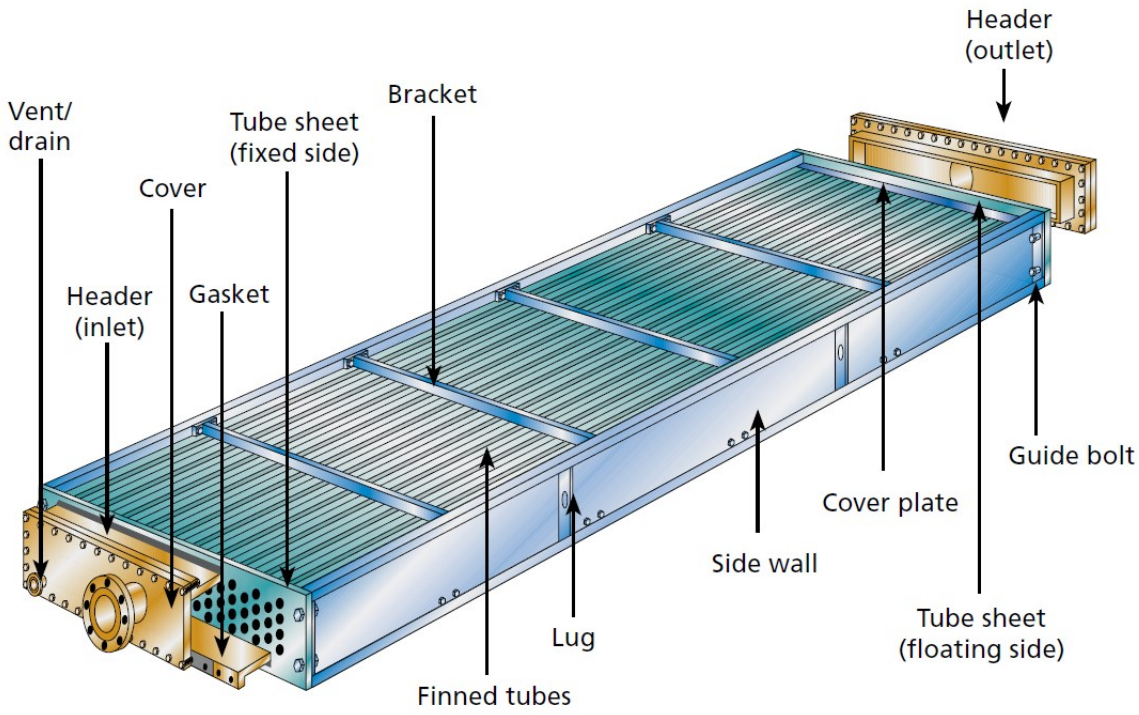

Figure 5. A typical ACC tube bundle (Kelvion 2017).

A tube bundle is an assembly of finned tubes, inlet and outlet header, tube supports and side supports. A typical construction is shown in Figure 5 with four staggered tube rows. It is a single pass bundle which means that the steam only flows once through the tube bundle, from the inlet header to the outlet header. All the condensation takes place within the tube length. The tubes are welded or expanded into the tube sheet. The inlet header provides a means of steam distribution across the finned tubes while the outlet header collects the condensate and drains it through the outlet nozzle. Tube bundles not only hold the finned tubes in a specific layout but also form the primary structure for the ACC.

The heat transfer performance of an ACC depends on the dry bulb temperature of the ambient air. In contrast, the performance of a water based evaporative cooling tower or wet cooling tower, depends on the wet bulb temperature of the ambient air. In most cases for a given location, the dry bulb temperature is always higher than the wet bulb temperature and experiences higher weather and seasonal changes. For these reasons, ACCs have lower performance efficiencies because of which they have larger areal foot prints and require higher operating power as compared to wet cooling towers. (Kröger 2004, p. 12.)

Most power plant ACC are quite large in size which can be seen on a human scale in Figure 6. Installation of a steam manifold in a single bay unit is shown on the left and a multi bay unit is shown on the right.

Figure 6. Typical industrial ACCs, left- steam manifold installation (Brighthub Engineering 2017), right- a multi bay unit (Virids 2017).

2.2 Air cooled condensers types

Based on the movement of cold air, ACCs are divided into two types, mechanical draft and natural draft. Mechanical draft ACC can be further categorized into forced and induced draft.

2.2.1 Mechanical draft ACCS

For most industrial applications, mechanical draft ACCs are used. In these, the cooling air is moved with the help of mechanical equipment, typically an axial flow fan run with a drive motor. Depending on the fan size a reduction gear box may or may not be used. They typically are smaller in size than natural draft cooling towers and incur a lower initial capital cost but a higher continuous running cost.

2.2.2 Forced draft ACCs

In forced draft ACCs the fans are located at the air stream inlet below the fin bundles as shown in Figure 7. This leads to having a lower power consumption per unit air mass flow rate as compared with induced draft configurations. Further since the fan drive units are located at the cooler side of the ACC, they are not exposed to high temperatures, thus making

maintenance easier while prolonging the service life. For condensers the fin bundles are normally inclined at an angle of 60° with the datum. (Kröger 2004, p. 13; Serth and Lestina 2014, p. 509.)

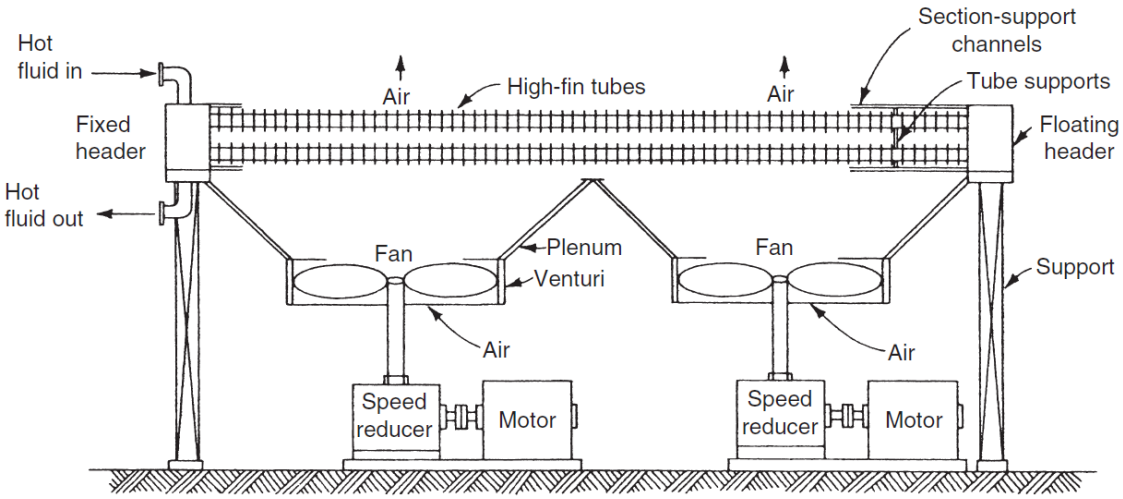

Figure 7. Forced draft Air Cooled Condenser (Kraus, Aziz and Welty 2001, p. 541).

On the downside, the escape velocity of the hot air escaping the tube bundles is lower about 2.5 to 3 m/s, than in the case of induced draft ACCs. This causes plume recirculation and can be severely critical due to other near-by ACC units or hindrances due to other structures. The air flow pattern is generally not as uniform as in the case of induced draft ACCs. Since the tube bundles are exposed to the open atmosphere, their performance is easily affected by the changes in the weather conditions including solar radiations, rain, wind and hail. Hail screens can be installed over the tubes but they affect the ACC performance. (Kröger 2004, p. 13.)

2.2.3 Induced draft ACCs

In induced draft ACCs, the fans are located at the exit of the hot air stream, above the tube bundles as shown in Figure 8. This leads to a higher escape velocity of the air stream exiting the unit, thus reducing the chances of plume recirculation. Further such type of configurations have a more uniform air flow pattern throughout the exchange unit. On the downside, they require a higher fan power per unit air mass flow rate. Since the fans and their drive units are subjected to higher temperatures, their material of construction and maintenance becomes more critical. (Kröger 2004, p. 13-14.)

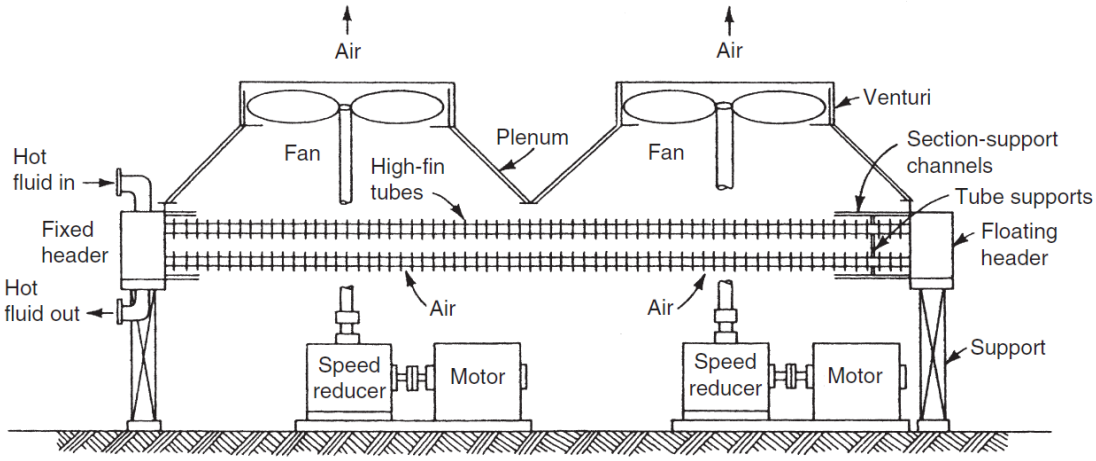

Figure 8. Induced draft air cooled condenser (Kraus, Aziz and Welty 2001, p. 540).

2.2.4 Natural draft ACCs

Natural draft ACCs use a hyperbolic tower that can be as high as 200 m in height. The schematics are shown in Figure 9. The required air draft is created due to the pressure difference between the denser ambient air and the heated humid air inside the tower. (Busch et al. 2002, p. 1510.)

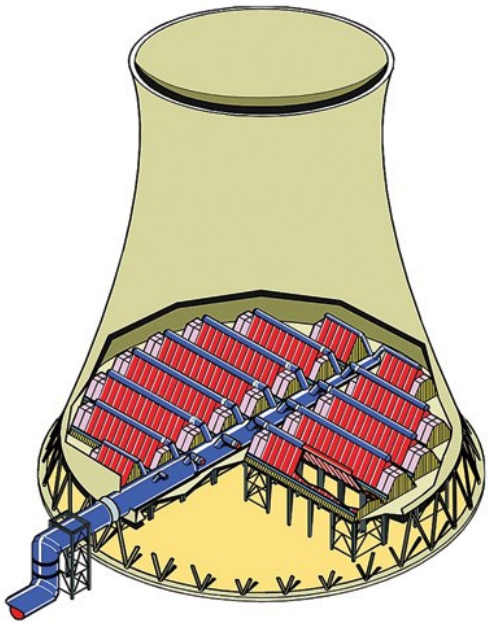

Figure 9. Natural draft air cooled condenser (Wurtz 2008, p. 1).

The height of the cooling tower can be reduced by installing axial flow fans at its base which is called a fan assisted natural draft cooling tower as shown in Figure 10. Although, this

reduces the construction cost of the tower, it is often offset by the capital and running costs of the fans. They are often used when plume recirculation become a problem in multibank mechanical draft ACCs. (Kröger 2004, p. 7.)

Figure 10. Fan assisted natural draft ACC (Hamon 2016).

2.3 Heat transfer through fins

ACCs consist of modules of fills that provide extended areas for heat transfer. The heat transfer performance of an ACC extensively depends on the fill performance. Conduction of heat takes place from the fluid (liquid or gas) through the tube to the fins and convection takes placed from the fins to the ambient air. Fins come in a variety of shapes, sizes and materials depending on their application. They may be round, elliptical, flattened or otherwise streamlined to reduce drag on the air-side. (Kröger 2004, p. 330.)

With time, the heat transfer performance of fins may decrease. The three mains reasons for increase in thermal resistances in fills are corrosion, fouling and loss of contact or bond pressure at the fill root.

Corrosion: Depending on the application and the environment an ACC is used in, air- borne contaminants such as salt in marine environments, mix with rain water and seep into the fin-tube interface. Since at the interface the temperature is higher, a reaction takes places that

corrodes the tube and fin materials to form metallic salts. These salt formations act like thermal barriers. (McHugh and Chapple 1999, p. 67.)

Fouling: With time, contaminants form the environment can deposited on the external fin surfaces. Depending on the fluid, the tubes can be prone to internal fouling as well. Both internal and external fouling can be cleaned off. Cleaning further reduces aerodynamic resistance. (McHugh and Chapple 1999, p. 67.)

Loss in fin-tube contact: With cyclic ACC operations over a period of time, the fins can lose their contact pressure on the tubes. This happens because the fins and the tubes expand during operation. This induces hoop stress on the inner fin circumference. When out of service, the fins being lesser resistant to thermal fluctuations, remain enlarged and eventually lose their contact pressure with the tubes. (McHugh and Chapple 1999, p. 67.)

Fin types

ACC finned tubes come in many different shaped and sizes, depending on their application and service life required off them. To enhance their thermal characteristics, they may be roughened, cut or perforated.

a) Wrapped-on finned tubes

A continuous metal strip with good thermal conductivity, usually aluminum is fed into a forming machine. The machine forms an ‘L’ or a ‘double L’ shaped foot on one edge of the strip which is tightly wound on to a steel tube. The fins are held tight on to the tube by either stapling or clamping on both ends of the tube. The L shaped foot increases the contact area with the base tube. Double L shaped fins not only offer good thermal conductivity but also better corrosion resistance. (McHugh and Chapple 1999, p. 67.) They both are shown in Figure 11. Wrapped-on aluminum finned tubes should not be used for temperatures higher than 120^{o}C. Due to the difference in coefficients of thermal expansions of the two metals, aluminum and steel, the thermal contact resistance increases rapidly. (Kröger 2004, p. 331.)

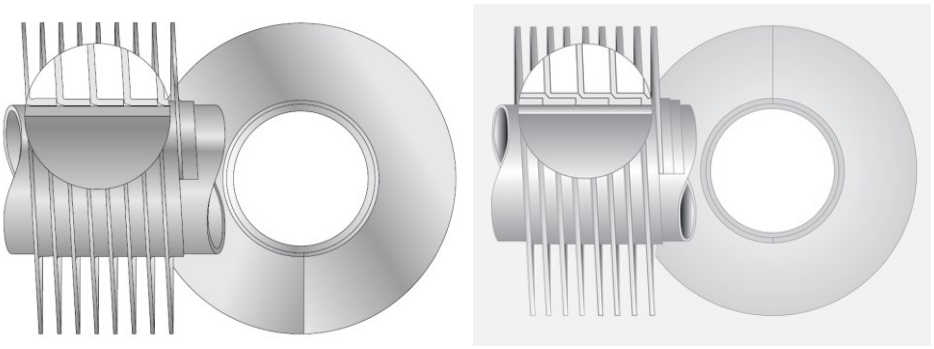

Figure 11. ‘L’ finned tube (left) (De.kelvion 2017) and ‘Double L’ finned tubes (right) (Salemtube 2017).

b) Embedded G-finned tubes

A continuous spiraling groove is machined on the outer tube surface into which a continuous strip of the fin material is inserted. The thickness of the tube should be high enough to allow for this groove. The finning machine then peens or rolls the tube material adjacent to the fin foot to secure the fins inside the groove. G fin is a type of embedded fins and is shown in the Figure 12. They can be used for service temperatures of up to 400ºC. (McHugh and Chapple 1999, p. 67.)

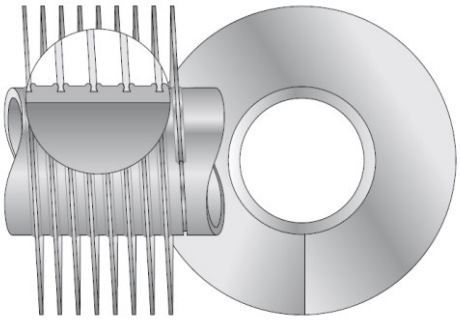

Figure 12. Embedded G-finned tube (De.kelvion 2017).

c) Bimetallic E-finned tubes

A base tube and an aluminum outer tube which lie concentric to one another, are fed into a finning machine. With the help of a set of rotating dies, the aluminum sleeve is plastically deformed to form fins. This extrusion process forms spiraling fins of a required height, leaving behind a sizable amount, about a millimeter of aluminum material enclosing the fluid handling, base tube as shown in Figure 13. (McHugh and Chapple 1999, p. 67.) The base

tube is made from a common tubing material with standard heat exchanger tubing dimensions. Since the contact between the inner and the outer tubes is not perfect, this poses a thermal contact resistance at the interface. Albeit, this resistance is not high for low temperatures but can increase from 10% to 25% of the total heat resistance when the tube-side fluid temperature is higher than 200ºC. (Serth and Lestina 2014, p. 511.)

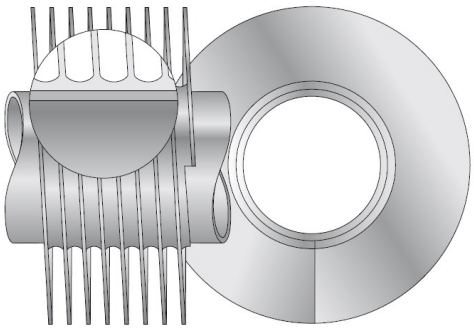

Figure 13. Extruded bimetallic E-finned tube (De.kelvion 2017).

d) Extruded K-finned tubes

They are used where corrosion is a major problem and temperatures are more than 200ºC. Soft and ductile metals including copper, cupronickel and aluminum are directly extruded without having a secondary inner tube. (Kröger, 2004, p. 333.)

Thermal and mechanical performance of ACC fins depend on the material they are made from. Aluminum, steel or copper are the three most common metals used, depending on the condenser duty conditions. Their advantages based on the application are summarized below.

Aluminum fins

Aluminum fins are the most common type of ACC fins because they offer good thermal conductivity and are cost effective. For most applications aluminum offer acceptable corrosion resistance. Its performance is better than steel but much cheaper than copper. (Hawkins 2013, p. 35.)

Steel fins

Galvanized steel fins are occasionally used in atmospheres where they have a better corrosion resistance than aluminum. They are also mechanically stronger than aluminum but have lower thermal conductivity. Therefore larger fin bundles are required for the same application. Even though cost of the material is about the same as aluminum but because larger fin bundles have to be used, they turn out to be more expensive. (Hawkins 2013, p. 35.)

Copper fins

The density of copper is about three times that of aluminum but has excellent thermal conductivity. Copper is used for fins where the fin thicknesses can be very low and are not dependent on the manufacturing process like in the case of circular helical fins. (Hawkins 2013, p. 35.)

2.4 Tube bundle headers types

Each tube bundle has two headers, one for the inlet and the other for the outlet. There are different types of headers designs as shown in Figure 14, depending on their applications. Some the most common ACC header designs are discussed in this section.

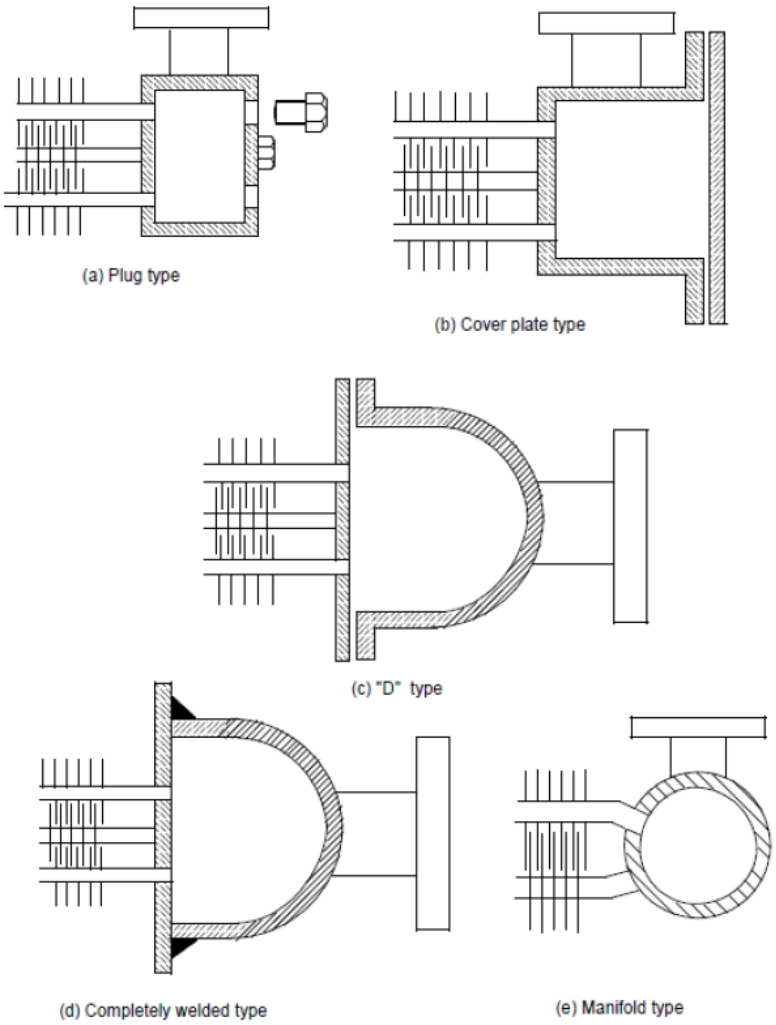

Figure 14. Header types (Hawkins 2013, p. 43).

a) Plug type header

This type of headers have as many screwed plugs as the finned tubes and are co-centric with the holes in the tube sheet. For maintenance and cleaning, the screwed plugs can be unscrewed to gain entry to the tube. (Serth and Lestina 2014, p. 512).

b) Cover plate type header

The inlet and the outlet nozzles are arranged at the top and at the bottom so the cover plate can be removed to have an unrestricted access to the tube sheet without dismantling any tubes. On the other hand this type is relatively more expensive than the rest and is susceptible to leakages because the large peripheral gasket is cumbersome to install accurately in place. This type is normally used in cases where the tubes need periodic maintenance and the service pressures are below 275 bars. (Serth and Lestina 2014, p. 512.)

c) D type header

They are cheaper than cover plate headers, can withstand higher service pressures. They give full access to the tube sheet, but the piping has to be dismantled (Hawkins 2013, p. 42). They are best suited on the outlet end for A-frame air cooled condensers because they are effective in collecting the condensate and discharging it through the outlet nozzles.

d) Completely welded type header

This type is an inexpensive design, normally used for clean fluids due to which, the headers do not require regular maintenance. The tubes are welded into the tube sheet and the D type header is welded with the required nozzles. (Hawkins 2013, p. 42.)

e) Manifold type header

For high pressure applications above 275 bars, the tubes are directly welded into a pipe of an appropriate schedule number to function as a header (Serth and Lestina 2014, p. 512).

2.5 Thermal performance

Condensation requires a large amount of heat transfer ($2.3 \cdot 10^6$ J/kg) to the atmosphere. The rate of heat transfer from the hot fluid to the ambient air is proportional to the temperature difference between the two. The condensing temperature is proportional to condensing pressure, which is the turbine back pressure minus any pressure drop in the steam lines up to the condenser inlet. The relationship between condensing temperature and pressure is shown in Figure 15. (Wilber 2005, p. 10.)

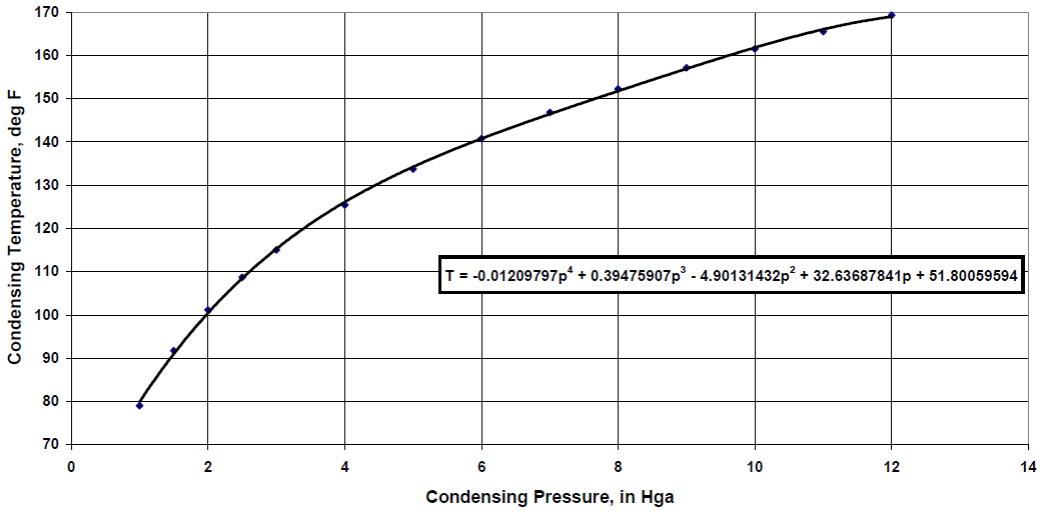

Figure 15. Condensing temperature vs pressure (Wilber 2005, p. 11).

The performance of an ACC is characterized by the difference between the condensing temperature (T_{cond}) and inlet temperature of the air-side stream (t_{in}) which is called ITD (Initial Temperature Difference).

$$ITD = T_{cond} - t_{in} \quad (1)$$

The heat load, Q of a given ACC is proportional to its ITD. The lower the initial temperature difference, the larger the ACC has to be in size (number of cells, heat transfer surfaces). This is expressed by the following relationship, (Wilber 2005, p. 11.)

$$ACC \text{ Size } \propto 1/ITD \quad (2)$$

2.6 Cold climate considerations

Sometime ACCs may run at lower load capacities and depending on the location, may operate at sub-freezing temperatures of the condensate, for at least during some parts of the year. Under such conditions, the problem of condensate freezing inside the tube bundles may occur. (Pat. US 4045961 1977, p. 2.)

A steam turbine is started slowly to protect the rotor and the stator from abrupt thermal distortions. This rate is prescribed by the turbine manufacturer above which large metal-temperature gradients occur. This poses a problem for the condenser at low ambient air temperatures. The heat exchange surfaces in the remote parts of the condenser must be bought above the freezing point of the condensate, which can be achieved by the following (Larinoff, Moles and Reichhelm 1978, p. 9)

a) Sequential start-up of the condenser by isolating different sections of the condenser by means of large steam valves.
b) Directly by-passing live steam from the boiler to the condenser to increase the total steam flow.
c) Using open flame torches to heat the heat exchange surfaces.
d) Making the inlet stream flow con-current with the cooling air. This method is especially used for viscous fluids with high pour points to avoid freezing and unacceptable pressure drop. It is done because con-current flow has the coldest air cooling

down the hottest fluid while the hottest air cools the coldest fluid. This helps to maintain a higher and uniform tube wall temperature. This is achieved by having the inlet nozzle at the bottom of the header while the pass arrangements upwards. (Price et al. 2004, p. 4.)

2.7 Air cooled condenser performance enhancement

The thermal performance of ACCs is drastically affected by the fluctuations in weather conditions. Designing ACCs for the peak temperatures incurs high capital and running costs. These costs can be brought down while maintaining the same thermal performance by adoption one of the following methods.

Hybrid cooling system

During hot summer months, the air cooled condenser performance drastically decreases which increases the turbine back pressure, thereby decreasing the turbine output. One way to deal with this problem is to connect an ACC with a wet cooling tower in parallel, equipped with a surface condenser as shown in Figure 16. During normal operation all the exhaust turbine steam is condensed by the ACC. At high ambient air temperatures, the ACC is coupled with a surface condenser such that the condensing pressure is the same in the two. The ACC reduces the total condensation pressure, which increase the turbine output. (Kröger 2004, p. 37.)

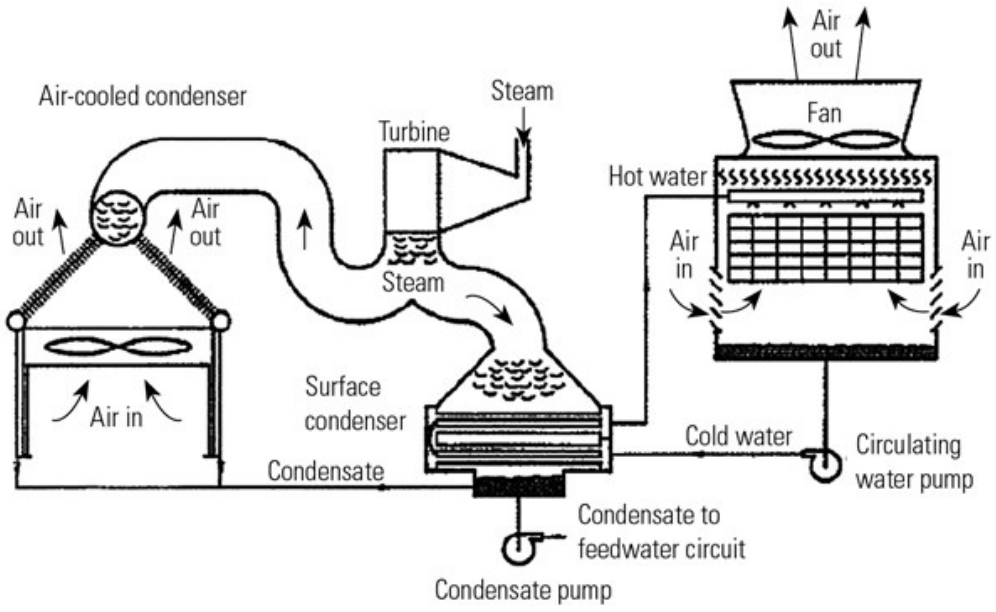

Figure 16. Air cooled condenser in parallel with a wet cooling tower (Kröger 2004, p. 38).

Such a system requires a much smaller ACC but on the other hand, requires additional equipment including a shell and tube surface condenser, an evaporative cooling tower, circulating water pumps and piping. Even with the added equipment requirements, the total system incurs lower capital and annual running costs when compared with a fully optimized all-dry cooling system. (Wilber 2005, p. 24.)

Spray enhancement

An alternative way of improving ACC performance is to install water sprays into the inlet air stream of the ACC for operations during hot summer months, as shown in Figure 17. This methods cools down the inlet air and cooling effects of 2.5 to 5 °C can be readily achieved eliminating the need of lowering the turbine load. This is a low cost approach which can be implemented into existing ACC installations. If the system is not correctly designed and implemented, it may scale or corrode the finned tube bundles from unevaporated water droplets, thereby damaging the heat transfer surfaces. (Wilber 2005, p. 25.)

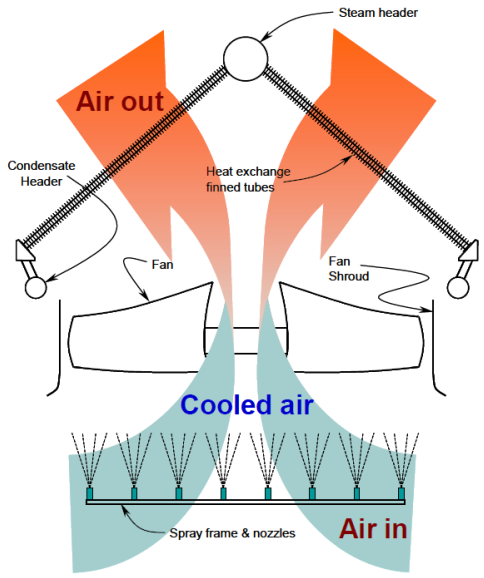

Figure 17. Water spray enhancement (Wilber 2005, p. 26).

2.8 Non- condensables in standard air cooled condensers

Sometimes non-condensable gases are present in the inlet steam which can accumulate inside the tubes of a standard ACC and cause a huge heat transfer efficiency loss. Standard frame ACCs with horizontal tubes are shown in Figure 18. A well designed system should be capable of continually collect and release non-condensable gases coming along with the

steam. These non-condensable gases are a result of atmospheric air leaks into the vacuum end of the steam turbine equipment and from water treatment chemicals for boiler feed. In addition, these non-condensables can be absorbed into the steam condensate causing metal corrosion. (Larinoff, Moles and Reichhelm 1978, p. 2.)

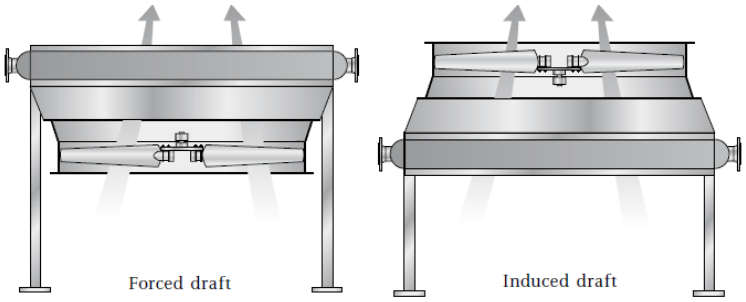

Figure 18. Standard frame ACC- forced draft (left), induced draft (right) (De.Kelvion 2017).

Pockets of non-condensable gases form inside the condenser tubes when the steam enters from two directions. This is illustrated in Figure 19 with two rows of tubes. The steam enters both the rows, through the steam inlet and moves towards the rear header. The lower condenser rows are subjected to cooler air than the upper rows because the air has a positive temperature gradient as it travels up in an ACC. This causes a higher amount of condensation in the lower rows and therefore a higher pressure drop than the upper rows. This leads to a back flow from the upper rows into the lower rows from the rear header which causes entrapment of the non-condensable gases. (Larinoff, Moles and Reichhelm 1978, p. 3.)

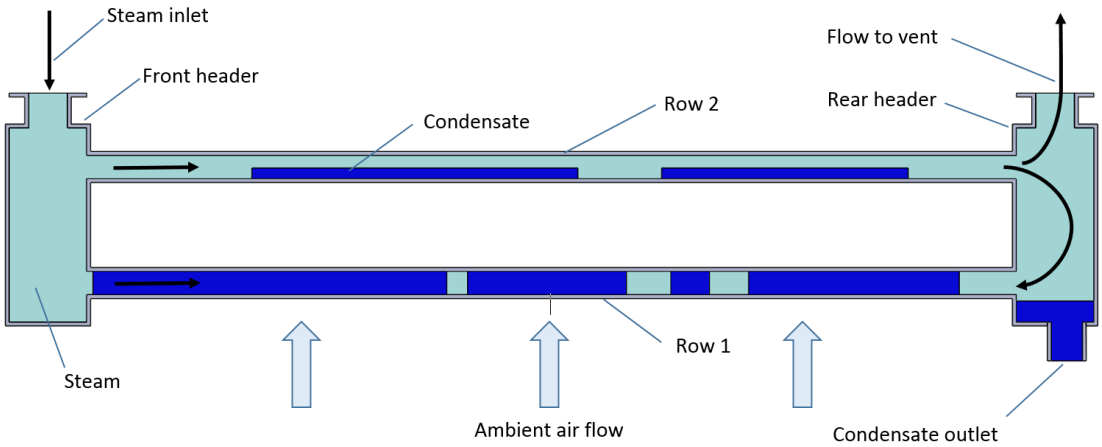

Figure 19. Trapping of non-condensable gases.

The non-condensable gases get entrapped inside the finned tubes above the condensate and form a vapor/ liquid interface. This causes a pressure rise inside the tubes and reduces the heat transfer coefficient. Ideally an ACC is meant to be a low pressure sink for the turbine exhaust steam but with an increased condenser pressure the efficiency of the turbine decreases. (Mohr, Mines and Bloomfield 2001, p. 1.)

Such entrapment of non-condensable gasses typically occurs in standard frame ACCs. Therefore in most cases for condensing steam coming from a turbine, A-frame ACCs are used. The non-condensable gases can be vented out though the installation of a dephlegmator, valves (manual/ automatic) and air venting devices (Paffel 2016).

2.9 Dephlegmator

Dephlegmators are commonly used to vent off non-condensable gases. An ACC normally consists of multiple A-framed bays. The majority of them form the primary bays and the rest secondary bays (dephlegmator). They are connected in series as shown in Figure 20. The incoming steam from the turbine is fed through the main steam header into the primary bay. Here partial condensation takes place with a con-current vapor/ condensate flow. The condensate drains into a tank through the condensate drain. The remaining steam enters the dephlegmator bay where secondary condensation takes place, with a counter-current vapor/ condensate flow. The condensate drains through a drain while the non-condensables are ejected through a vent at the top. (Larinoff, Moles and Reichhelm 1978, p. 3.)

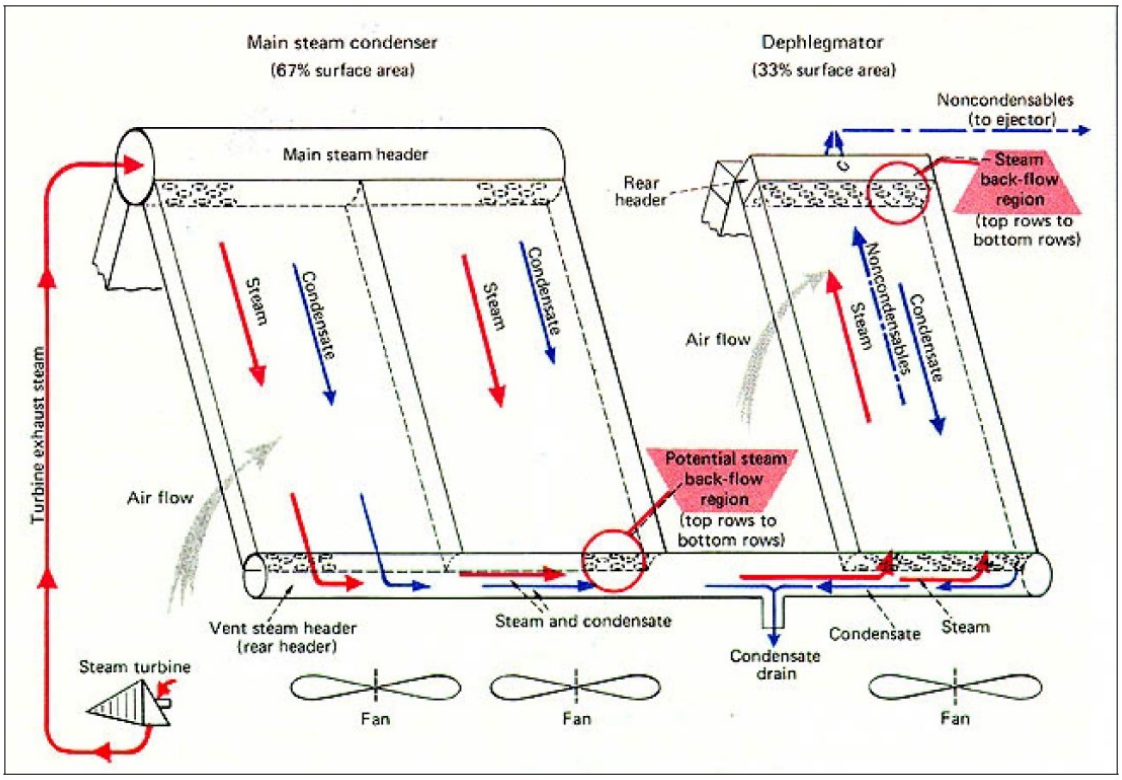

Figure 20. Dephlegmator design (Larinoff, Moles and Reichhelm 1978, p. 15).

2.10 Air cooled condenser thermal specifications

To fully design an ACC system capable of performing at the expected operational conditions, the following design parameters are needed to be specified (Larinoff, Moles and Reichhelm, 1978, p. 7; Wilber 2005, p. 1)

1) Steam flow rate
2) Turbine exhaust steam quality
3) Turbine back pressure
4) Design ambient dry bulb air temperature
5) Site elevation above sea level
6) Maximum ambient air temperature
7) Minimum ambient air temperature
8) Lowest optimum turbine exhaust pressure
9) Highest permissible turbine exhaust pressure

The full load fluid properties are given by the first three parameters. The design exhaust pressure is measured at the turbine exhaust flange if the piping to the ACC is under the

manufacturer's scope of supply. During peak summer months at high ambient temperatures, the rate of heat rejection to the ambient air from the ACC decreases. This increases the unit's pressure which should be lower than the maximum exhaust pressure that the turbine can withstand. A turbine's output efficiency is adversely affected with the increase in its exhaust pressure. Since the turbine output decreases, plants normally establish an upper pressure limit. Furthermore turbine manufacturers have a prescribed upper pressure limit for the turbine for mechanical and metallurgical reasons. Normally the upper pressure limit for a vacuum turbine ranges from 12 to 15 cm Hg. (Larinoff, Moles and Reichhelm, 1978, p. 8.)

Since an ACC's efficiency decreases at high ambient temperatures, it has to be over designed for such situations, thereby increasing its capital costs. An economic ACC design is determined by sizing an ACC based on a number of possible high ambient air temperature values, and then comparing its capital cost with the savings from turbine outputs.

The minimum ambient air temperature helps determine the type and degree of freeze protection required. Measures to prevent the freezing of condensate in the finned tubes include, heating through steam coils, incorporating louvers, reversing the fan rotation, or decreasing the fan pitch (Mukherjee 2007, p. 12).

The ACC has to be designed such that initial capital costs of the heat transfer surfaces are balanced with the fan operational costs. Depending on the space constraints, the areal footprint of an ACC can be decreased by increasing the fan power and vice versa. (Larinoff, Moles and Reichhelm 1978, p. 8.)

Steam flow is the total amount of fluid flowing from the turbine, available to the condenser which includes both dry steam and water droplets. Steam quality is the fraction of dry steam in the total steam flow coming from the turbine. Fully saturated dry steam has a quality of 100% (x=1).

3 CONDENSER DESIGN THEORY

The initial capital and running costs of ACCs in a power plant significantly contribute to the overall total power plant project cost. The capital cost of an ACC is proportional to the area of heat transfer surfaces and the running cost is proportional to the total fan power. For these reasons accurate theoretical calculations for condenser design are very important (Palen 2006, p. 8). This section of the report goes through detailed theoretical methods and principles for the accurate design calculations.

3.1 Mean temperature difference

The MTD (Mean Temperature Difference) is used to determine the driving force for heat transfer between two fluid streams. The heat rate at every location of the ACC can be determined with known heat transfer coefficients. For practical applications, the overall heat transfer rate of a unit is of interest, since the process fluid temperature changes as it flows. (Stewart and Lewis 2013, p. 23.)

The calculation method for mean temperature difference in cross flow air cooled condensers is presented here. It is a graphical method, for which it is important to know the four terminal temperatures of the condenser. The correction factor, F is calculated from the graph for 4 rows and 1 pass arrangement using the corresponding values for the ratio of effectiveness, R and the thermal effectiveness of air, P. This approach is based on empirical equations based on a specific flow arrangement. (Roetzel and Nicole 1975, p. 5-8.)

Step 1) The logarithmic mean temperature difference, ΔT_{lm} is calculated by the following equation,

$$\Delta T_{lm} = \frac{(T_{in} - t_{out}) - (T_{out} - t_{in})}{ln\frac{T_{in} - t_{out}}{T_{out} - t_{in}}} \tag{3}$$

where, T_{in} is the inlet temperature of the tube-side stream, T_{out} is the outlet temperature of the tube-side stream, t_{in} is the inlet temperature of the air-side stream and t_{out} is the outlet temperature of the air-side stream (Echarte 1981, p. 1).

Step 2) The ratio of effectiveness, R is given by the following equation (Echarte 1981, p. 1),

$$R = \frac{T_{in} - T_{out}}{t_{out} - t_{in}} \tag{4}$$

Step 3) The thermal effectiveness, P of air is given by the following equation (Echarte 1981, p. 2),

$$P = \frac{t_{out} - t_{in}}{T_{in} - t_{in}} \tag{5}$$

Step 4) The cross-flow correction factor, F is determined form the values of R, P and the corresponding graph for 4 rows and 1 pass as shown in Figure 21. F is used to compensate for deviation from a pure counter-current flow. For a pure counter-current flow, F is taken to be 1 (Farrant 1995, p. 5).

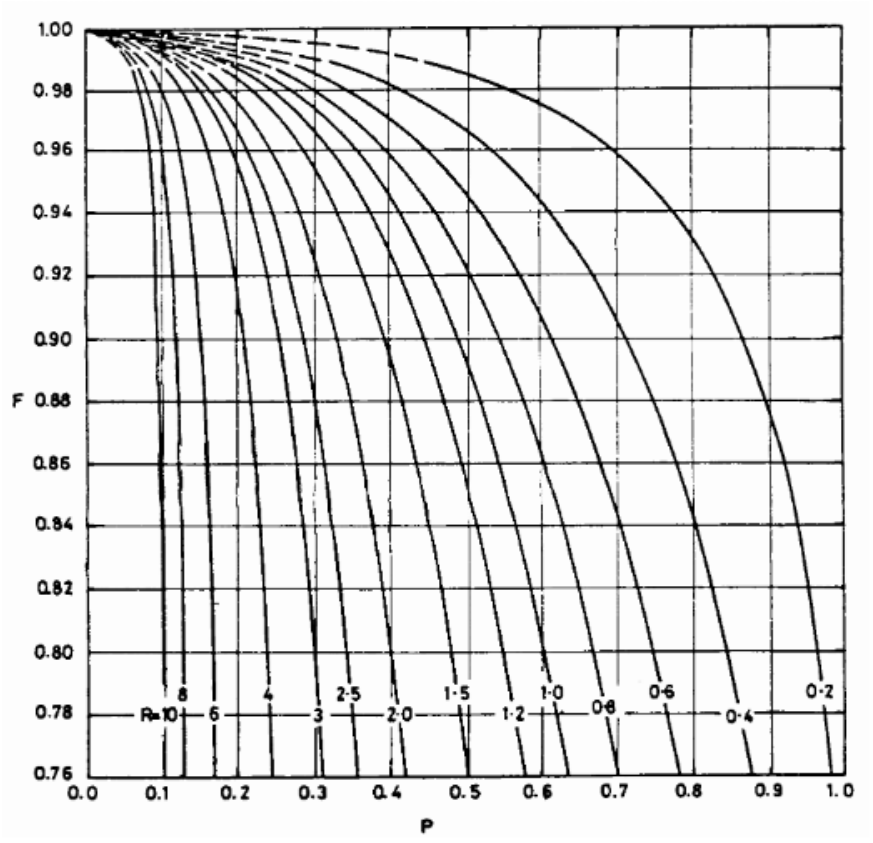

Figure 21. Correction factor for 4 rows and 1 pass (Echarte 1981, p. 7).

Step 5) The mean temperature difference, ΔT_m is given by the following equation,

$$\Delta T_m = \Delta T_{lm} F \tag{6}$$

where, ΔT_{lm} is the log mean temperature difference (Echarte 1981, p. 2).

Overall heat transfer rate

The amount of heat transferred during condensation, $\dot{q}_{cond}$ is given by the following equation,

$$\dot{q}_{cond} = \dot{m}_{fluid} h_e \tag{7}$$

where, $\dot{q}_{cond}$ is the rate of heat transfer during condensation in kcal/ hr, $\dot{m}_{fluid}$ is the tube-side fluid mass flow rate in kg/ hr and h_e is the specific enthalpy of evaporation for steam in kcal/ kg (U.S. Department of Energy 1992, p. 110).

The amount of heat exchanged during a temperature drop from T_{in} to T_{out} is given by,

$$\dot{q}_{\Delta t} = \dot{m}_{fluid} C_{p\,cond} \Delta t \tag{8}$$

where, $\dot{q}_{\Delta t}$ is the amount of heat exchanged for a temperature drop from T_{in} to T_{out} , $C_{p\,cond}$ is the specify heat capacity of the condensate in kcal/ kg-C and Δt is the change in temperature in ^{o}C (U.S. Department of Energy 1992, p. 47). Therefore the total rate of heat transfer, $\dot{q}_{total}$ is given by,

$$\dot{q}_{total} = \dot{q}_{cond} + \dot{q}_{\Delta t} \tag{9}$$

3.2 Surface area of the condenser

The overall heat flow rate in an air cooled heat exchanger is defined in terms its overall heat transfer coefficient which is referred to the total surface area for heat transfer.

$$\dot{q}_{total} = U\ A\ F\ \Delta T_{lm} \tag{10}$$

where, $\dot{q}_{total}$ is the total rate of heat transfer in kcal/h, U is the overall heat transfer coefficient in Kcal/ hr. m^2 ^oC and A is the total surface area of the condenser in m^2 (Henry 1995, p. 7).

3.3 Number of tube rows, tube length and number of tubes

Total face area of bundles for a standard fan velocity is given by,

$$A_{face} = \frac{\dot{m}_{air}}{\rho_{std} V_{face}} \tag{11}$$

where, A_{face} is the total face area of all the tube bundles in m^2, $\dot{m}_{air}$ is the outside air mass flow rate, ρ_{std} is standard air density in kg/m^3 and V_{face} is standard face velocity for axial flow fans for ACC in m/hr (Lee, Ralston and McNaught 2013, p. 9).

Once the total face area of the bundles is calculated, it can be divided into smaller practically sized bundles. Since steam condensers are generally A-frame, the number of bundles have to an even number as each bay has to have the same number of bundles on each side. Also, the area of each bundle is maximized such that large diameter fans can be installed in the bays. By having large diameter fans, it is possible to reduce the number of fans required for the same air flow. This makes the design more cost effective and easier to maintain.

Number of tubes is given by the following equation,

$$n_t = \frac{A}{A_{total} L} \tag{12}$$

where, n_t is the number of tubes, A_{total} is the total surface area of the finned tubes per meter length and L is the tube length.

3.4 Number of tube passes

The tube-side coefficient of heat transfer is dependent on the stream velocity. Tube-side fluid (steam) velocity gain is proportional to the increase in pressure drop which is achieved by increasing the number of tube passes. For a high coefficient of heat transfer, the fluid should have a turbulent flow and therefore a Reynold's number greater than 4000. (Mukherjee 2007,

p. 41.) On the other hand, since increasing the number of passes also increases the pressure drop in the tube bundles, ACCs are designed with the least number of passes. A larger number of passes also increases complexity for fabrication. Therefore during thermal designing, the Reynolds number is first calculated for the fluid velocity corresponding to a single pass.

The tube-side fluid velocity, V_{steam} is given by,

$$V_{steam} = \frac{\dot{m}_{air}\,(n_p/n_t)}{\rho_{steam}\ \pi\ D_i^2/4} \tag{13}$$

where, $\dot{m}_{air}$ is the out-side air mass flow rate in kg/s, n_p is the number of tube passes, ρ_{steam} is the steam density in kg/m^3 and D_i is the inner diameter of the tubes in m (Serth and Lestina 2014, p. 522).

Reynold's number for tube-side fluid, $Re_{tube\ side}$ is given by,

$$Re_{tube\ side} = \frac{\rho_{steam}\ V_{steam}\ D_i}{\mu_{steam}} \tag{14}$$

where, μ_{steam} is the dynamic viscosity of steam (Kröger 2004, p. 69).

On substituting for steam velocity, V_{steam} in equation 15,

$$Re_{tube\ side} = \frac{4\ \dot{m}\ (n_p/n_t)}{\pi\ D_i\ \mu_{steam}} \tag{15}$$

For a flow to be turbulent, the Reynold's number needs to be greater than 4000 (The Engineering toolBox 2017).

3.5 Tube to fin diameter ratio

In the case of steam condensers and low viscous tube-side streams, the air-side heat transfer coefficient is much lower than the tube-side. Since the air-side heat transfer coefficient is controlling, there becomes a need for high fin density (fin number per unit tube length) and fin height to bring the lower coefficient closer to that of the tube-side. In such cases, a fin

density of 433 fins per meter and fin height of 25.4 mm is used. On the other hand in applications with high tube-side fluid viscosities, the tube-side heat transfer coefficient is much lower. Therefore, it becomes more reasonable to have lower fin densities (197-276 per meter) and a lower height of 12.7 mm. In some extreme cases, even bare tube (without fins) may be used (Mukherjee 2007, p. 36).

3.6 Tube-side heat transfer coefficient

The tube-side heat transfer coefficient is a function of the tube inner diameter, Reynolds number and the Prandtl number. By increasing the tube-side fluid velocity, the fluid flow is made turbulent which increases the heat transfer coefficient. (Mukherjee 2007, p. 41-42.)

This section describes the theory behind the tube-side heat transfer coefficient calculations on a vertical tube inner surfaces. It applies to condensation inside finned tubes where the film thickness is lower than the tube diameter. Vapor condensation on a vertical tube surface is shown in Figure 22 where the vapor shear effects are negligible and the condensate flows downwards dues to gravity. A short laminar condensate film exists at the top which transitions into a laminar wavy regimes. This transition often occurs at film Reynold's number great than 30. (Butterworth 1974, p. 1.)

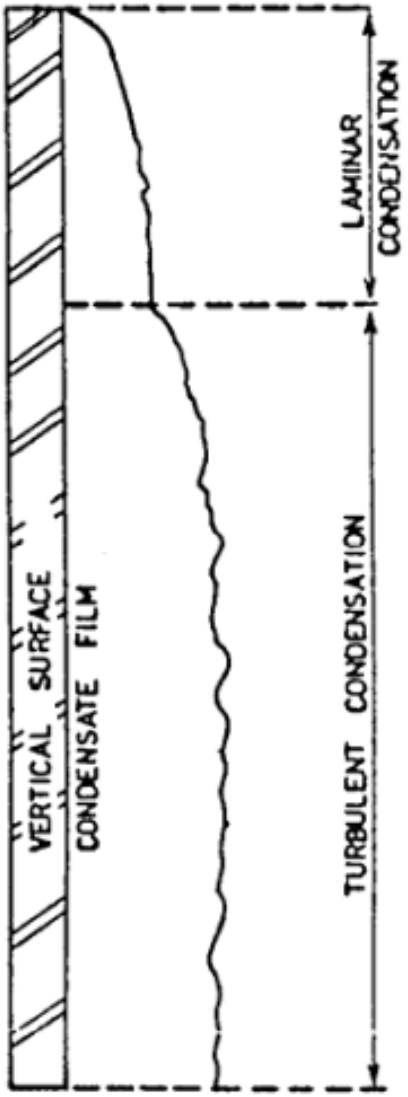

Figure 22. Film-wise condensation on a vertical surface with negligible vapor shear (Butterworth 1974, p. 1).

Figure 23 describes the local heat transfer coefficients with respect to film Reynold's number which is dependent on the flow velocity. In the laminar-wavy region, the heat transfer coefficient decreases as shown in Figure 23, since the film flow rate and thickness increases. Further accumulation of the condensate down the tube length causes the flow to become turbulent as the film thickness increases due to increased effective viscosity. The thermal diffusivity increases with the increase in flow rate which increases the coefficient of heat transfer.

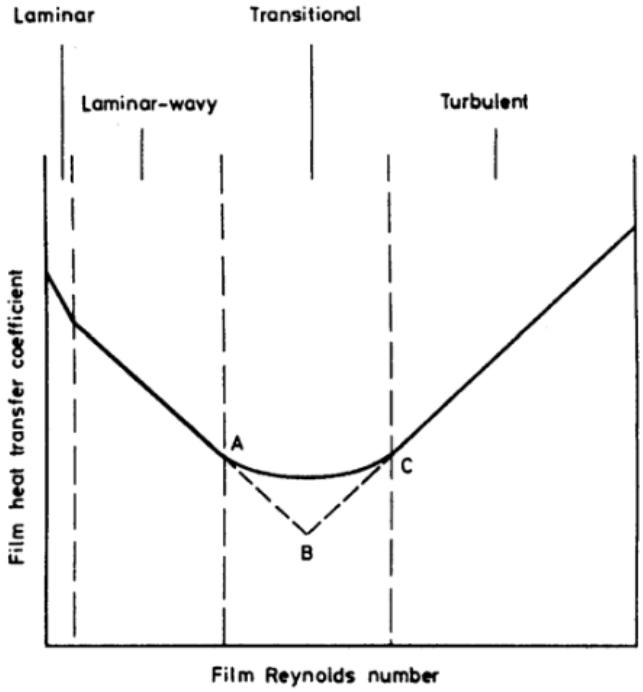

Figure 23. Variation in condensate heat transfer coefficient with film Reynold's number (Butterworth 1974, p. 2).

3.7 Tube-side heat transfer coefficient calculations

This method applies to the calculation of the tube-side heat transfer coefficient for condensate on the tube inner surfaces. Since, in an air cooled condenser, the tubes are inclined at an angle of 60 degrees, the condensate flows under the action of gravity. Therefore, this calculation procedure takes into account gravity controlled film-wise condensation. The local condensate flow rate is given by,

$$\tau_{cond} = \frac{\dot{m}_{cond}}{D_i \, n_t} \tag{16}$$

where, τ_{cond} is the local condensate flow rate in kg/s m, $\dot{m}_{cond}$ is the condensate mass flow rate kg/s, D_i is the tube inner diameter in m and n_t is the total number of tube (McNaught and Walker 1987, p. 1).

The local condensate Reynold's number is given by,

$$Re_{cond} = \frac{4 \, \tau_{cond}}{\mu_{cond}} \tag{17}$$

where, Re_{cond} is the local condensate Reynold's number, τ_{cond} is the local condensate flow rate in kg/s m and μ_{cond} is the dynamic viscosity of the condensate in N s/m^2 (McNaught and Walker 1987, p. 2).

Condensate Prandtl number is given by,

$$Pr_{cond} = \frac{C_{p\ cond}\,\mu_{cond}}{k_{cond}} \tag{18}$$

where, Pr_{cond} is the condensate Prandtl number, $C_{p\ cond}$ is the specific heat of the condensate in J/kg. K, μ_{cond} is the dynamic viscosity of the condensate in N s/m^2 and k_{cond} is the thermal conductivity of the condensate in W/m K (McNaught and Walker 1987, p. 2).

An ACC is designed such that the tube-side fluid flow is fully turbulent. This increases the tube-side heat transfer coefficient as shown in Figure 23. Therefore the equations for heat transfer coefficient, for a fully turbulent flow are used,

$$\alpha_c^* = 0.0038\, Re_{cond}^{0.4}\, Pr_{cond}^{0.65} \tag{19}$$

where, α_c^* is the dimensionless local heat transfer coefficient for turbulent region (McNaught and Walker 1987, p. 3).

The tube-side heat transfer coefficient is given by,

$$h_{tube\ side} = k_{cond}\,\alpha_c^* \left(\left(\frac{\rho_{cond}(\rho_{cond} - \rho_{steam}) g_n}{\mu_{cond}^2} \right) \right)^{0.333} \tag{20}$$

where, $h_{tube\ side}$ is the tube-side heat transfer equation in W/m^2 K, ρ_{cond} is the condensate density in kg/ m^3, ρ_{steam} is the steam density in kg/ m^3 and g_n is the acceleration due to gravity in m/s^2 (McNaught and Walker 1987, p. 3).

Since the ACC is an A-frame condenser with a tube angle of 60^o, we introduce a sin component in equation 20. Therefore we get,

$$h_{tube\ side} = k_{cond}\,\alpha_c^* \left(\left(\frac{\rho_{cond}(\rho_{cond}-\rho_{steam}) g_n\, Sin\theta}{\mu_{cond}^2} \right) \right)^{0.333} \quad (21)$$

3.8 Air-side coefficient of heat transfer

This section describes the procedure to calculate the air-side heat transfer coefficient flow across finned tube bundles. The heat transfer coefficient is based on the total surface area, tube arrangement and the number of tube rows. This methods is applicable for tube bundles with at least two tube rows. (Hoyle, 1985 p. 25.)

In our design a staggered tube bundle is used as shown in Figure 24. Finned tube bundle geometry (Butterworth 1980, p. 1).

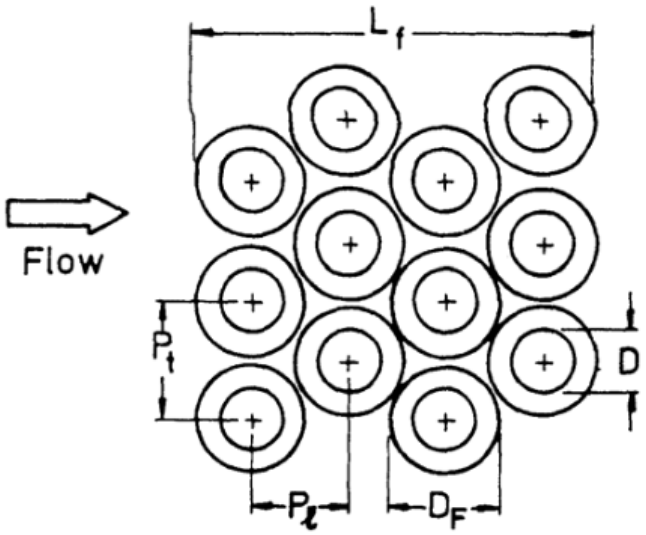

Figure 24. Finned tube bundle geometry (Butterworth 1980, p. 1).

The minimum flow area is given by,

$$S_{min} = (P_t - D_R - n_F S(D_f - D_R))L_T N_T \quad (22)$$

where, S_{min} is the minimum flow area in m^2, P_t is the transverse pitch in m, D_R is the outer diameter of root tube in m, n_F is the fin frequency per meter length, S is the fin thickness in m, D_f is the fin outer diameter in m, L_T is the length of finned tubes exposed to the air flow in m, N_T is the number of tubes in a row (Butterworth 1980, p. 2).

The maximum mass velocity, which is based on S_{min} is given by,

$$\dot{m}_{max} = \frac{\dot{m}_{air}}{S_{min}} \tag{23}$$

where, $\dot{m}_{max}$ is the maximum mass velocity in kg/s and $\dot{m}_{air}$ is the outside air mass flow rate in kg/s (Butterworth 1980, p. 2).

The air-side Reynold's number is given by,

$$Re_{air\ side} = \frac{\dot{m}_{air}\, D_r}{\mu_{air}} \tag{24}$$

where, $Re_{air\ side}$ is the air-side Reynold's number (Butterworth 1980, p. 2).

The area ratio, which gives the area of the total extended surfaces to the root tube is given by,

$$A_r = 1 + 2\, n_f\, H \left(1 + \frac{H+s}{D_r}\right) \tag{25}$$

where, A_r is the area ratio, H is the fin height in m (Hoyle 1985, p. 25).

The j-factor for the finned tubes is given by,

$$j_R = 0.29\, Re_{air\ side}^{-0.367}\, A_r^{-0.17} \tag{26}$$

where, j_R is the j-factor for round finned tubes (Hoyle 1985, p. 25).

The air-side Prandtl number is given by,

$$Pr_{air\ side} = \frac{C_{p\ air}\, \mu_{air}}{k_{air}} \tag{27}$$

where, $Pr_{air\ side}$ is the air Prandtl number, $C_{p\ air}$ is the specific heat of air in J/ kg K, μ_{air} is the dynamic viscosity of air in Ns/ m^2 and k_{air} is the thermal conductivity of air in W/m K (Hoyle 1985, p. 26).

Air-side heat transfer coefficient is given by,

$$h_{air\ side} = j_R\ C_{p\ air}\ \dot{m}_{max}\ Pr_{air\ side}^{-2/3} \tag{28}$$

where, $h_{air\ side}$ is the air-side heat transfer coefficient in W/m^2 K (Hoyle 1985, p. 26).

3.9 Fin efficiency calculations

Extended surfaces are required for both conduction and convection because the heat transfer coefficient of air and other gases is much lower than for fluids. Albeit, fins come in a variety of shapes and sizes, annual (transverse or radial) fin type as shown in Figure 25 are the most common. Since fins are made from very thin strips of metal attached to the base tubes, a significantly large surface area is attained with using a small amount of extra metal.

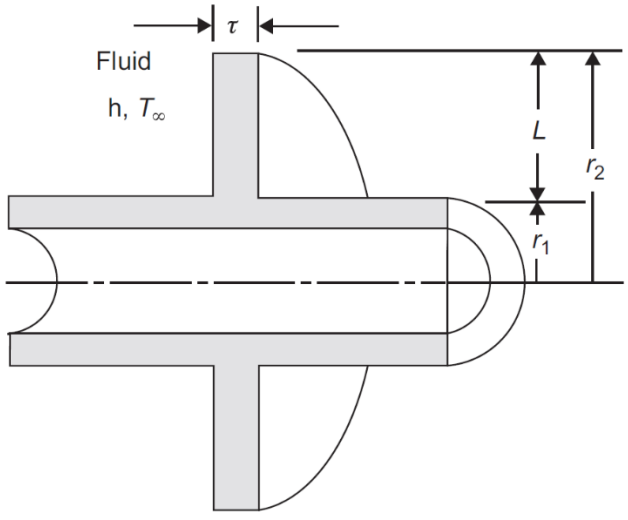

Figure 25. Radial fin attached to a base tube (Serth and Lestina 2014, p. 34).

First heat is transferred to the fins from the base tube through conduction and then to the ambient air through convection. Since the fins extend radially for the base tube, there exists a thermal gradient along the length. The temperature at the fin base is very close to that of the base tube and at the fin tip the temperature is close to that of the ambient air. This results

in a decrease in a temperature difference for convective heat transfer along the radial length of the fins. Therefore the extended surfaces are lower in efficiency than the base tube for heat transfer. For this reason, it is important to calculate fin efficiency to design an efficient ACC (Serth and Lestina 2014, p. 33).

Fin efficiency is given by,

$$\eta_f \cong \frac{\tanh(m\psi)}{m\psi} \tag{29}$$

where, η_f is the fin efficiency, m is the fin parameter and ψ is the effective fin height in m (Serth and Lestina 2014, p. 36).

The fin parameter is given by,

$$m = \left(\frac{2\, h_{air\ side}}{k\, S}\right)^{0.5} \tag{30}$$

where, m is the fin parameter, k is the thermal conductivity of the metal, the fins are made from, in W/m K and S is the fin thickness in m (Serth and Lestina 2014, p. 550).

The effective fin height, ψ is given by,

$$\psi = (r_{2c} - r_1)\left(1 + 0.35 \ln\left(\frac{r_{2c}}{r_1}\right)\right) \tag{31}$$

where, r_1 is the fin inner radius or tube outer radius in m, and r_{2c} is the corrected fin radius in m (Serth and Lestina 2014, p. 36).

And the corrected fin radius is given by,

$$r_{2c} = r_2 + \frac{S}{2} \tag{32}$$

where, r_{2c} is the corrected fin radius in m and r_2 is the fin outer radius in m (Serth and Lestina 2014, p. 34).

The surface area of fins is given by,

$$A_{fins} = 2\, n_f \pi (r_{2c}^2 - r_1^2) \tag{33}$$

where, A_{fins} is the fin surface area and n_f is the number of fins per meter length (Serth and Lestina 2014, p. 170).

The prime surface area is given by,

$$A_{prime} = 2\pi r_1 (L - n_f S) \tag{34}$$

where, A_{prime} is the prime surface area and L is the tube length (Serth and Lestina 2014, p. 170).

The weighed efficiency of the finned surface is given by,

$$\eta_w = \left(\frac{A_{prime}}{A_{Total}}\right) + \eta_f \left(\frac{A_{fin}}{A_{total}}\right) \tag{35}$$

where, η_w is the weighed efficiency of the finned surface (Serth and Lestina 2014, p. 36).

3.10 Overall heat transfer coefficient

The overall heat transfer coefficient is based on the total external surface area of the finned tubes which is given by,

$$U_c = \left(\frac{A_{total}/A_i}{h_{tube\ side}} + \frac{(A_{total}/L)\ln(D_r/D_i)}{2\pi k_{tube}} + \frac{1}{\eta_w h_{air\ side}}\right)^{-1} \tag{36}$$

where, U_c is the clean overall heat transfer coefficient W/m^2 K, A_i is the internal surface area of the tubes in m^2 (Serth and Lestina 2014, p. 517).

3.11 Fouling resistance

The total fouling resistance is given by,

$$R_D = R_{Di}(A_{total}/A_i) + R_{D0}/\eta_w \quad (37)$$

where, R_D is the total fouling resistance in m^2 K/W, R_{Di} is the tube-side fouling resistance in W/m^2 K, R_{D0} is the air-side fouling resistance in m^2 K/W (Serth and Lestina, 2014, p. 122).

Design overall heat transfer coefficient:

$$U_D = (\frac{1}{U_c} + R_D)^{-1} \quad (38)$$

where, U_D is the design overall heat transfer coefficient in W/m^2 K (Serth and Lestina 2014, p. 122).

3.12 Tube-side pressure drop

The total tube-side pressure drop in an ACC is the sum of the pressure drops in the finned tubes due to frictional forces and tube entrance and exit losses.

The tube-side pressure drop due to fluid friction inside the tubes is given by,

$$\Delta P_{f-tube\ side} = \frac{f\ n_p\ L\ G^2_{tube\ side}}{2000\ D_i\ s\ \emptyset} \quad (39)$$

where, $\Delta P_{f-tube\ side}$ is the tube-side pressure due to friction in Pa, f is Darcy friction factor, $G_{tube\ side}$ is the tube-side stream mass flux in kg/s m^2, s is specific gravity, $\emptyset$ is the viscosity correction factor (Serth and Lestina 2014, p. 189).

For turbulent flow, the viscosity correction factor is given by,

$$\emptyset = \left(\frac{\mu_{steam}}{\mu_{w\ steam}}\right)^{0.14} \quad (40)$$

where, μ_{steam} is the tube-side stream dynamic viscosity in N s/m^2 and $\mu_{w\ steam}$ is the tube-side stream dynamic viscosity at average tube wall temperature in N s/m^2 (Serth and Lestina 2014, p. 189).

Darcy friction factor is given by,

$$f = 0.4137\ Re_{tube\ side}^{-0.2585} \tag{41}$$

where, f is the Darcy friction factor (Serth and Lestina 2014, p. 152).

The tube-side mass flux is given by,

$$G_{tube\ side} = \frac{(\dot{m}_{fluid}/bundle)\left(\frac{n_p}{\frac{n_t}{bundle}}\right)}{\frac{\pi D_i^2}{4}} \tag{42}$$

where, $G_{tube\ side}$ is the tube-side mass flux in kg/s m^2 (Serth and Lestina 2014, p. 524).

The tube-side pressure drop due to tube entrance and exit losses, $\Delta P_{r-tube\ side}$ is given by,

$$\Delta P_{r-tube\ side} = 5.0 * 10^{-4}\ \alpha_r\ \left(\frac{G_{tube\ side}^2}{s}\right) \tag{43}$$

where, α_r is the number of velocity heads for tube-side pressure losses (Serth and Lestina 2014, p. 189).

For regular tubes with turbulent fluid flow (Serth and Lestina 2014, p. 152),

$$\alpha_r = 2n_p - 1.5 = 0.5 \tag{44}$$

The total tube-side pressure drop is given by the sum of all the frictional forces inside the tubes and pressure drop due to tube entrance, exit losses.

$$\Delta P_{tube\ side} = \Delta P_{f-tube\ side} + \Delta P_{r-tube\ side} \tag{45}$$

3.13 Air-side pressure drop

Air-side pressure drop due to friction with the tube bundles of high fin heights given by,

$$\Delta P_{f-air\ side} = \frac{2 f_{fr}\, N_r\, G_{air\ side}^2}{\rho_{std}} \tag{46}$$

where, $\Delta P_{f-air\ side}$ is the air-side pressure drop due friction in Pa, f_{fr} is the friction correction factor for air flow across tube bundles with an equilateral pitch, N_r is the number of rows, $G_{air\ side}$ which is given by $\rho_{std} V_{max}$ is the air-side mass flux in kg/s m^2, ρ_{std} is the standard air density in Kg/ m^3 and V_{max} is the maximum air velocity in tube bundles in m/s (Serth and Lestina 2014, p. 516).

For air flow through equilateral triangle pitched tubes in tube bundles, the friction factor, f_{fr} is given by,

$$f_{fr} = (1 + \frac{2e^{-(m/4)}}{1+m})(0.021 + \frac{27.2}{Re_{eff}} + \frac{0.29}{Re_{eff}^{0.2}}) \tag{47}$$

where, m is the fin parameter and Re_{eff} is the effective Reynold's number (Ganguli, Tung and Taborek 1985, p. 122-128).

The fin parameter is given by,

$$m = \frac{P_t - D_f}{D_r} \tag{48}$$

where, P_t is the transverse tube pitch in m, D_f is the fin outer diameter in m and D_r is the tube root diameter in m (Serth and Lestina 2014, p. 517). The effective Reynold's number is given by,

$$Re_{eff} = Re_{air\ side}(l/H) \tag{49}$$

where, Re_{eff} is the effective Reynold's number, l is the fin spacing and H is the fin height in m (Serth and Lestina 2014, p. 517).

The fin spacing is obtained from the number of fins per unit length. It is given by,

$$l = \frac{1}{n_f} - S \tag{50}$$

where, l is the fin spacing (Serth and Lestina 2014, p. 515).

The maximum velocity in the tube bundles is related to the face velocity which is the average air velocity entering the first rows of the tube bundles. The relationship is given by,

$$\frac{V_{max}}{V_{face}} = \frac{A_{face}}{A_{min}} \tag{51}$$

where, A_{face} is the face area and A_{min} is the minimum flow area. In a tube bundle with equilateral triangle tube pitch, the minimum flow area is the space between the adjacent tubes, refer to Figure 24. The area between the adjacent tubes is given by, $(P_t - D_r)L$, where L is the tube length. The area taken up by fins on both side of the tubes is given by, $2n_f\ L\ H\ S$ (Serth and Lestina 2014, p. 515). Therefore, the minimum flow area is given by,

$$A_{min} = (P_t - D_r)L - 2n_f\ L\ H\ S \tag{52}$$

The air passing through the gap between the tubes, approaches the tube bundles over the length, L (tube length) and width (P_t), extending from the center of one tube to the center of the adjacent tube. Thus the corresponding area, A_{face} is given by, $P_t\,L$. From substituting the values for A_{face} and A_{min} in equation 53, we get,

$$V_{max} = \frac{P_t\,V_{face}}{P_t - D_r - 2n_f\,H\,S} \tag{53}$$

where, V_{max} is the maximum air velocity in the tube bundles in m/s (Serth and Lestina 2014, p. 515).

3.14 Motor sizing

A fans performance is defined by its static pressure. The total pressure in an air stream flowing due to a fan is equal to the sum of the static and dynamic (velocity) pressures. The dynamic pressure comprises of kinetic energy in the Bernoulli's equation (Serth and Lestina 2014, p. 517). Therefore, the total pressure change across the fan is given by,

$$\Delta P_{total-fan} = \text{FSP} + \frac{\alpha_{fan}\,\rho_{fan} V_{fan}^2}{2\,g_c} \tag{54}$$

where, $\Delta P_{total-fan}$ is the total pressure change across the fan in Pa, FSP (Fans Static Pressure) is in Pa, α_{fan} is the kinetic energy correction factor for air leaving the fan, ρ_{fan} is the density of air leaving the fan in kg/m^3, V_{fan} is the velocity of air leaving the fan in m/h and g_c is the unit conversion factor (Serth and Lestina 2014, p. 518).

The velocity of air leaving the fan is given by,

$$V_{fan} = \frac{\dot{V}_{fan}}{\frac{\pi}{4}\cdot D_{fan}^2} \tag{55}$$

where, $\dot{V}_{fan}$ is the volumetric flow per fan in m^3/h and D_{fan} is the fan diameter in m (Serth and Lestina 2014, p. 526).

The break down fan power is given by,

$$\dot{W}_{fan} = \frac{\Delta P_{total-fan}\,\dot{V}_{fan}}{\eta_{fan}} \tag{56}$$

where, $\dot{W}_{fan}$ is the break down fan power in KW and η_{fan} is the total fan efficiency (Serth and Lestina 2014, p. 518).

4 THERMAL DESIGN

This section of the thesis goes through the thermal design of air cooled heat exchangers. A comprehensive commercial thermal design softwares, Aspen EDR (Exchanger Design and Rating) from Aspen Technology, Inc. is used for simulating real world input design parameters. The input parameters are obtained from the company, 'North Street Cooling Towers P Ltd.' for which this thesis is written. The output results from the software are compared with theoretical formulations.

The input process parameters to design the ACC are given in Table 1. The ACC will be used for condensing steam coming from a steam turbine. As depicted in the table, since the in-stream vapor mass fraction is 1 (pure steam), the design is made for a single stream component. A vapor mass fraction of 0 at the outlet means that full vapor condensation is required.

Table 1. Process parameters.

Tube-side stream data – Steam	Outside stream data – Air
Flow rate: 35300 kgs/hr	Dry bulb temperature: 36 ºC
Inlet temperature: 53.57 ºC	Elevation: 0 m
Vapor mass fraction (in/out): 1/0	Allowable pressure drop: 2942 Pa
Operating pressure: 14.71 kPa	Fouling factor: 0.0001 m^2 K/W
Allowable pressure drop: 0.03 kgs/cm^2	Outside tube application: dry air

4.1 Aspen EDR

This section of the thesis presents all the steps and methods for the simulation of an A- frame air cooled condenser based on the input process parameters, given in Table 1. Aspen offers a set of property methods and models based on the heat exchanger application, the process fluid and number of phases present. In depth explanation for the selection of these has been given. To arrive at an optimized condenser design, Aspen offers different design modes which are discussed in this section.

4.1.1 Run modes

In order to arrive at a fully optimized ACC design, three different run modes, ‘Design with varying outside flow’, ‘Rating/ Checking’ and ‘Simulation’ are used in the software.

Design with varying outside flow

In this mode of the software, the tube-side inlet and outlet process parameters and ambient air temperature are specified. The software during execution, varies the air-side flow rate to determine the outlet temperature of the flow. For each iteration of the exchanger configuration, the software determines the number of tubes per bundle, number of tube rows, tube length, bundles per bay, fans per bay and bays per unit. The final optimization is chosen based on the final capital and operating cost of the exchanger. In this mode, the software only offers an option of choosing a standard exchanger design with horizontal tubes for forced and induced draft configurations, as shown in Figure 26.

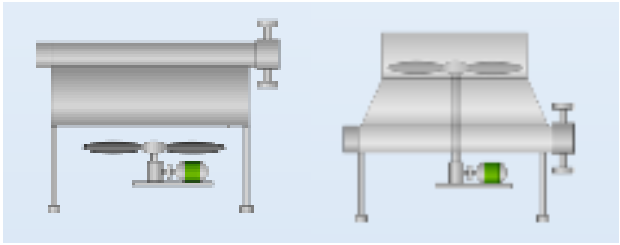

Figure 26. Standard forced draft type (left), standard induced draft type (right)

Rating/ Checking

In this mode of the software, the performance requirements in terms of the inlet and outlet process conditions are transferred from the ‘Design with varying outside flow’. Also, the specific exchanger configuration is specified in this mode. In this case the exchanger type is changed from a standard frame to A-frame. A schematic diagram of an A-frame condenser is shown in Figure 27. The software checks if the new configuration meets, the required heat exchange and maximum pressure drop requirements.

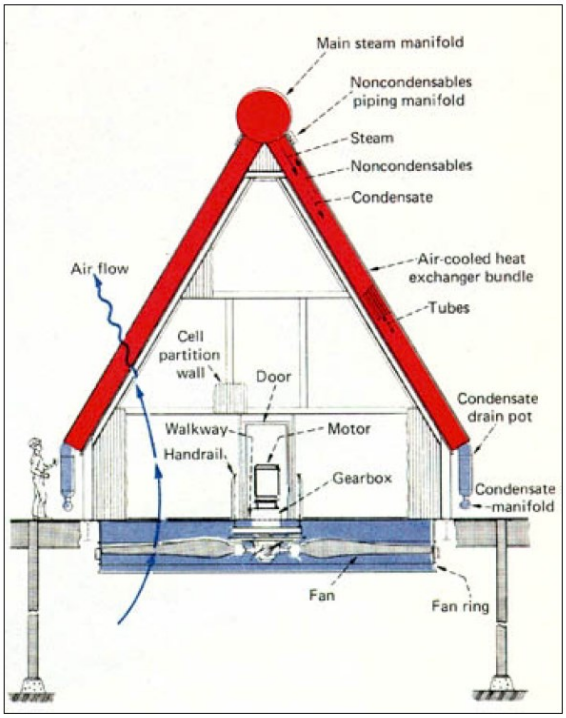

Figure 27. A-frame ACC (Larinoff, Moles and Reichhelm 1978, p. 12).

Simulation

In this mode, the specific heat exchanger configuration and some combination of stream process conditions are specified. The software predicts one or more of the unknown conditions of the two streams. There are a number of program options available in this mode to choose from, which can be chosen to simulate exact exchanger running conditions.

4.1.2 Design of a standard forced draft condenser

To begin with, the software is switched to 'Design with varying outside flow' mode and the following program settings are used, as shown in Table 2.

Table 2. Application options.

Program calculation mode	Design with varying outside flow
Tube-side application	Phase change
Outside tube application	Dry air
Simulation calculation	Set default

The run mode, ‘Design with varying outside flow’ finds the optimum geometry of an air-cooled condenser for minimum cost with the corresponding required outside air flow rate. Since a condenser condenses steam vapors into water, ‘phase change’ is chosen in the tube-side application option. Dry air is input into the air-side tube application field according to the process parameters. In this design mode only default simulation settings are available.

Process parameters form Table 1 are entered for the tube-side and air-side stream process conditions as shown in Table 3. Not all fields are compulsory to fill because in this mode the software finds an optimum solution though iterations. Pure steam has a vapor mass fraction of 1 and a fully saturated condensate has a vapor fraction of 0. The field for the condensate outlet temperature is kept blank for the software to calculate the highest temperature at which the tube-side stream will exist in a liquid phase under the specified pressure conditions.

Table 3. Process data.

Tube-side			
		In	Out
Fluid name	Steam		
Mass flow rate (total)	kg/h	35300	
Temperature	°C	53.57	
Vapor mass fraction		1	0
Operating pressure (absolute)	kPa	14.71	
Heat exchanged	kW		
Allowable pressure drop	Pa	2942	
Fouling resistance	m²-K/W	0	
Outside Tube			
Fluid name	Air		
Air/Gas mass flow rate	kg/h		
Face velocity	m/s		
Required bundle pressure drop	Pa		
		In	Out
Air/Gas dry bulb design	°C	36	
Minimum ambient temperature	°C	10	

Table 3 continues. Process data.

Operating pressure specification	Altitude and gauge pressure	
Altitude above sea level	m	0
Inlet pressure (gauge)	Pa	0
Inlet pressure (absolute)	bar	
Allowable pressure drop	Pa	200
Inlet humidity parameter	No humidity (dry air)	

The property package and method used for simulation are shown in Table 4. To calculate transport and thermodynamic properties, Aspen EDR uses property methods. These methods are a set of models and methods which are specific to the tube-side stream. (Aspen Technology 2000, p. 169.)

Table 4. Tube-side databank.

Physical property package	Aspen properties
Tube-side composition specifications	Weight flowrate or %
Aspen property method	PENG-ROB
Property model	STEAMNBS
Aspen flash option	Flash3: Vapor – liquid – liquid

Aspen property method, PENG-ROB (Peng Robinson) is chosen because water is a non-polar and real fluid. It is a recommend property method for water as shown in Figure 28, as it predicts vapor phase at any given pressure.

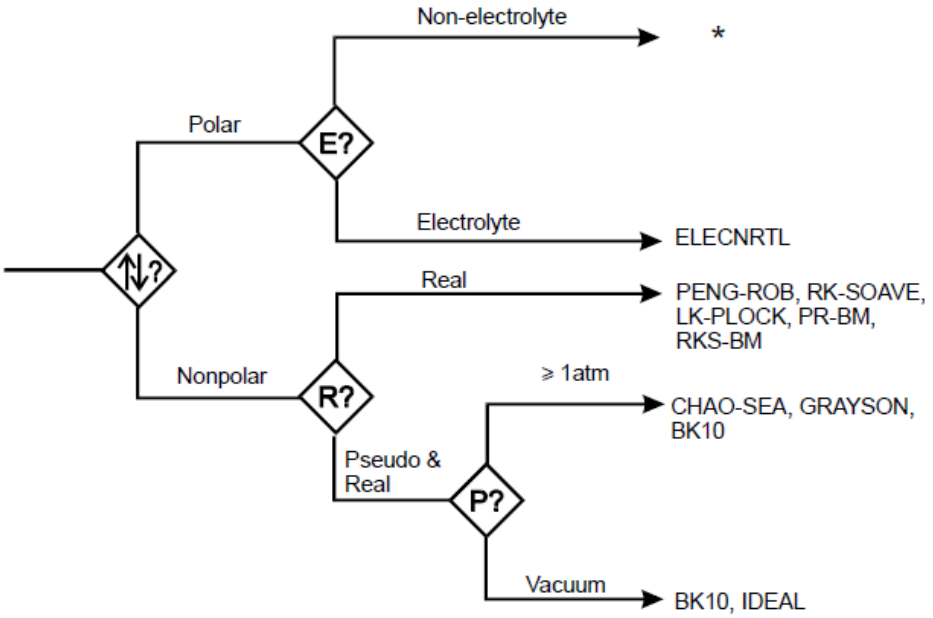

Figure 28. Flow diagram for choosing a property method (Aspen Technology 2000, p. 178).

Following are the two methods available to calculate steam and water properties.

1) STEAM-TA 1967 ASME (American Society of Mechanical Engineers) Steam Tables
2) STEAMNBS the method of the International Association of Properties of Steam

STEAM-TA method uses multiple correlations, each converging different region of Pressure-Temperature space. Since these correlation do not provide continuity at the boundaries, they cause inaccurate convergences and predict incorrect trends. Since, STEAMNBS method does not have these problems and has accurate extrapolations, it is recommended for pure water systems and for free-water calculations. Therefore, STEAMNBS method has been used in this case. (Aspen Technology 2000, p. 177.)

For one or more inlet streams, flash models in Aspen determine the thermal and phase conditions of a mixture. Based on the specifications, they perform phase equilibrium flash calculations. (Aspen Plus 2000, p. 263.)

Aspen flash option, Flash3: Vapor-Liquid-Liquid has been chosen because a single vapor outlet stream and two liquid outlet streams are produced through rigorous 3 phase vapor-liquid-liquid equilibrium calculations (Aspen Plus 2000, p. 263.) When the pressure of a liquid is equal to or greater than its bubble point and there is a sudden reduction in pressure, flashing takes place. This produces a two-phase system of vapor and liquid in equilibrium. (Shojaei, Movaghar and Dehghani 2015, p. 1485.)

Tube stream properties

The temperature range for the tube stream properties is set from 36 ºC to 53.57 ºC as shown in Figure 29. This is because 36 ºC is the lowest temperature to which the condensate can cool to, while being exposed to the inlet air. 53.57 ºC is the highest inlet steam temperature. For the highest accuracy in results, the maximum temperature points of 24 are chosen. All tube-side steam properties are calculated at these 24 temperature points corresponding to the operating pressures.

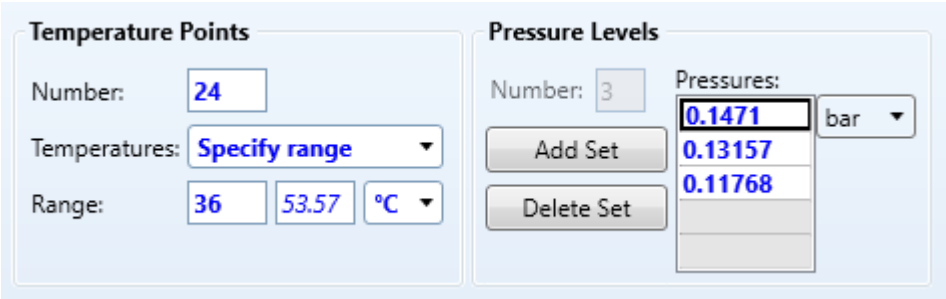

Figure 29. Tube stream temperature and pressure range.

Condenser geometry

The specifications shown in Table 5 are used in Aspen EDR. Standard industrial fin and tube sizes are chosen. Since, steam is a volumetric fluid, a large tube diameter is chosen with an intermediate fin height. This is because, the heat transfer coefficient of bare tubes is higher than the fins because there exists a decrease in the temperature difference along the fin lengths. Further a larger tube diameter keeps the pressure drop within the required operation limits.

Table 5. Condenser geometric specifications.

Tube specifications	
Tube outer / inner diameter	38.1/ 34.8 mm
Tube wall thickness	Birmingham Wire Gauge (BWG): 16
	1.65 mm
Tube material	Carbon steel
Fin specifications	
Fin type	G-finned
Fin material	Aluminum 1060
Fin frequency	433 fins per meter
Mean fin thickness	0.4 mm
Bundle specifications	
Bundle type	Staggered: Even rows to right
Transverse pitch	90 mm
Longitudinal pitch	77.94 mm
Tube layout angle	30 degrees
Unit geometry	
Tube-side to air-side flow orientation	Counter current
Angle of air-side flow	0 degrees
Tube-side flow direction	Horizontal
Fan configuration	Forced

A tube layout for a staggered tube arrangement is shown in Figure 30. In the mode ‘Design with varying outside flow’ only standard frame air cooled condensers can be designed.

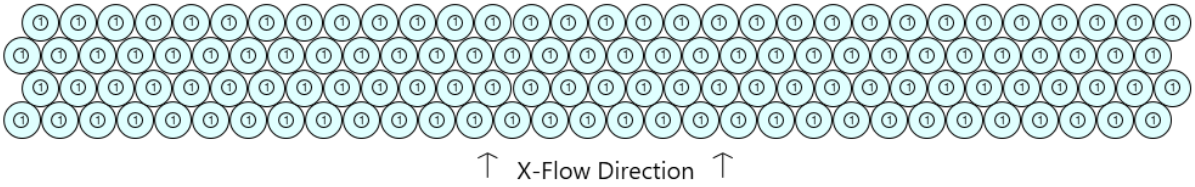

Figure 30. Staggered finned tube bundle

The design codes and standards used for simulation are shown in

Table *6*. Simulating a design using a suitable design code and material standard makes sure that all components of the ACC will not only be thermally suitable but also have mechanically durability. ANSI dimensional standard is used so that all off the shelf buy outs are easily available in the market.

Table 6. Design codes and standards.

Design code	ASME Code Sec VIII Div 1
Material standard	ASME
Dimensional standard	ANSI – American

The design limits used for simulation are given in Table 7. The number of tube passes per bundle are chose depending on the resulting tub-side Reynold's number. For a start, a single pass is tested with. The maximum air-side fluid face velocity is set to 3 m/sec because it is a practical value for conventional axial flow fans for air cooled heat exchangers.

Table 7. Design limits.

		Minimum	Maximum
Geometry limits			
Tube length	m	2	10
Tube rows deep		3	4
Tube passes per bundle		1	1
Process limits			
Tube-side fluid velocity	m/s	-	100
Outside fluid face velocity	m/s	-	3

Simulation results from the design mode are given in Table 8. The software come with a large number of bays and fans for the unit which will be impractical to manufacturing with high capital and running costs and high maintenance.

Table 8. Results from design mode.

Unit			
Bays in parallel per unit	14	A or V frame	None
Bundles in parallel per bay	2	Tube inclination	0
Fans per bay	2	Tube-side flow orientation	Counter- current
Bay width	5.7 m	Outside stream flow direction	0 deg.
Fan power	14.5 kW	Total surface area	106278.4 m^2
Bundle width	2.745 m	Fan diameter	3.657 m
Unit length	10.29 m	Plenum depth	1.463 m
Unit width	81.06 m	Ground clearance	5.4864 m
Bundle			
Tubes per bundle	90	Number of tube types	1
Tube rows per bundle	3	Tube row arrangement	Staggered
Tubes per row per bundle	30	Tube transverse pitch	90 mm
Tube passes per bundle	1	Tube row longitudinal pitch	77.94 mm
Total tube length	9.5 m	Layout angle	30 deg.
Effective tube length	9.299 m	Area ratio finned to bare	37.89
Tube sheet thickness	76.2 mm	Total surface effectiveness	0.76
Tube support width	25 mm	Bundle face area	25.5 m^2
Number of tube supports	5		

The performance data for the generated results is given in Table 9. The steam gets fully condensed at the outlet but the condenser is over-surfaced by 9%. The outlet condensate temperature is lower than the dew point of 51.98 ^oC.

Table 9. Performance data.

Design with varying outside flow		Outside		Tube-side	
Total mass flow rate	kg/h	8431560		35300	
		In	Out	In	Out
Vapor mass	kg/h	8431560	8431560	35300	0
Liquid mass	kg/h	0	0	0	35300
Vapor mass quality		1	1	1	0
Temperature	°C	36	45.97	53.57	49.04
Dew point	°C			53.57	51.98
Film coefficient	W/m^2K	1286.5		3354.7	
Pressure drop (allow./ calc.)	Pa	200/ 117		2942/1098.8	
Reynold's number		14035.19		13930.43	
Total heat exchanged		23494.6 kW			
Condenser surface area		106278.4 m^2			
Area ratio: actual/ required		1.09			

For the tube-side flow to be fully turbulent, the Reynold's number needs to be greater than 4000 (The Engineering toolBox 2017). Since the Reynold's number from Table 9 is 13930.43, the tube-side flow is fully turbulent. Therefore a single pass design is sufficient to achieve a high tube-side coefficient of heat transfer.

A plan view for a standard-frame ACC unit obtained from Aspen EDR is shown in Figure 31. It is a 14 bay unit with two fans per bay. It can be seen that each bay has two tube bundles with one outlet nozzle for each tube bundle. Not all 14 bays of the unit have been depicted in the plan view.

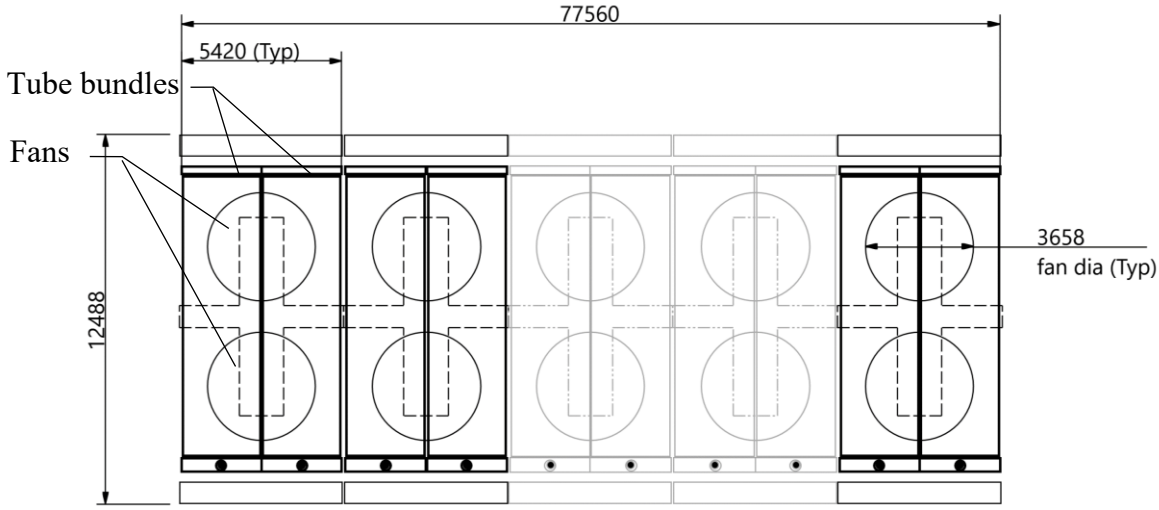

Figure 31. Plan view of the standard frame condenser.

Side view

A side view of the standard-frame ACC unit obtained from Aspen EDR is shown in Figure 32. From the figure, it can be seen that the finned tubes lie horizontal with a forced draft configuration. Underneath the two fans are two motor drives.

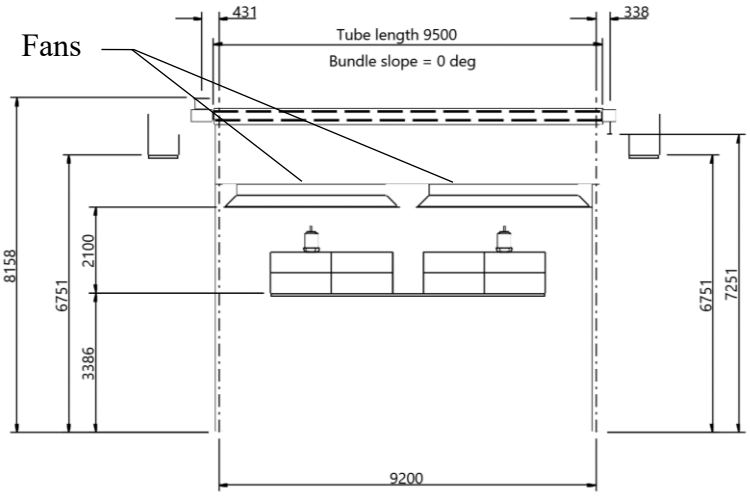

Figure 32. Side view of the standard frame condenser.

4.1.3 Design of an A-frame condenser

The software is switched to the second mode, 'Rating/ Checking' in which the standard ACC frame is changed to a suitable A-frame condenser to meet the desired process conditions. The input process parameters from Table 1 remains the same and the simulation is re-run in this mode. The new output design geometry summary is shown in Table 10. The number of

bays are reduced to 3 with an A frame type geometry. The number of bundles per bay has to be an even number, to maintain symmetry on both sides of the bay. The tube length is increased to 11.5 m to accommodate a large fan diameter with a frame angle of 60º. The tube-side flow direction is set to downwards. The rest of the tube and fin parameters remain the same as in the previous mode.

Table 10. Final design geometry summary.

Unit		Tubes	
Bays per unit	3	Tube OD/ ID	38.1/ 34.8 mm
Bundles per bay	6	Tube wall thickness	1.65 mm
Fans per bay	1	Tube length	11.5 m
Exchanger type/ angle	A frame/ 60º	Fin tip diameter	88.9 mm
Draft	Forced draft	Fin frequency	433 fins/ m
Tube-side flow direction	Downwards	Mean fin thickness	0.4 mm
Tube layout			
Number of tube/ bundle	128	Bundle type	Staggered
Tube rows deep	4	Transverse pitch	100 mm
Tube passes	1	Longitudinal pitch	86.6 mm
Tube rows per pass	4	Tube layout angle	30º

Performance data for the new simulation is shown in Table 11. The condenser comes to be slightly under surfaced, that is the area ratio is 0.99. This is because the condensate gets sub-cooled below its due point to 49.09 ºC.

Table 11. Performance data form Rating/Checking mode.

Rating/ Checking		Outside		Tube-side	
Total mass flow rate	kg/h	8267580		35300	
		In	Out	In	Out
Vapor mass	kg/h	8267580	8267580	35300	0
Liquid mass	kg/h	0	0	0	35300
Vapor mass quality		1	1	1	0
Temperature	ºC	36	45.97	53.57	49.09

Table 11 continues. Performance data form Rating/Checking mode.

Rating/ Checking		Outside		Tube-side	
Total mass flow rate	kg/h	8267580		35300	
		In	Out	In	Out
Dew point	°C			53.57	52.13
Film coefficient	W/m^2K	1277.1		2401	
Operating pressure	Pa	98652	98652	14710	13713.8
Pressure drop (allow./ calc.)	Pa	200/ 153		2942/ 996.2	
Reynold's number		13770.72		15236.41	
Total heat exchanged		23493.1 kW			
Fan diameter		10 m			
Fan power		153.76 kW/ per fan			
Condenser surface area		114945.7 m^2	Area ratio: actual/ required		0.99

4.1.4 Simulation

Simulation calculation: Outlet temperature on both sides (method 1)

This method calculates the tube and air-side outlet temperatures, the tube-side inlet temperature, pressure and flow rate, and the air-side inlet and flow rate. It follows a combined forward and backward iteration technique to get a faster converged solution.

Tube-side flow distribution

In the simulation mode of the software, the tube-side flow distribution is activated which adjusts the tube-side flowrate within each pass to equalize the tube pressure drop through each tube. This is effective in the present situations where the lower tube rows that first come in contact with the inlet air, due to greater temperature difference, condense more vapor than the other tube rows. This function in the 'Simulation' mode offers a greater accuracy than the 'Rating/ Checking' mode. The final design performance data is given in Table 12.

Table 12. Final design performance data from Simulation mode.

Simulation		Outside		Tube-side	
Total mass flow rate	kg/h	8267580		35300	
		In	Out	In	Out
Vapor mass	kg/h	8267580	8267580	35300	29
Liquid mass	kg/h	0	0	0	35271
Vapor mass quality		1	1	1	0.0008
Temperature	^oC	36	46.07	53.57	51.48
Dew point	^oC			53.57	51.48
Film coefficient	W/m^2K	1272.7		2406.6	
Operating pressure	Pa	101326	101326	14710	13706.6
Pressure drop (allow./ calc.)	Pa	200/ 148		2942/ 1003.4	
Reynold's number		13770.72		15236.41	
Total heat exchanged		23348.6 kW			
Fan diameter		10 m			
Fan power		142.124 kW/ per fan			
Condenser surface area		114945.7 m^2	Area ratio: actual/ required		1

From Table 12 it can be seen that, to achieve full condensation of the vapor stream, that is, for the outlet vapor quality to be 0, the condenser is under-surfaced, but only by a small fraction of 0.01. For most industrial applications this area ratio is acceptable because increasing the condenser surface area will further increase the capital costs for a very small increase in performance.

Final design

An isometric view of the final design is shown in figure Figure 33. The ACC unit has three bays with a single fan per bay. The schematics of steam flow across the steam manifold, distribution across the tube bundles and condensate flow are represented with arrows.

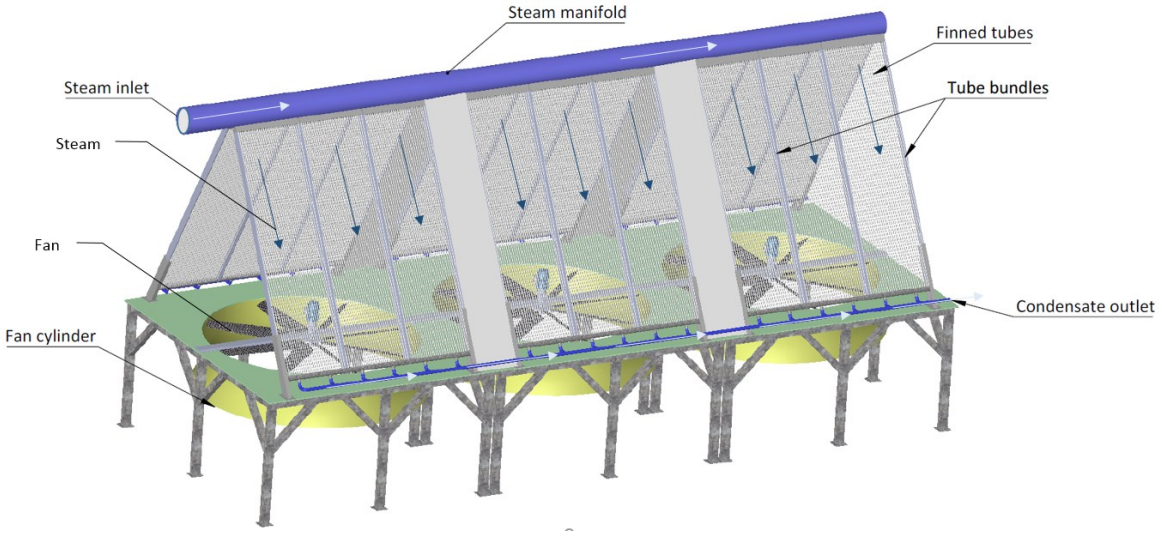

Figure 33. Isometric view of the ACC.

The side view of the ACC unit is shown in Figure 34. A single fan unit is visible in figure which is driven by a motor and a gear box mounted on top. The fan assembly is housed within a fan cylinder. A fan cylinder forms a hyperbolic shaped structure that enhances efficient air flow through the bay.

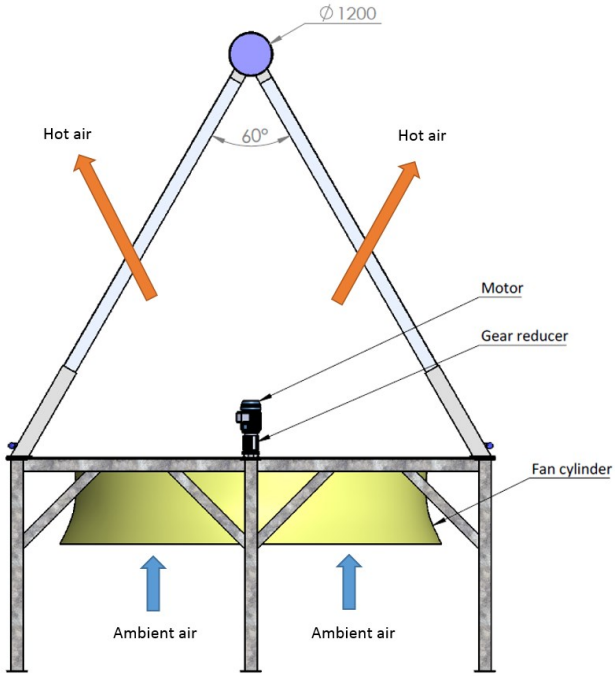

Figure 34. Side view of the ACC.

The front view of the ACC is shown in Figure 35. A human figure has been placed next to the scaled drawing of the ACC unit to give a perspective on its size.

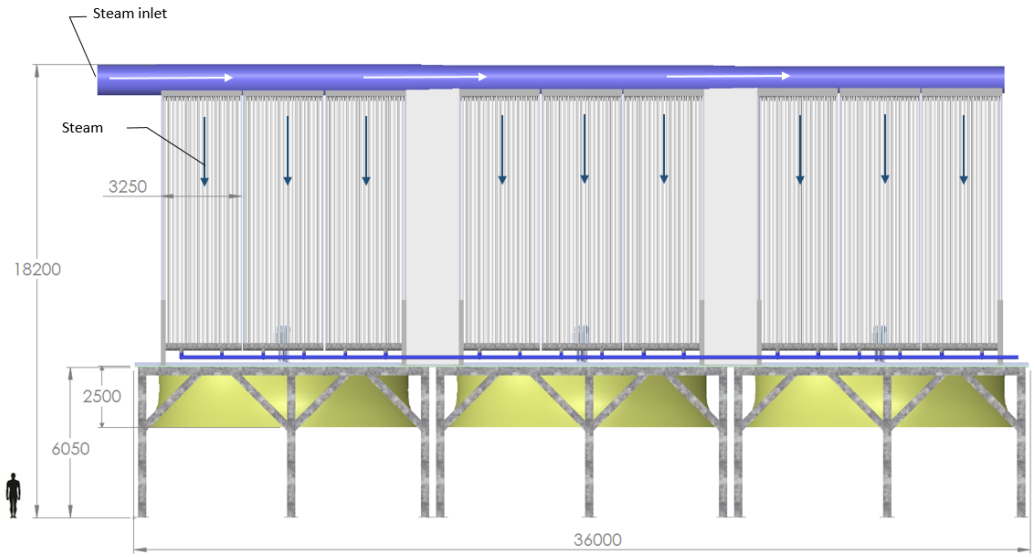

Figure 35. Front view of the ACC.

4.2 Theoretical formulations

The design of air cooled condensers is challenging because, there are infinite possibilities to choose from, as there are a number of degrees of freedom. Therefore a stepwise design procedure has to be followed to come up with a reasonable and practical design. All detailed theoretical formulations based on the 'Condenser Design Theory' are given in the appendix III of the report. The methodology involves the use of parameters including, fin sizing, exchanger type, number of heat transfer units and exchanger heat effectiveness for a single component condensing stream. It uses the classical approach of using cross flow correction factor and log mean temperature difference.

4.2.1 ACC geometry

Before the start of the design process, an appropriate condenser geometry is chosen in accordance with the application. For this particular case, since it is a steam condenser an A-type design is chosen with forced draft air flow. Also, a large tube diameter with a medium fin height is chosen. Since steam is a volumetric fluid, a manifold type header in an A-frame condenser allows for an efficient stream distribution into the inclined tube bundles. The condensate flows downwards due to gravity through D-type outlet headers into the condensate tank.

4.2.2 Design procedure

The first phase of the design procedure is to calculate the required surface area based on the overall heat transfer rate for the condensing stream. This surface area is then divided into practical bundle sizes that can be served by axial flow fans with minimum motor power ratings. The 'tube diameter', 'fin height' and 'thickness', 'tube arrangement' and the 'tube pitch' are pre-determined based on the application. The parameters that remain unknown are, 'number of tube passes', 'number of tubes', 'number of tube rows', 'tube length' and 'fan sizing and power'. Once a few preliminary parameters are set, the rest can be made to vary to obtain a suitable ACC design.

Parametric values are calculated including the 'Reynold's numbers', 'heat transfer coefficients', 'fin efficiency' and 'pressure drops' to make sure that the obtained design is capable of meeting the process requirements and is fully optimized with respect to its areal size and operating power.

The tube-side Reynold's number is determined to make sure that the tube-side stream flow is fully turbulent which helps raise the heat transfer coefficient. Fin efficiency helps determine the root diameter to fin height ratio. Pressure drops should be within the process allowable limits. The ACC specifications used for the calculations are given in Table 13.

Table 13. ACC specifications.

ACC type	
Draft type	Forced draft
Frame type	A-frame
Tube specifications	
Outer diameter of root tube, D_r	38.1 mm
Inner diameter of root tube, D_i	34.8 mm
Fin height	25.4 mm
Fin thickness	0.4 mm
Tube material	Carbon steel
Fin material	Aluminum 1060
Fin type	G- fins

Table 13 continue. ACC specifications.

Tube bundle specifications	
Bundle type	Staggered
Tube layout angle	30 degrees
Transverse pitch, P_t	95 mm
Header specifications	
Material and construction type	Carbon steel manifold type

4.3 Design optimization

In order to achieve an optimized solution, input parameters are varied as shown in Table 14. Only feasible designs which suffice the process requirements within a reasonable range of condenser surface area and fan power are reported in this section.

Table 14. Unit parameters for design optimization.

Parameters	Design 1	Design 2	Design 3	Design 4	Design 5	Design 6
Bays/ unit	3	4	3	3	3	3
Bundles/ bay	6	6	6	6	6	6
Tube OD (mm)	25.4	25.4	31.75	38.1	38.1	38.1
Tube ID (mm)	22.1	22.1	28.45	34.8	34.8	34.8
Fin height	25.4	15.875	25.4	38.1	25.4	25.4
Tubes/ bundle	250	200	140	108	132	128
Rows	5	5	4	4	4	4
Transverse pitch (mm)	80	60	90	117	100	100
Longitudinal pitch (mm)	69.28	51.96	77.94	101.32	86.6	86.6
Condenser type	A-frame		Tube layout		30^o – staggered	
Fin thickness	0.4 mm		Tube length		11. 5 m	
Fin frequency	433 fins/ m		Tube passes		1	
Fans/ bay	1		Tube thickness		1.65 mm	

Design 1

The performance data for design 1 is given in Table 15. The steam does not condense completely, though the quantity of the steam in the outlet is small which is acceptable for most scenarios.

Table 15. Performance data for design 1.

Simulation		Outside		Tube-side	
Total mass flow rate	kg/h	8431560		35300	
		In	Out	In	Out
Vapor mass	kg/h	8431560	8431560	35300	311
Liquid mass	kg/h	0	0	0	34989
Vapor mass quality		1	1	1	0.0088
Temperature	^oC	36	45.84	53.57	49.8
Dew point	^oC			53.57	49.8
Film coefficient	W/m^2K	1357.8		2217.6	
Operating pressure	Pa	101326	101326	14710	12226.4
Pressure drop (allow./ calc.)	Pa	200/ 128		2942/2483.6	
Reynold's number		7778.53		12284.4	
Total heat exchanged		23228.6 kW			
Fan diameter		10 m			
Fan power		155 kW/ per fan			
Condenser surface area		159943.6 m^2			

Design 2

The performance data for design 2 is given in Table 16. A higher rate of steam condensation takes place as compared with design 1 but at the expense of a higher total fan power. Steam condenses at a higher temperature because of a lower tube-side pressure drop.

Table 16. Performance data for design 2.

Simulation		Outside		Tube-side	
Total mass flow rate	kg/h	8267580		35300	
		In	Out	In	Out
Vapor mass	kg/h	8267580	8267580	35300	36
Liquid mass	kg/h	0	0	0	35264
Vapor mass quality		1	1	1	0.001
Temperature	ºC	36	45.93	53.57	50.57
Dew point	ºC			53.57	50.57
Film coefficient	W/m^2K	1131.7		2000.9	
Operating pressure	Pa	101326	101326	14710	12700.6
Pressure drop (allow./ calc.)	Pa	200/ 172		2942/2009.3	
Reynold's number		10186.55		11516.63	
Total heat exchanged		23408.3 kW			
Fan diameter		6.97 m			
Fan power		125.9 kW/ per fan			
Condenser surface area		99249.8 m^2			

Design 3

The performance data for design 3 is given in Table 17. From the data, this design gives a very low rate of steam condensation at the outlet.

Table 17. Performance data for design 3.

Simulation		Outside		Tube-side	
Total mass flow rate	kg/h	8267580		35300	
		In	Out	In	Out
Vapor mass	kg/h	8267580	8267580	35300	688
Liquid mass	kg/h	0	0	0	34612
Vapor mass quality		1	1	1	0.0195
Temperature	ºC	36	45.75	53.57	50.34
Dew point	ºC			53.57	50.34

Table 17 continues. Performance data for design 3.

Simulation		Outside		Tube-side	
Total mass flow rate	kg/h	8267580		35300	
		In	Out	In	Out
Film coefficient	W/m^2K	1194.1		2071.8	
Operating pressure	Pa	101326	101326	14710	12554.6
Pressure drop (allow./ calc.)	Pa	200/ 143		2942/2155.4	
Reynold's number		10247.05		15292.2	
Total heat exchanged		22985.8 kW			
Fan diameter		10 m			
Fan power		139.8 kW/ per fan			
Condenser surface area		113005.1 m^2			

Design 4

The performance data for design 4 is given in Table 18. Full steam condensation at the outlet takes place but requires a high total fan power.

Table 18. Performance data for design 4.

Simulation		Outside		Tube-side	
Total mass flow rate	kg/h	8267580		35300	
		In	Out	In	Out
Vapor mass	kg/h	8267580	8267580	35300	0
Liquid mass	kg/h	0	0	0	35300
Vapor mass quality		1	1	1	0
Temperature	°C	36	45.75	53.57	51.37
Dew point	°C			53.57	52.05
Film coefficient	W/m^2K	1594.2		2682.8	
Operating pressure	Pa	98652	98652	14710	13660
Pressure drop (allow./ calc.)	Pa	200/ 192		2942/1050	
Reynold's number		13373.56		18057.97	

Table 18 continues. Performance data for design 4.

Simulation		Outside		Tube-side	
Total mass flow rate	kg/h	8267580		35300	
		In	Out	In	Out
Total heat exchanged		23398.4 kW			
Fan diameter		10 m			
Fan power		192.8 kW/ per fan			
Condenser surface area		172348.8 m^2			

Design 5

The performance data for design 5 is given in Table 19. Full steam condensation at the outlet takes place, at a low total fan power but with a larger condenser surface area.

Table 19. Performance data for design 5.

Simulation		Outside		Tube-side	
Total mass flow rate	kg/h	8267580		35300	
		In	Out	In	Out
Vapor mass	kg/h	8267580	8267580	35300	0
Liquid mass	kg/h	0	0	0	35300
Vapor mass quality		1	1	1	0
Temperature	ºC	36	46.13	53.57	49.88
Dew point	ºC			53.57	52.18
Film coefficient	W/m^2K	1252.4		2379.6	
Operating pressure	Pa	101326	101326	14710	13744.8
Pressure drop (allow./ calc.)	Pa	200/ 140		2942/ 965.2	
Reynold's number		13353.43		14774.7	
Total heat exchanged		23460.3 kW			
Fan diameter		10 m			
Fan power		135.14 kW/ per fan			
Condenser surface area		118537.7 m^2			

Design 6

The performance data for design 6 is given in Table 20. A small very amount of uncondensed steam remains at the outlet but the condensate temperature is the highest.

Table 20. Performance data for design 6.

Simulation		Outside		Tube-side	
Total mass flow rate	kg/h	8267580		35300	
		In	Out	In	Out
Vapor mass	kg/h	8267580	8267580	35300	29
Liquid mass	kg/h	0	0	0	35271
Vapor mass quality		1	1	1	0.0008
Temperature	ºC	36	46.07	53.57	51.48
Dew point	ºC			53.57	51.48
Film coefficient	W/m^2K	1272.7		2406.6	
Operating pressure	Pa	101326	101326	14710	13706.6
Pressure drop (allow./ calc.)	Pa	200/ 148		2942/1003.4	
Reynold's number		13770.72		15236.41	
Total heat exchanged		23348.6 kW			
Fan diameter		10 m			
Fan power		142.12 kW/ per fan			
Condenser surface area		114945.7 m^2			

4.3.1 Design comparison

A design comparison of the six design outputs is shown in Figure 36. Only those designs that suffice the process parameters have been compared here. The comparison takes into account the outlet vapor quality, total condenser surface area, total fan power and condensate temperature. To get maximum condensation at the outlet, the outlet vapor quality should be as low as possible. The condenser surface area and total fan power should be as low as possible because they are indicative of the capital and running costs respectively. The condensate outlet temperature should be as high as possible because it will help save energy when recirculated back to the boiler to produce steam to feed the steam turbine.

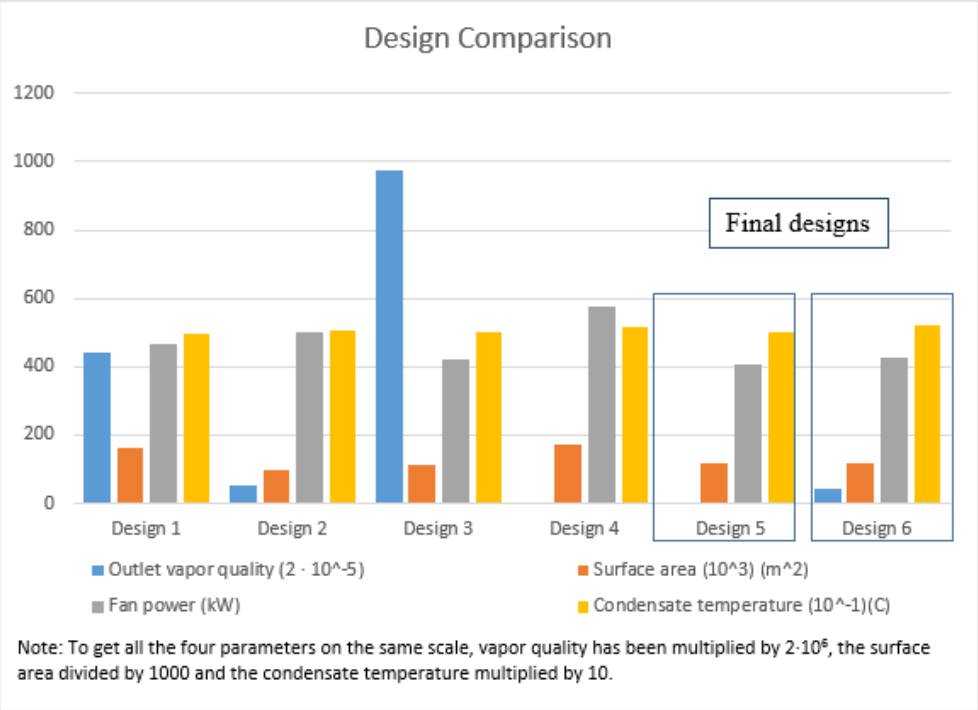

Figure 36. Design comparison

Final designs selection

Two of the six designs, compared in Figure 36 have been chosen. They both have some advantages and drawbacks over each other which have been discussed in the following section.

Design 5

This design is chosen because full steam condensation takes place at the lowest fan power. A lower fan power is required because this design is over-surfaced by 2% because of which a lower *FSP* (Fan Static Pressure) of 140 Pa is required. This results in a lower fan power of 135.14 kW. On the downside since the condenser is over surfaced, sub-cooling of the condensate takes place, down to a temperature of 49.88 ºC.

Design 6

This design is chosen for its highest outlet condensate temperature of 51.48ºC and a lower condenser surface area. On the downside since the condenser is under surfaced by 1%, a higher *FSP* of 148 Pa is required. This results in a higher fan power of 142.12 kW than in design 5. Also the vapor quality at the outlet is 0.0008, which is a small amount of vapor mass of 29 kg/hr. Since the vapor quality is very low, the design is acceptable.

5 RESULTS AND ANALYSIS

The final design results from optimization are compared with the theoretical formulation results, which are given in Table 21. The data for output parameters given in the table for designs 5 and 6 are available in appendices I and II and for theoretical formulations in appendix III.

Table 21. Output comparison.

Design parameter	Aspen EDR (Design 5)	Aspen EDR (Design 6)	Theoretical formulations
Mean temperature difference, ΔT_m (°C)	10.11	10.24	10.99
Total rate of heat transfer, $\dot{q}_{total}$ (kcal/h)	20,172,236	20,076,139	20,051,899
Fin surface area, A_{fins} (m^2)	118,537.7	114,945.7	118,677.2
Air mass flow rate, $\dot{m}_{air}$ (kg/h)	8,267,580	8,267,580	8,285,908
Tube-side Reynold's number, $Re_{tube\ side}$	14,774.7	15,236	13,943
Air-side Reynold's number, $Re_{air\ side}$	13,353	13,770	14,397
Tube-side Prandtl number for condensate, Pr_{cond}	3.55	3.45	3.461
Air-side Prandtl number, $Pr_{air\ side}$	0.71	0.71	0.7123
Tube-side heat-transfer coefficient, $h_{tube\ side}$ (W/m^2K)	2379.6	2406.6	2437.9
Fin efficiency, η_w	0.76	0.76	0.768

Table 21 continues. Output comparison.

Design parameter	Aspen EDR (Design 5)	Aspen EDR (Design 6)	Theoretical formulations
Total pressure drop for tube-side fluid, $\Delta P_{tube\ side}$ (Pa)	1,239	1,426.9	1,560
Total air-side pressure loss, $\Delta P_{air\ side}$ (Pa)	140	148	117.7
Fan power (KW)	135.13	142.12	152.8

The designs obtained through Aspen EDR and theoretical formulations are very similar as shown in Table 22. The unit and bundle specifications given in the table for designs 5 and 6 are available in appendices I and II and for theoretical formulations in appendix III.

Table 22. Design comparison.

Unit specifications	Aspen EDR (Design 5)	Aspen EDR (Design 6)	Theoretical formulations
Number of bays	3	3	3
Tube bundles per bay	6	6	6
Fans per bay	1	1	1
Fan diameter	10	10 m	10 m
Bundle specifications			
Tube length	11.5 m	11.5 m	10.25 m
Bundle width	3.35 m	3.25 m	3.42 m
Tube transverse pitch	100 mm	100 mm	95 mm
Number of tubes per bundle	132	128	144
Number of rows	4	4	4
Tube passes	Single	Single	Single

The most critical physical properties of the tube side vapor-liquid stream, which affect condenser performance have been discussed below,

Vapor fraction along the tube lengths for each row

In an air cooled heat exchanger, the tubes in the lower rows get exposed to the inlet air when it is at its lowest temperature. The air temperature rises as it flows through the tube bundles. Figure 37 which corresponds to design 6, shows the vapor fraction of the tube-side stream as it flows along the tube lengths. Since the tubes in row 1 get exposed to the lowest air temperature, the steam condenses the fastest at the least distance of its travel along the tube bundle length. On the other hand, since the tubes in row 4 get exposed to already heated air, the steam requires a long time to condense and a fraction of the stream remains in the vapor state. From the overall summary given in the appendix II, it can be seem that there exists a very small amount (29 kg/h) of steam in the tube-side outlet. This small value is acceptable in most industrial scenarios because in order to fully condense a stream, the condenser surface area will have to be increased unnecessarily increasing the capital and running costs.

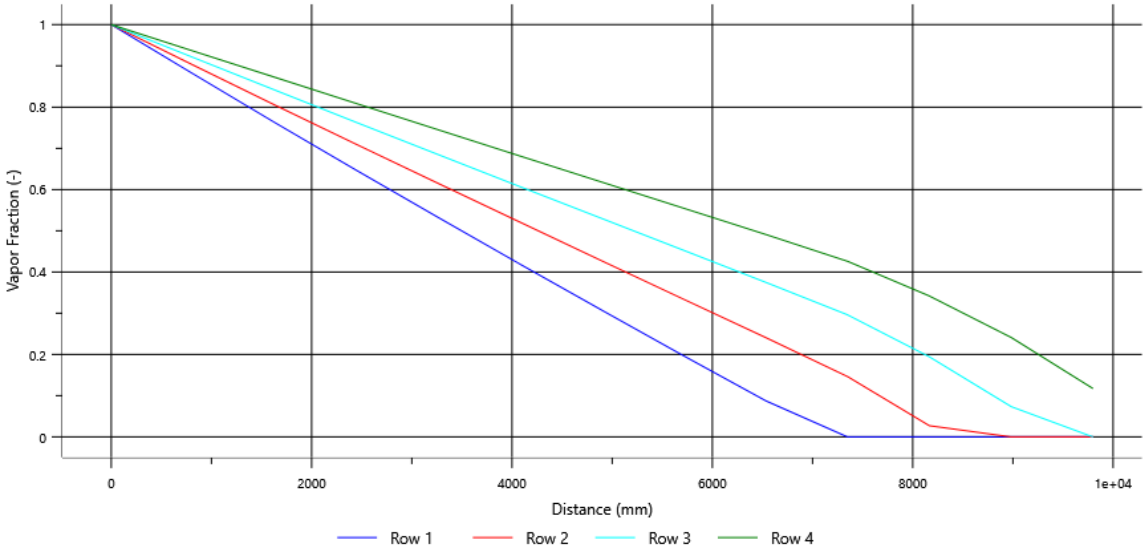

Figure 37. Vapor fraction along the tube lengths for each row.

Inlet air temperature along the tube lengths for each row

The inlet air temperature for each tube row is shown in

Figure **38**. It can be seen from the graph that air warms up as it passes through the tube bundles. Also, its temperature is lower at greater tube lengths as the tube-side stream cools down along the tube length.

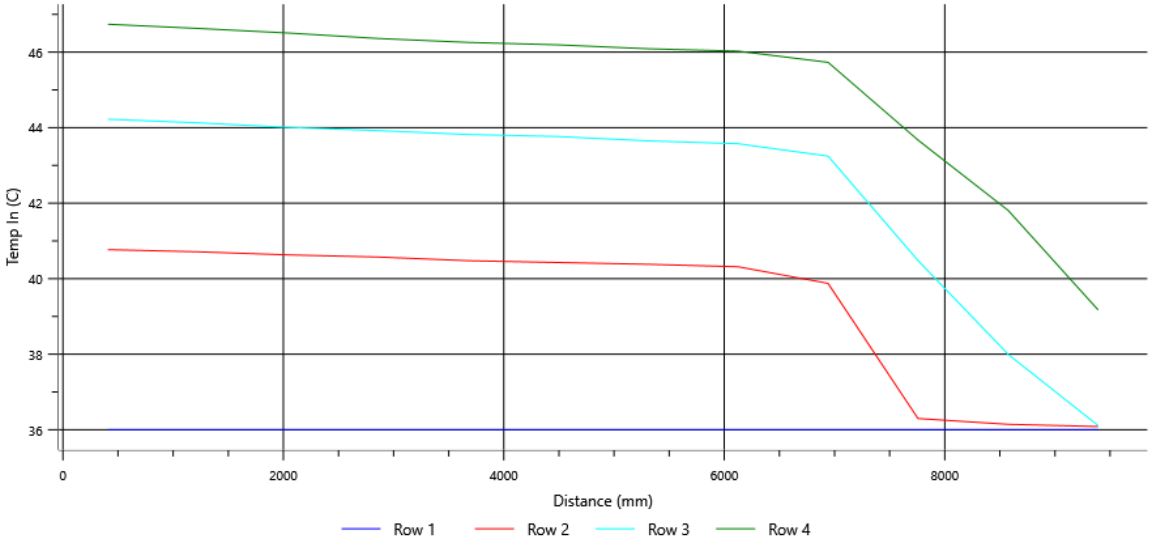

Figure 38. Inlet air temperature along the tube lengths for each row.

Pressure drop along the tube lengths for each row

When steam condenses into water, there is a reduction in volume which leads to a pressure drop. Since rapid condensation occurs in tubes in the lower rows as compared with the tubes in the higher rows, there is a greater pressure drop in the lower rows as shown in Figure 39. The final pressure vales at the tube outlets in all rows reach the approximately the same pressure value.

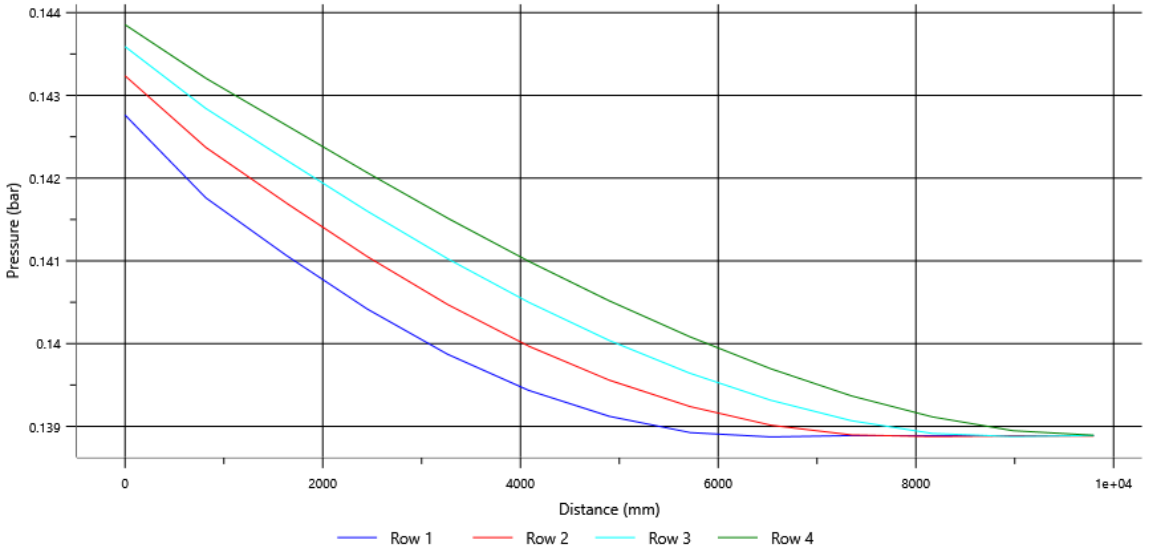

Figure 39. Pressure drop along the tube lengths for each row.

Vapor flow rate along the tube lengths for each row

At the inlet of the tubes, there exists a vapor fraction of 1 since there is 100 % saturated steam. As the steam vapors flow down the tubes they condense into a liquid and hence the vapor fraction decreases. The fastest decrease in vapor fraction occurs in row 1 as it reaches a vapor fraction of 0 at a tube length of 6.4 m. Subsequently, the rate of condensation along the tube lengths decreases in higher tubes as shown in Figure 40. A small amount of uncondensed steam remains at the outlet of row four.

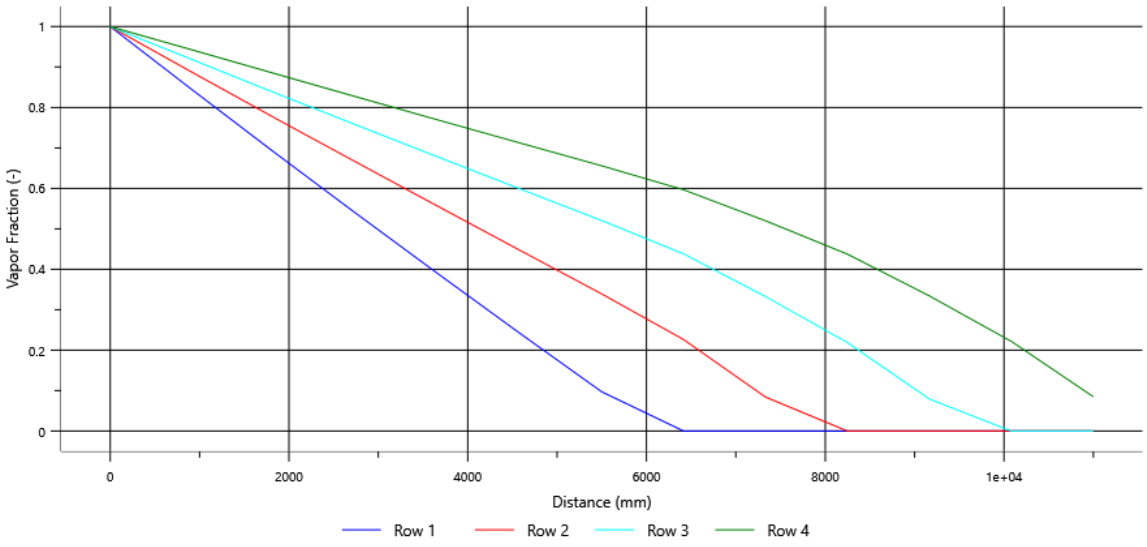

Figure 40. Vapor flow rate along the tube lengths for each row.

Sub-cooling in tubes

Sub-cooling in the tubes in rows 1, 2 and 3 takes place as shown in Figure 41. This is because the condensate keeps getting exposed to the cooling air. The points at which sub-cooling takes places in each row, correspond with the points at which condensation completes.

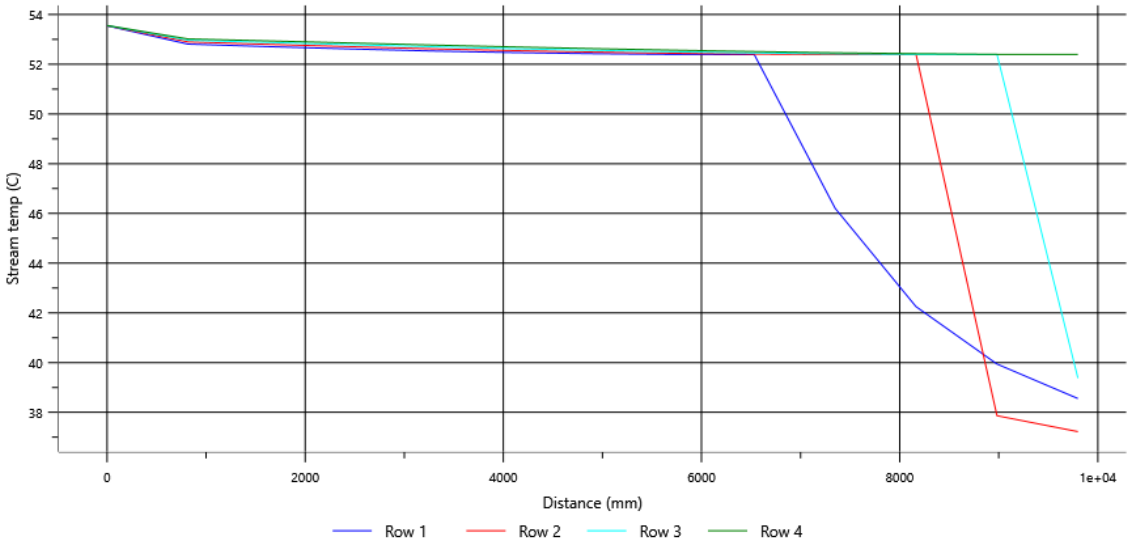

Figure 41. Sub-cooling in tubes.

Variation in the heat transfer coefficients along the tube lengths for each row

The tube-side heat transfer coefficient is a function of the temperature difference between the hot (steam) and the cold medium (ambient air) and Reynold's number for the stream flow. The coefficient, $h_{tube\ side}$ increases with the increase of the aforementioned. This can be explained through Figure 42. At distance zero, there exists the greatest temperature difference because of which, $h_{tube\ side}$ starts off with a high value. As the tube-side stream accelerates under gravity, its Reynold's number increases and so $h_{tube\ side}$ is the maximum at about 800 mm of the tube length. After this point the coefficient decreases as the stream cools down and so the temperature difference reduces, thereby constantly reducing the coefficient along the tube length.

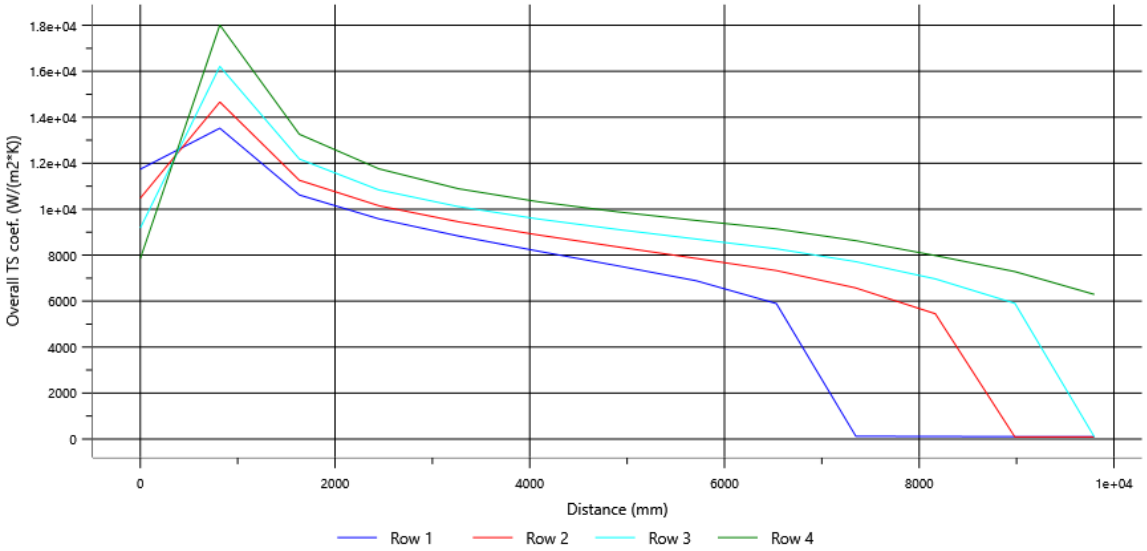

Figure 42. Variation in the heat transfer coefficients along the tube lengths, for each row.

6 CONCLUSION

In the thesis, thermal design and optimization of ACCs was performed on process parameters provided by North Street Cooling Towers P Ltd. For the particular given requirements the thesis involved, selecting the most suitable ACC type, design configuration, material of construction and parametric design and optimization. All design results were obtained from Aspen EDR which were validated through, theoretical formulations based on condenser design theories. Six suitable designs which would suffice the process requirements were obtained through software simulations by varying the crucial input parameters. Off these two designs were chosen based on the outlet vapor quality, condensate temperature, condenser surface area and fan operating power.

Thermal optimization of ACCs is based on their thermal-hydraulic performance which represents the relationship between the total heat exchanged, pressure drop and the condenser surface area. In the project, a comprehensive design methodology to obtain an effective thermal design for ACCs through Aspen EDR and theoretical formulations has been established. The methodologies include ways to calculate the condenser surface area, the number of finned tubes, total fan power, tube-side and air-side heat transfer coefficients, pressure drops and condenser frame selection.

The results obtained from Aspen EDR and theoretical formulations are within the acceptable range. Since, steam is a volumetric fluid it is necessary to have large tube diameters to have pressure drop within the allowable range. The heat transfer coefficient of bare tubes is higher than the fins because there exists a decrease in the temperature difference along the fin length. Therefore, it makes more sense to have a large inner tube diameter of 34.8 mm and medium fin height of 25.4 mm for this application. This is because there is not a large temperature difference between the ambient air and tube-side fluid temperature. This makes the tube bundles smaller and so the number of fans required to cover the face area. This in turn helps in saving capital (size of the ACC) and running costs (fan power).

Since the tube-side Reynold's number in all designs is well above 4000, the fluid flow is turbulent and hence the corresponding heat transfer coefficients are optimized as per the

design principles. On the other hand the tube-side stream velocity increases with the increase in pressure drop (Bernoulli's effect). But this increase in pressure drop is limited by the process requirements and hence the tube diameters and numbers are calculated not to breach this limit. This is because tube diameter is inversely proportional to the fluid velocity.

For the given requirements, an A-frame, three bay condenser unit comes to be the most efficient design. Each bay is serviced by a single 10 m diameter fan. This gives a good bundle face area coverage. Having large bays and a lower number of fans decreases capital and maintenance costs.

The higher is the condenser operating pressure, the higher is the condensation dew point. Since design 6 has the highest operating pressure of 13,706.6 Pa, the corresponding dew point is the highest, which is 51.48^{o}C. This is the highest across all designs.

In the thesis A-framed ACCs have been focused on, but the devised design methodologies can be used for other ACC configurations as well. Since the first development of ACCs, the industry has seen a continuous improvement in terms of both thermal design and performance capabilities. Currently from a maintenance point of view, corrosion and fouling are still major challenges. This can be solved through the development of new types of finned tubes, manufactured from newer materials.

LIST OF REFERENCES

Aspen Technology. 2000. Aspen Plus ® Aspen Plus User guide [web document]. February 2000 [Referred 19.12.2016]. Version 10.2. Available: https://web.ist.utl.pt/ist11038/acad/Aspen/AspUserGuide10.pdf.

Benchmark Power International. 2016. Home [web document]. Published 2016. [Referred 22.3.2017]. Available: http://www.benchmarkpowerintl.org.

Brighthub Engineering. 2017. Air Cooled Condensers or Dry Cooling Tower: Steam or Steam Power Plant Water Usage [web document]. Published 2016. [Referred 6.3.2017]. Available: http://www.brighthubengineering.com/power-plants/64903-steam-power-plant-condenser-cooling-part-three-the-air-cooled-condenser/#imgn_0.

Busch, D., Harte, R., Krätzig, W. and Montag, U. 2002. New natural draft cooling tower of 200 m of height. Engineering Structures, 24: 12. P. 1509-1521.

Butterworth, D. 1974. CP2: Condensate Film Resistance on Vertical Surfaces (including tubes). AERE Harwell: Engineering Sciences Division. P. 1-4.

Butterworth, D. 1980. AM3: Airside Pressure Drop for Staggered and In-Line Arrays of Finned Tubes. AERE Harwell: Engineering Sciences Division. P. 1-4.

De.Kelvion. 2017. Rippenrohre [web document]. Published 2017. [Referred 5.3.2017]. Available: https://de.kelvion.com/de/produkte/luftgekuehlte-waermetauscher/rippen-rohrluftkuehler/rippenrohre.

Echarte, R. 1981. AM11: Cross Flow Correction Factors for Temperature Difference. Bahia Blanca, Argentina: Engineering Sciences Division P. 1-9.

Farrant, P. 1995. A fresh approach to designing air cooled heat exchangers. AERE Harwell: HTFS Heat Transfer Research. P. 1-9.

Ganguli, A., Tung, S. and Taborek, J. 1985. Parametric study of air-cooled heat exchanger finned tube geometry. Proceedings of the 1985 Symposium on National Heat Transfer Conference, Denver, CO, USA. AIChE Series. Pp. 122-128.

Hamon. 2016. Fan Assisted Natural Draft cooling towers [web document]. Published 2016. [Referred 26.10.2016]. Available: http://www.hamon.com/en/cooling-systems/wet-cooling-systems/natural-draft-cooling-towers/fan-assisted-natural-draft.

Hamon. 2017. Air Cooled Condensers [web document]. Published 2017. [Referred 3.3.2017]. Available: http://www.hamon.com/index/cms/page/air-cooled-condensers/lang/en.

Hawkins, G. 2013. Process Engineering Guide: Air Cooled Heat Exchanger Design [web document]. N.d. [Referred 27.12.2016]. Available: https://www.academia.edu/3641527/Air_Cooled_Heat_Exchanger_Design.User name and password needed.a fresh

Henry, J. 1995. [Chapter 1:] Heat Transfer in ACHEs. In: Aspen HTFS Handbook. Amsterdam: Kellog Continental B.V. Pp. 7-14.

Hoyle, D. 1985. [Chapter 3:] Airside Heat Transfer Coefficients for Staggered and In-Line Arrays of Finned Tubes. In: Aspen HTFS Handbook. Amsterdam: Kellog Continental B.V. Pp. 25-28.

Kelvion. 2017. Aéroréfrigérants [web document]. Published 2017. [Referred 5.3.2017] Available: https://fr.kelvion.com/fr/produits/echangeurs-avec-tubes-a-ailettes/aerorefrigerants.

Kraus, A., Aziz, A. and Welty, J. 2001. Extended surface heat transfer. New York: John Wiley & Sons, Inc. 1073 p.

Kröger, D. 2004. Air-Cooled Heat Exchangers and Cooling Towers: Thermal-Flow Performance Evaluation and Design, Vol. 1. Tulsa: PennWell Corporation. 502 p.

Larinoff, M., W. Moles and Reichhelm, R. 1978. Design and Specification of Air- Cooled Steam Condensers. Huston: Hudson Products Corporation. 20 p.

Lee, S., Ralston, T. and McNaught, J. 2013. Design an A-Framed Vacuum Steam Condenser Using Aspen Air Cooled Exchanger. Massachusetts: Aspen Technology, Inc. 18 p.

McHugh, S. and Chapple, S. 1999. Specify the right fin type for air-cooled heat exchangers. Hydrocarbon Processing. Pp. 67-72.

McNaught, J. and Walker, I. 1987. Heat transfer during gravity-controlled filmwise condensation in vertical condensers. Proceedings of 1987 Symposium on HTFS Research, 743. Pp. 1-4.

Mendrinos, D., Kontoleontos, E. and Karytsas, C. 2006. Geothermal Binary Plants: Water Or Air Cooled. Centre for Renewable Energy Sources. Pp. 1-2.

Mohr, C., Mines, G. and Bloomfield, K. 2001. Continual Removal of Non-Condensable Gases for Binary Power Plant Condensers. Geothermal Resources Council Transactions, 25: 1. Pp. 1-1.

Mukherjee, R. 2007. Practical thermal design of air-cooled heat exchangers. Redding: Begell House, Inc. 151 p.

Palen, J. 2006. [Chapter 8:] Heat Exchangers, Vaporizers, Condensers Typographical. In: Engineer's Handbook: Mechanical Energy and Power. 3rd Edition. [Hoboken:] John Wiley & Sons, Inc. Pp. 295-334.

Paffel, K. 2016. Removal of non-condensable gases, air is critical in a steam system | Plant Engineering [web document]. Published 2016. [Referred 28.10.2016]. Available: http://www.plantengineering.com/single-article/removal-of-non-condensable-gases-air-is-critical-in-a-steam-system/79fa6a7fd7616f5cce50120f709d8d2c.html

Pat. US 4045961. 1977. Control of freezing in air-cooled steam condensers. The Lummus Company, Schoonman, W. Appl. US 591677, 1975-06-30. Publ. 1997-08-06. 2 p.

Price, B., Russel, F., Morgan D. and Kramer. J. 2004. Engineering Data Book. 12th Edition. Tusla: Gas Processors Suppliers Association. 821 p.

Roetzel, W. and Nicole, F.J.L. 1975. Mean temperature difference for heat exchanger design a general approximate explicit equation. J. Heat Transfer, 97: 1. Pp. 5−8.

Salemtube. 2017. Helical High and Extruded Finned Tube [web document]. Published 2017. [Referred 5.3.2017]. Available: http://www.salemtube.net/helical-high-and-extruded-finned-tube.

Serth, R. and Lestina, T. 2014. Process Heat Transfer: Principles, Applications and Rules of Thumb. 2nd Edition. San Diego: Academic Press. 609 p.

Stewart, M. and Lewis, O. 2013. Heat exchanger equipment field manual. Waltham: Gulf Professional Pub. 461 p.

The Engineering ToolBox. 2017. Laminar, Transitional or Turbulent Flow [web document]. Published 2017. [Referred 9.2.2017]. Available: http://www.engineeringtoolbox.com/laminar-transitional-turbulent-flow-d_577.html.

U.S. Department of Energy. 1992. DOE Fundamental Handbook Thermodynamics, Heat Transfer and Fluid Flow [web document]. June 1992 [Referred 02.01.2017]. Volume 1 of 3. Available: https://energy.gov/sites/prod/files/2013/06/f2/h1012v1.pdf.

Virids. 2017. Home - Viridis [web document]. Published 2017. [Referred 5.3.2017]. Available: http://viridisperunding.com.

Wilber, K. 2005. Air-Cooled Condenser Design, Specification, and Operation Guidelines. Santa Rosa: Electric Power Research Institute. 176 p.

Wurtz, W. 2008. Air-cooled condensers eliminate plant water use [web document]. POWER Magazine. [Referred 26.10.2016]. Available: http://www.powermag.com/air-cooled-condensers-eliminate-plant-water-use.

All condenser data and specification sheets for design 5 are given in Appendix I.

Condenser specification sheet from Aspen EDR, corresponding to design 5.

Air-Cooled Heat Exchanger Specification Sheet

Company:										
Location:										
Service of Unit:		Our Reference:								
Item No.:		Your Reference:								
Date:	Rev No.:	Job No.:								
Size & Type	12.1464	/ 63	m	Type	Forced		Number of Bays		3	
Surf/Unit-Finned Tube		118537.7	m²	Bare area/bundle		173.8	m²	Ratio (Total/Bare)		37.89
Heat exchanged		23460.3	kW		MTD, Eff		10.11	°C		
Transfer Rate-Finned	16.8	Bare, Service		638.1	Clean		689.2	kcal/(h-m²-C)		
PERFORMANCE DATA - TUBE SIDE										
Fluid Circulated		Steam					In	/	Out	
Total Fluid Entering	kg/h	35300		Density, Liq	kg/m³			/	987.82	
		In	/ Out	Density, Vap	kg/m³		0.1	/		
Temperature	°C	53.57	/ 49.88	Specific Heat, Liq	kJ/(kg-K)			/	4.191	
Liquid	kg/h	0	/ 35300	Specific Heat, Vap	kJ/(kg-K)		1.884	/		
Vapor	kg/s	9.8056	/ 0	Therm. Cond, Liq	W/(m-K)			/	0.6431	
Noncondensable	kg/s	0	/ 0	Therm. Cond, Vap	W/(m-K)		0.0201	/		
Steam	kg/s		/	Freeze Point	°C					
Water			/	Bubble / Dew point	°C		51.77	/	53.57	
Molecular wt, Vap		18.0151	/ 18.0151	Latent heat	kJ/kg					
Molecular wt, NC				Inlet pressure (abs)	Pa		14710			
Viscosity, Liq	mPa-s		/ 0.5452	Pres Drop, Allow/Calc	Pa		2942	/	1239	
Viscosity, Vap	mPa-s	0.0102	/	Fouling resistance	m²-K/W		0			
PERFORMANCE DATA - AIR SIDE										
Air Quantity, Total		8267580	kg/h	Altitude		0	m			
Air Quantity/Fan		670.312	m³/s	Temperature In		36	°C			
Static Pressure		140	Pa	Temperature Out		46.13	°C			
Face Velocity	3.03 m/s	Mass velocity	3.46 kg/s/m²	Design Ambient		10	°C			
DESIGN-MATERIALS-CONSTRUCTION										
Design/Vac./Test Pres	1	/ /	bar	Design temperature	200 °C					
TUBE BUNDLE		**Header**		**Tube**						
Size	m 12.1464	Type	Manifold	Material	Carbon Steel					
Number/bay	6	Material	Carbon Steel	Specifications						
Tube Rows	4	Passes	1	OD	38.1	Min Thk.	1.65	mm		
Arrangement		Plug Mat.		No./Bun	132	Lng	11.5	m		
Bundles	6 par	Gasket Mat.		Pitch	100 / 86.6	30	Degrees			
Bays	3 par	Corr. Allow.	mm	**FIN**						
Bundle frame		Inlet nozzle (1)	501.65 mm	Type	G-finned					
MISCELLANEOUS		Outlet nozzle (1)	33.99 mm	Material	Aluminum 1060					
Struct. Mount.		Special Nozzles		OD	88.9	Tks	0.4	mm		
Surf.Prep		Rating	Program	No. 433	#/m	Design Temp	°C			
Louvers		TI	PI	Code	ASME Code Sec VIII Div 1					
Vibration Switches		Chem Cleaning		Stamp	Yes	Specs				
MECHANICAL EQUIPMENT										
Fan,Mfr., Model		Driver, Type	Program	Speed Reducer, Type						
No./Bay	1 RPM	Mfr.		Mfr.&Model						
Dia.	10 m Blade(s)	No./Bay		No./Bay						
Pitch	Angle	RPM		Rating	hp					
Blade(s)	Hub	Enclosure		Ratio						
hp/Fan	135.136kW MinAmb	V/Phase/Hz	/ /	Support						
Control Action on Air Failure-				Louvers						
Degree Control of Outlet Process Temperature										
Recirculation				Steam Coil	No					
Plot Area	m²	Drawing No.		Wt.Bundle	7681.1	Wt. Unit	138260	kg		
Notes:										

Design summary from Aspen EDR, corresponding to design 5.

Unit Length/Width/Height	12.1464	/	63	/	0.3464	m		Tube inclination			-59.99999
Baysperunit	3	Bundles per bay	6	Tube Rows	4	Passes	1	X-side flow direction	60		Degrees
Staggered-even rows to right								Tube flow orientation	[1-pass crossflow]		
Total surface	118537.7	Ext surface/bundle	6585.4	Bare/Bundle	173.8	m²		Ratio (Total/Bare)			37.89

Simulation	Performance of the Unit									
		Tube Side		X-Side		Heat Transfer Parameters				
Process Data		In	Out	In	Out	Total head load	kW		23460.3	
Total Flow	kg/h	35300		8267580		Effective MTD	°C		10.11	
Gas				8267580	8267580	Actual/Reqd area ratio(dirty/clean)		1	/	1.08
Vapor		35300	0							
Liquid		0	35300	0	0	Coef/Resist (Bare)	W/(m²-K)	m²-K/W	%	
Cond./Evap.		35300		0		Tube side film	2379.6	0.00042	31.18	
Temperature	°C	53.57	49.88	36	46.13	Tube side fouling		0	0	
Quality		1	0			Tube wall	34584.4	3E-05	2.15	
Humidity ratio						Outside fouling	10000	0.0001	7.42	
Pressure (abs)	Pa	14710	13471			Outside film	1252.4	0.0008	59.25	
	Pa			101326	101326	Overall fouled	742.1	0.00135		
DP		1239		140		Overall clean	801.5	0.00125		
Velocity	m/s	44.31	0	5.8	5.99					

Liquid Properties			Tube Side Pressure Drop	Pa	%
Density	kg/m³	987.82	Inlet nozzle	178.3	14.39
Viscosity	mPa-s	0.5452	Inlet header	157.4	12.7
Specific heat	kJ/(kg-K)	4.191	Inside tubes	629.5	50.81
Th Cond	W/(m-K)	0.6431	Across pass	0	0
Surface	N/m		Other header	0	0
Vapor Properties			Outlet nozzle	273.8	22.1
Density	kg/m³	0.1	1.14	1.11	Outside Pressure Drop	Pa	%
Viscosity	mPa-s	0.0102	0.0189	0.0193	Ground clearance	0	0
Specific heat	kJ/(kg-K)	1.884	1.007	1.008	Fan inlet	12	7.95
Th Cond	W/(m-K)	0.0201	0.027	0.0277	Bundle	144	91.7
Two-Phase Properties					Louvers	0	0
Latent	kJ/kg				Steam Coil	0	0
Molecular weight		18.0151		28.96	Plenum	9	5.55

Heat Transfer Parameters					Heat Load	kW
Reynolds No. vapor	14774.7		13353.43	13035.34	Vapor	15.7
Reynolds No. liquid		276.94			Cond./Evap	23328.6
Prandtl No. vapor	0.96		0.71	0.7	Liquid	116
Prandtl No. Liquid		3.55			Input/Actual duty ratio	1

Tubes / Fin			Last row number		4				
Tubes per bundle		132	Tube OD / ID	mm	38.1	/	34.8	/	/	/
Tube material		Carbon Steel	Fin type		G-finned				
Length effective	m	11	Fin material		Aluminum 1060				
Length actual	m	11.5	Fin tip diameter	mm	88.9				
Transverse pitch	mm	100	Fin thickness	mm	0.4				
Longitudinal pitch	mm	86.6	Fin frequency	#/m	433				
Pitch angle		30	Root diameter	mm	38.1				
Th Cond	W/(m-K)	59.6853	Th cond	W/(m-K)	230.1618				
Surface effectiveness		0.76	Surface effectiveness		0.76				

X-side and Fan				Header and Nozzles				Weights	kg
Type draft		Forced				Inlet	Other	Inlet header	0
Fans/bay		1		Header type		Manifold	Manifold	Other header	0
Vol./fan(Act/Std)	m³/s	670.312	638.09	Header depth	mm	346.41	300	Inlet nozzle	274.9
Face vel. (Act/Std)	m/s	3.03	2.89			In	Out	Outlet nozzle	1.8
Fan diam./% cov.	m	10	33.98	No. of nozzles		1	1	Tubes and fins	5777.7
Sum./Win. des. Temp	°C	36	10	Nozzle ID	mm	501.65	33.99	Side frms/supports	1626.7
Abs pwr/fan-Winter	kW	135.136		Hom. Velocity	m/s	28.14	0.61	Bundle - dry	7681.1
Abs pwr/fan-Summer	kW	123.771		Rho*V2	kg/(m-s²)	78	365	Bundle - wet	9669.1
Drive efficiency		95						Unit bundles - dry	138260
Fan efficiency		80						Unit bundles - wet	174043.2

Overall summary from Aspen EDR, corresponding to design 5.

Overall Performance

Simulation			OutSide		Tube Side	
Total mass flow rate		kg/h	8267580		35300	
Vapor mass		kg/h	8267580	8267580	35300	0
Liquid mass		kg/h	0	0	0	35300
Vapour mass quality			1	1	1	0
Temperature		°C	36	46.13	53.57	49.88
Dew point / Bubble point temperatures		°C			53.57	51.77
Humidity ratio						
Operating pressure	Pa / Pa		101326	101326	14710	13471
Film coefficients		W/(m²-K)	1252.4		2379.6	
Fouling resistance		m²-K/W	0.0001		0	
Velocity (highest)		m/s	5.8 / 5.99		44.31 / 0	
Pressure drop (allow./calc.)	Pa / Pa		200 / 140		2942 / 1239	
Total heat exchanged	kW	23460.3	Bay per unit	3	Tube OD	38.1 mm
Overall bare coef. (dirty/clean)	W/(m²-K)	742.1 / 801.5	Bundles/bay	6	Tube tks	1.65 mm
Effective MTD	°C	10.11	Tubes/bundle	132	Tube length	11.5 m
Effective surface (bare tube)	m²	3128.3	Rows deep	4	Fin OD	88.9 mm
Effective surface (total)	m²	118537.7	Tube passes	1	Fin tks	0.4 mm
Area ratio: actual/required		1	Fans/bay	1	Fin frequency	433 #/m

Heat Transfer Resistance

Outside / Fouling / Wall / Fouling / Tube side

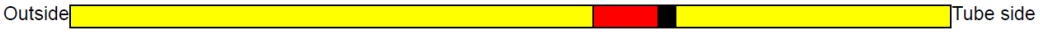

All condenser data and specification sheets for design 5 are given in Appendix I

Condenser specification sheet from Aspen EDR, corresponding to design 6.

Air-Cooled Heat Exchanger Specification Sheet

Company: North Steet Cooling Towers P Ltd									
Location:									
Service of Unit: ACC			Our Reference:						
Item No.:			Your Reference:						
Date: 06/03/2017			Rev No.:		Job No.:				
Size & Type	12.1464	/ 61.2	m	Type	Forced		Number of Bays		3
Surf/Unit-Finned Tube		114945.7	m²	Bare area/bundle		168.5 m²	Ratio (Total/Bare)		37.89
Heat exchanged		20076140	kcal/h			MTD, Eff	10.24	°C	
Transfer Rate-Finned	17.1	Bare, Service		646.4	Clean		699	kcal/(h-m²-C)	

PERFORMANCE DATA - TUBE SIDE

Fluid Circulated		Steam				In	/	Out
Total Fluid Entering	kg/h	35300		Density, Liq	kg/m³		/	987.08
		In	/ Out	Density, Vap	kg/m³	0.1	/	0.09
Temperature	°C	53.57	/ 51.48	Specific Heat, Liq	kJ/(kg-K)		/	4.192
Liquid	kg/h	0	/ 35271	Specific Heat, Vap	kJ/(kg-K)	1.884	/	1.879
Vapor	kg/s	9.8056	/ 0.008	Therm. Cond, Liq	W/(m-K)		/	0.6448
Noncondensable	kg/s	0	/ 0	Therm. Cond, Vap	W/(m-K)	0.0201	/	0.02
Steam	kg/s		/	Freeze Point	°C			
Water			/	Bubble / Dew point	°C	51.48	/	53.57
Molecular wt, Vap		18.0151	/ 18.0151	Latent heat	kJ/kg			
Molecular wt, NC				Inlet pressure (abs)	Pa	14710		
Viscosity, Liq	mPa-s		/ 0.5308	Pres Drop, Allow/Calc	kgf/cm²	0.03	/	0.015
Viscosity, Vap	mPa-s	0.0102	/ 0.0101	Fouling resistance	m²-K/W	0		

PERFORMANCE DATA - AIR SIDE

Air Quantity, Total	8267580	kg/h		Altitude	0	m	
Air Quantity/Fan	670.312	m³/s		Temperature In	36	°C	
Static Pressure	148	Pa		Temperature Out	46.07	°C	
Face Velocity	3.12 m/s	Mass velocity	3.56 kg/s/m²	Design Ambient	10	°C	

DESIGN-MATERIALS-CONSTRUCTION

Design/Vac./Test Pres	1	/	/	bar	Design temperature	200	°C	
TUBE BUNDLE		**Header**			**Tube**			
Size	m 12.1464	Type	Manifold		Material	Carbon Steel		
Number/bay	6	Material	Carbon Steel		Specifications			
Tube Rows	4	Passes	1		OD	38.1	Min Thk. 1.65	mm
Arrangement		Plug Mat.			No./Bun	128	Lng 11.5	m
Bundles	6 par	Gasket Mat.			Pitch	100 / 86.6	30	Degrees
Bays	3 par	Corr. Allow.	mm		**FIN**			
Bundle frame		Inlet nozzle (1)	501.65 mm		Type	G-finned		
MISCELLANEOUS		Outlet nozzle (1)	53.98 mm		Material	Aluminum 1060		
Struct. Mount.		Special Nozzles			OD	88.9	Tks 0.4	mm
Surf.Prep		Rating	Program		No.	433 #/m	Design Temp	°C
Louvers		TI	PI		Code	ASME Code Sec VIII Div 1		
Vibration Switches		Chem Cleaning			Stamp	Yes	Specs	

MECHANICAL EQUIPMENT

Fan,Mfr., Model		Driver, Type	Program		Speed Reducer, Type			
No./Bay	1 RPM	Mfr.			Mfr.&Model			
Dia.	10 m Blade(s)	No./Bay			No./Bay			
Pitch	Angle	RPM			Rating			hp
Blade(s)	Hub	Enclosure			Ratio			
hp/Fan	142.124kW MinAmb	V/Phase/Hz	/ /		Support			
Control Action on Air Failure-					Louvers			
Degree Control of Outlet Process Temperature								
Recirculation					Steam Coil		No	
Plot Area	m²	Drawing No.		Wt.Bundle	7489.9	Wt. Unit	134818.5	kg
Notes:								

Design summary from Aspen EDR, corresponding to design 6.

Unit Length/Width/Height	12.1464	/	61.2	/	0.3464	m		Tube inclination			-59.99999
Baysperunit	3	Bundles per bay	6	Tube Rows	4	Passes	1	X-side flow direction		60	Degrees
Staggered-even rows to right								Tube flow orientation		[1-pass crossflow]	
Total surface	114945.7	Ext surface/bundle	6385.9	Bare/Bundle	168.5	m²		Ratio (Total/Bare)			37.89

Simulation	Performance of the Unit									
		Tube Side		X-Side		Heat Transfer Parameters				
Process Data		In	Out	In	Out	Total head load	kcal/h			20076140
Total Flow	kg/h	35300		8267580		Effective MTD	°C			10.24
Gas				8267580	8267580	Actual/Reqd area ratio(dirty/clean)			1 /	1.08
Vapor		35300	29							
Liquid		0	35271	0	0	Coef/Resist (Bare)	W/(m²-K)	m²-K/W		%
Cond./Evap.		35271		0		Tube side film	2406.6	0.00042		31.24
Temperature	°C	53.57	51.48	36	46.07	Tube side fouling		0		0
Quality		1	0.0008			Tube wall	34584.5	3E-05		2.17
Humidity ratio						Outside fouling	10000	0.0001		7.52
Pressure (abs)	Pa	14710	13283.1			Outside film	1272.7	0.00079		59.07
	Pa			101326	101326	Overall fouled	751.8	0.00133		
DP		1426.9		148		Overall clean	812.9	0.00123		
Velocity	m/s	45.69	0.1	5.98	6.17					

Liquid Properties						Tube Side Pressure Drop	kgf/cm²	%
Density	kg/m³		987.08			Inlet nozzle	0.002	12.5
Viscosity	mPa-s		0.5308			Inlet header	0.002	11.06
Specific heat	kJ/(kg-K)		4.192			Inside tubes	0.007	46.77
Th Cond	W/(m-K)		0.6448			Across pass	0	0
Surface	N/m					Other header	0	0.01
Vapor Properties						Outlet nozzle	0.004	29.67
Density	kg/m³	0.1	0.09	1.14	1.11	Outside Pressure Drop	Pa	%
Viscosity	mPa-s	0.0102	0.0101	0.0189	0.0193	Ground clearance	0	0
Specific heat	kJ/(kg-K)	1.884	1.879	1.007	1.008	Fan inlet	12	7.6
Th Cond	W/(m-K)	0.0201	0.02	0.027	0.0277	Bundle	151	91.95
Two-Phase Properties						Louvers	0	0
Latent	kJ/kg		2382.1			Steam Coil	0	0
Molecular weight		18.0151		28.96		Plenum	9	5.33

Heat Transfer Parameters					Heat Load	kW
Reynolds No. vapor	15236.41	30.08	13770.72	13444.52	Vapor	18
Reynolds No. liquid		292.82			Cond./Evap	23330.5
Prandtl No. vapor	0.96	0.96	0.71	0.7	Liquid	0
Prandtl No. Liquid		3.45			Input/Actual duty ratio	0.99

Tubes / Fin			Last row number		4				
Tubes per bundle		128	Tube OD / ID	mm	38.1 / 34.8	/	/	/	
Tube material		Carbon Steel	Fin type		G-finned				
Length effective	m	11	Fin material		Aluminum 1060				
Length actual	m	11.5	Fin tip diameter	mm	88.9				
Transverse pitch	mm	100	Fin thickness	mm	0.4				
Longitudinal pitch	mm	86.6	Fin frequency	#/m	433				
Pitch angle		30	Root diameter	mm	38.1				
Th Cond	W/(m-K)	59.6853	Th cond	W/(m-K)	230.1619				
Surface effectiveness		0.76	Surface effectiveness		0.76				

X-side and Fan				Header and Nozzles				Weights	kg
Type draft		Forced				Inlet	Other	Inlet header	0
Fans/bay		1		Header type		Manifold	Manifold	Other header	0
Vol./fan(Act/Std)	m³/s	670.312	638.09	Header depth	mm	346.41	300	Inlet nozzle	274.9
Face vel. (Act/Std)	m/s	3.12	2.97			In	Out	Outlet nozzle	3.9
Fan diam./% cov.	m	10	35.02	No. of nozzles		1	1	Tubes and fins	5602.6
Sum./Win. des. Temp	°C	36	10	Nozzle ID	mm	501.65	53.98	Side frms/supports	1608.5
Abs pwr/fan-Winter	kW	142.124		Hom. Velocity	m/s	28.14	5.48	Bundle - dry	7489.9
Abs pwr/fan-Summer	kW	130.171		Rho*V2	kg/(m-s²)	78	1305	Bundle - wet	9417.6
Drive efficiency		95						Unit bundles - dry	134818.5
Fan efficiency		80						Unit bundles - wet	169517.3

Overall summary from Aspen EDR, corresponding to design 6.

Overall Performance

Simulation			OutSide		Tube Side	
Total mass flow rate		kg/h	8267580		35300	
Vapor mass		kg/h	8267580	8267580	35300	29
Liquid mass		kg/h	0	0	0	35271
Vapour mass quality			1	1	1	0.0008
Temperature		°C	36	46.07	53.57	51.48
Dew point / Bubble point temperatures		°C			53.57	51.48
Humidity ratio						
Operating pressure	Pa / Pa		101326	101326	14710	13283.1
Film coefficients		W/(m²-K)	1272.7		2406.6	
Fouling resistance		m²-K/W	0.0001		0	
Velocity (highest)		m/s	5.98 / 6.17		45.69 / 0.1	
Pressure drop (allow./calc.)	Pa / Pa		200 / 148		2942 / 1426.9	

Total heat exchanged	kcal/h	20076140	Bay per unit	3	Tube OD	38.1 mm
Overall bare coef. (dirty/clean)	W/(m²-K)	751.8 / 812.9	Bundles/bay	6	Tube tks	1.65 mm
Effective MTD	°C	10.24	Tubes/bundle	128	Tube length	11.5 m
Effective surface (bare tube)	m²	3033.5	Rows deep	4	Fin OD	88.9 mm
Effective surface (total)	m²	114945.7	Tube passes	1	Fin tks	0.4 mm
Area ratio: actual/required		1	Fans/bay	1	Fin frequency	433 #/m

Heat Transfer Resistance

Outside / Fouling / Wall / Fouling / Tube side

Theoretical formulations

Mean temperature difference calculation, ΔT_m

From the given data for the air cooled condenser process conditions, we have,

T_{in}, the inlet temperature of the tube-side stream is 53.57 ºC

T_{out}, the outlet temperature of the tube-side stream is 51.53 ºC

t_{in}, the inlet temperature of the air-side stream is 36 ºC

t_{out}, the outlet temperature of the air-side stream is 46 ºC

The logarithmic mean temperature difference is given by equation 3. On substituting the temperature values in the equation we get,

$$\Delta T_{lm} = \frac{(53.57-46)-(51.53-36)}{ln\frac{53.57-46}{51.53-36}} = 11.21\ ^{o}C$$

The ratio of effectiveness is given by equation 4. On substituting the temperature values in the equation we get,

$$R = \frac{T_{in}-T_{out}}{t_{out}-t_{in}} = \frac{53.57-51.53}{46-36} = 0.204$$

The thermal effectiveness of air is given by the equation 5. On substituting the temperature values in the equation we get,

$$P = \frac{t_{out}-t_{in}}{T_{in}-t_{in}} = \frac{46-36}{53.57-36} = 0.57$$

The correction factor, F is determined form the values of R, P and the corresponding graph for 4 rows and 1 pass as shown in Figure 43.

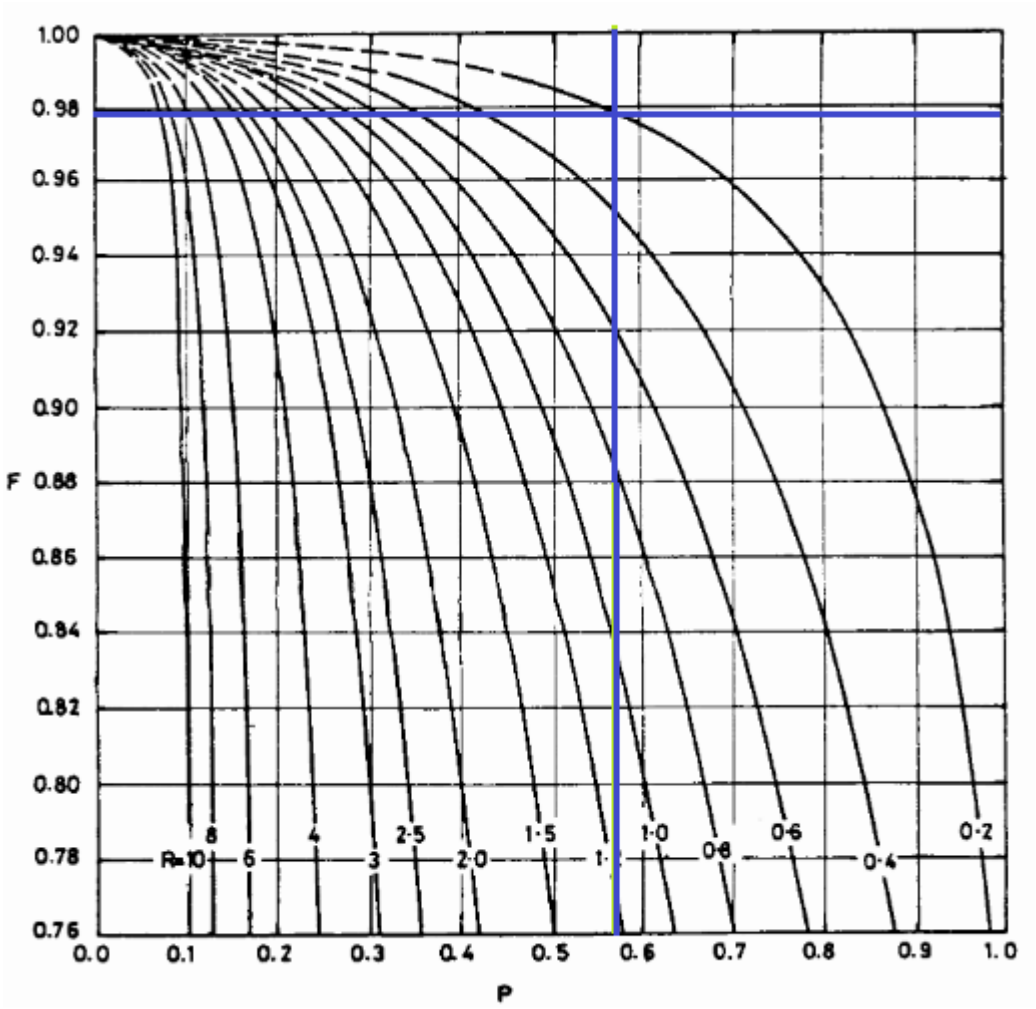

Figure 43. Correction factor for 4 rows and 1 pass (Echarte 1981, p. 7).

From the graph, $F = 0.98$

The mean temperature difference, ΔT_m is given by equation 6. By substituting the values for the correction factor, F and log mean temperature difference, ΔT_{lm} we get,

$$\Delta T_m = 11.21 \cdot 0.98 = 10.99\ ℃$$

Overall heat transfer rate, $\dot{q}_{total}$

The amount of heat transferred during condensation, $\dot{q}_{cond}$ is given by equation 7. By substituting the values for $\dot{m}_{fluid}$, the tube-side stream flow rate in kg/ hr and h_e, the specific enthalpy of evaporation for steam in kcal/ kg, we get,

$$\dot{q}_{cond} = 35300 \cdot 566 = 19{,}979{,}800 \frac{kcal}{hr}$$

The amount of heat exchanged, $\dot{q_{\Delta t}}$ is given by equation 8 for a temperature drop from 53.57 ^{o}C to 51.33 ^{o}C,

$$\dot{q_{\Delta t}} = 35300 \cdot 1.0012 \cdot (53.57\,℃ - 51.53\,℃) = 72098.4 \frac{kcal}{hr}$$

The total rate of heat transfer, $\dot{q}_{total}$ is given by equation 9, we get,

$$\dot{q}_{total} = 20{,}051{,}899 \frac{kcal}{hr}$$

Surface area of the exchanger, A

The total surface area of the condenser is given by equation 10,

$$A = \frac{20{,}051{,}899}{15.38 \cdot 0.98 \cdot 11.21} = 118{,}677.2\ m^2$$

Outside air mass flow rate, $\dot{m}_{air}$

The Outside air mass flow rate is calculated by rearranging the equation 8,

$$\dot{m}_{air} = \frac{20{,}051{,}899}{(0.242 \cdot 10)_{air}} = 8{,}285{,}908 \frac{kg}{hr}$$

Number of tube rows, tube length and number of tubes

The total face area of all the tube bundles is given by equation 11,

$$A_{face} = \frac{8{,}285{,}908}{1.22 \cdot 10800} = 628.9\ m^2$$

$$A_{face} \cong 629\ m^2$$

Since the ACC will is a forced draft, A-frame unit, it is necessary to have an even number of tube bundles. For a bundle face are of 629 m^2, it is reasonable to have the following specifications as show in Table 23, from a manufacturing and operational point of view,

Table 23. Number of bays

Number of bays	3
Number of tube bundles per bay	6
Total number of tube bundles	18
Face area of each bundle	629/18 ≈ 35 m^2

Single large tube bundles can be difficult to manufacture and heavy for transport. Further multiple bay condensers are easier to maintain and service as, one bay at a time can be put under maintenance and the rest could be working.

Bundle area = $L \cdot W = 35\ m^2$

Based on the design guidelines, the tube length, L should be three times of the bundle width, W. Therefore, bundle area = $3 \cdot W^2 = 35\ m^2$
So, $W = 3.42\ m$ and $L = 10.25\ m$

For a fin outside diameter, D_f of 88.9 mm and root diameter, D_r of 38.1 mm,
The surface area of a single fin $= 0.0101\ m^2$
Fin frequency, $n_f = 433/$ m
Fin area per meter length $= 0.0101 \cdot 433 = 4.37\ m^2$
Bare tube surface area per meter = $\pi\ D_f h = \pi \cdot 0.0381 \cdot 1 = 0.1197\ m^2$
Total surface area of the finned tubes per meter length, $A_{total} = 4.37 + 0.1197 = 4.5\ m^2$

Number of tubes, n_t is given by equation 12,

$$n_t = \frac{118677.2}{4.5 \cdot 10.25} = 2572.9 \cong 2573$$

Number of bundles = 18

Therefore, tubes per bundle = 2573/18 = 142.9 ≈ 143

Number of rows = 4

Number of tubes per row, N_T = 143/4 = 35.75 ≈ 36

Taking whole integers,

Actual number of tubes per bundle = 36 · 4 = 144

Actual total number of tubes in the ACC = 144 · 18 = 2592

Calculating bundle width form the number of tubes,

Width of the tube bundles, W = (N_T · P_t) + clearance on each side

Therefore, W = (36 · 0.095) + 0.05 = 3.47 m

Face area of each bundle = WL = 3.47 · 10.25 = 35.57 m^2

Total face area of all the bundles, A_{face} = 35.57 · 18 = 640.22 m^2

The actual face velocity, $V_{face,\ act}$ is given by rearranging equation 11,

$$V_{face,\ act} = \frac{\dot{m}_{air}}{\rho_{std}\, A_{face}}$$

$$V_{face,\ act} = \frac{8{,}285{,}908}{1.22 \cdot 640.22} = 10608\frac{m}{s} = 2.95\frac{m}{hr}$$

Number of tube passes, n_p

According to thermal design principles, it is preferred to have the least number of tube passes to limit the tube-side pressure drop. Therefore during the thermal design the tube-side Reyn-old's number is first calculated for tube-side velocity corresponding to a single tube pass.

The tube-side fluid (steam) velocity, V_{steam} is given by equation 13, which gives,

$$V_{steam} = \frac{\frac{35300}{3600} \cdot (1/2573)}{(0.1)\ \pi\ (0.0348)^2/4} = 40.1\ m/s$$

Here, ρ_{steam} = 0.1 kg/m^3 at 0.15 kg/cm^2 (Serth and Lestina, 2014, p. 560)

Reynold's number for tube-side fluid (steam), $Re_{tube\ side}$ is given by equation 15, which gives,

$$Re_{tube\ side} = \frac{4 \cdot \left(\frac{35300}{3600}\right) \cdot (1/2573)}{\pi \cdot 0.0348 \cdot 10^{-5}} = 13{,}943$$

Here the fluid viscosity, μ_{steam} = 10^{-5} kg/m-s (Serth and Lestina, 2014, p. 565)

For a flow to be turbulent, the Reynold's number needs to be greater than 4000 (The Engineering toolBox 2017). Since the $Re_{tube\ side}$ is 13943 the tube-side stream is fully turbulent. Therefore for this case a single tube pass is sufficient to achieve an optimum heat transfer coefficient.

Tube-side heat transfer coefficient calculations, $h_{tube\ side}$

All the following condensate properties are taken at temperature 51.53 ºC

Condensate specific heat, $C_{p\ cond}$ = 4180 J/kg. K

Condensate mass flow rate, $\dot{m}_{cond}$ = 9.8 kg/s

Condensate dynamic viscosity, μ_{cond} = 0.00053 N s/m^2

Condensate thermal conductivity, k_{cond} = 0.64 W/m K

Condensate density, ρ_{cond} = 986 kg/m^3

Steam density, ρ_{steam} = 0.089 kg/m^3

Tube data,

Tube inner diameter D_i = 0.0348 m

Number of tubes, n_t = 2592

The local condensate flow rate, τ_{cond} is given by the equation 16, which gives,

$$\tau_{cond} = \frac{9.8}{0.0348 \cdot 2592} = 0.108 \frac{kg}{m\ s}$$

The local condensate Reynold's number, Re_{cond} is given by equation 17, which gives,

$$Re_{cond} = \frac{4 \cdot 0.108}{0.00053} = 819.9$$

The condensate Prandtl number, Pr_{cond} is given by equation 18, which gives,

$$Pr_{cond} = \frac{4180 \cdot 0.00053}{0.64} = 3.461$$

Using equation 19, for the dimensionless local heat transfer coefficient, α_c^* for turbulent region, we get,

$$\alpha_c^* = 0.0038 \cdot 819.0^{0.4} \cdot 3.461^{0.65} = 0.124$$

The tube-side heat transfer coefficient, $h_{tube\ side}$ for an A frame ACC is calculated using equation 21. Since the ACC is an A frame with an angle of 60°, θ = 60 and so we get,

$$h_{tube\ side} = 0.64 \cdot 0.124 \left(\left(\frac{986 \cdot (986 - 0.089) \cdot 9.807 \cdot \sin 60}{0.00053^2} \right) \right)^{0.333}$$
$$= 2437.9 \frac{W}{m^2 K}$$

Air-side coefficient of heat transfer, $h_{air\ side}$

The minimum flow area, S_{min} is given by equation 22, we get,

$$S_{min} = \big(0.095 - 0.0381 - 433 * 0.0004(0.0889 - 0.0381)\big)10.25 \cdot 648$$
$$= 319.48\, m^2$$

The maximum mass velocity, $\dot{m}_{max}$ which is based on S_{min} is given by equation 23, we get,

$$\dot{m}_{max} = \frac{8267580/3600}{319.48} = 7.18 \frac{kg}{s\ m^2}$$

The air-side Reynold's number, $Re_{air\ side}$ is given by equation 24, we get,

$$Re_{air\ side} = \frac{7.18 \cdot 0.0381}{19 \cdot 10^{-6}} = 14{,}397$$

The area ratio, A_r which gives the area of the total extended surfaces to the root tube is given by equation 25,

$$A_r = 1 + 2 \cdot 433 \cdot 0.0254 \left(1 + \frac{0.0254 + 0.0004}{0.0381}\right) = 37.89$$

Here, H is the fin height which 0.0254 m

The j-factor for the finned tubes is given by equation 26,

$$j_R = 0.29 \cdot 14{,}397.7^{-0.367} \cdot 37.89^{-0.17} = 0.00465$$

The air-side Prandtl number, Pr_{air} is given by equation 27,

$$Pr_{air} = \frac{1007 \cdot 19 \cdot 10^{-6}}{26.86 \cdot 10^{-3}} = 0.7123$$

Air-side heat transfer coefficient, $h_{air\ side}$ is given by equation 28,

$$h_{air\ side} = 0.00465 \cdot 1007 \cdot 7.18 \cdot 0.7123^{-\frac{2}{3}} = 42.15\ W/m^2K$$

Fin efficiency calculations

r_1 = tube root radius = 0.0381/2 = 0.01905 m

r_2 = r_1 + fin height = 0.01905 + 0.0254 = 0.04445 m

r_{2c} = r_2 + fin thickness/2 = 0.04445 + 0.0004/2 = 0.04465 m

The effective fin height, ψ is given by equation 31,

$$\psi = (0.04465 - 0.01905\ )\left(1 + 0.35\ln\left(\frac{0.04465}{0.01905}\right)\right) = 0.03323\ m$$

The fin parameter, m is given by equation 30,

$$m = \left(\frac{2 \cdot 42.15}{238 \cdot 0.0004}\right)^{0.5} = 29.75$$

Here, the thermal conductivity of aluminum, k = 238 W/m K (Serth and Lestina, 2014, p. 555)

$$m\psi = 29.75 \cdot 0.03323 = 0.988$$

Fin efficiency, η_f is given by equation 29,

$$\eta_f \cong \frac{\tanh(0.988)}{0.988} = 0.765$$

The surface area of fins, A_{fins} is given by equation 33,

$$A_{fins} = \ 2 \cdot 433 \cdot \pi(0.04465^{\ 2} - 0.01905^2) = 4.4365\ m^2$$

The prime surface area, A_{prime} is given by equation 34,

$$A_{prime} = 2 \cdot \pi \cdot 0.01905\big(1.0 - (433 \cdot 0.0004)\big) = 0.0989\ m^2$$

$$\frac{A_{fin}}{A_{Total}} = \frac{4.4365}{4.5} = 0.985$$

$$\frac{A_{prime}}{A_{Total}} = 1 - 0.985 = 0.015$$

The weighed efficiency of the finned surface is given by equation 35,

$$\eta_w = 0.015 + (0.765 \cdot 0.985) = 0.768$$

Overall heat transfer coefficient

The internal surface area, A_i of the tubes per meter length,

$$A_i = \pi D_i L = \pi \cdot 0.0348 \cdot 1 = 0.109\, m^2$$

The clean overall heat transfer coefficient, U_c is given by equation 36,

$$U_c = \left(\frac{4.5/0.109}{2437.9} + \frac{(4.5/1)\ln(0.0381/0.0348)}{2 \cdot \pi \cdot 54} + \frac{1}{0.768 \cdot 42.15}\right)^{-1} = 20.39 \frac{W}{m^2\, K}$$

Here, the thermal conductivity, k_{tube} of carbon steel is 54 W/m K

Fouling resistance

The given tube-side fouling resistance, $R_{Di}$is given to be zero.

The air-side fouling resistance, R_{D0} is 0.0001 m^2 K/W

Since, R_{Di} for this case is zero, the total fouling resistance, R_D is given by equation 37,

$$R_D = \frac{R_{D0}}{\eta_w} = \frac{0.0001}{0.768} = 0.00013 \frac{m^2 K}{W}$$

Design overall heat transfer coefficient

The design overall heat transfer coefficient, U_D is given by equation 38,

$$U_D = (\frac{1}{20.39} + 0.00013)^{-1} = 20.33 \frac{W}{m^2\ K}$$

Required overall heat transfer coefficient

The required overall heat transfer coefficient, U_{req} is calculated by rearranging equation 10,

$$U_{req} = \frac{20{,}051{,}899}{2592 \cdot 4.5 \cdot 10.25 \cdot 0.98 \cdot 11.21} = 15.26 \frac{W}{m^2\ K}$$

Since, $U_D > U_{req}$, the ACC design is thermally feasible.

Tube-side pressure drop

The tube-side stream dynamic viscosity at average tube wall temperature, $\mu_{w\ steam}$ is given by,

$$\mu_{w\ steam} = \frac{\mu_{steam\ at\ 53.57℃} + \mu_{steam\ at\ 51.53℃}}{2}$$

$$= \frac{(1.07 \cdot 10^{-5}) + (1.066 \cdot 10^{-5})}{2} = 1.068 \cdot 10^{-5}\ N \frac{s}{m^2}$$

The viscosity correction factor, $\emptyset$ is given by equation 40,

$$\emptyset = \left(\frac{\mu_{steam\ at\ 0.147\ bar}}{\mu_{w\ steam}}\right)^{0.14} = \left(\frac{1.07 \cdot 10^{-5}}{1.068 \cdot 10^{-5}}\right)^{0.14} = 1$$

The specific gravity, s is given by,

$$s = \frac{\rho_{steam\ at\ 53.57℃}}{\rho_{fluid\ at\ 0℃}} = \frac{0.098}{1000} = 9.8 \cdot 10^{-5}$$

The Darcy friction factor, f is given by equation 41,

$$f = 0.4137 \cdot 13{,}943^{-0.2585} = 0.0351$$

The mass flux, $G_{tube\ side}$ is given by equation 42,

$$G_{tube\ side} = \frac{\left(\frac{9.8}{18}\right) \cdot \left(\frac{1}{144}\right)}{\frac{\pi \cdot 0.0348^2}{4}} = 3.97 \frac{kg}{s\ m^2}$$

The tube-side pressure drop due to friction, $\Delta P_{f-tube\ side}$ is given by equation 39,

$$\Delta P_{f-tube\ side} = \frac{0.0351 \cdot\ 1 \cdot 10.25 \cdot 3.97^2}{2000 \cdot 0.0348 \cdot\ 9.8 \cdot 10^{-5} \cdot 1} = 834.4\ Pa$$

The number of velocity heads for tube-side pressure losses, α_r for regular tubes with turbulent fluid flow is given by equation 44,

$$\alpha_r = 2n_p - 1.5 = 0.5$$

The tube-side pressure drop due to tube entrance and exit losses, $\Delta P_{r-tube\ side}$ is given by equation 43,

$$\Delta P_{r-tube\ side} = 5.0 \cdot 10^{-4} \cdot 0.5 \left(\frac{3.97^2}{9.8 \cdot 10^{-5}}\right) = 40.34\ Pa\ per\ tube\ bundle$$

From equation 45,

Therefore, $\Delta P_{tube\ side} = \Delta P_{f-tube\ side} + \Delta P_{r-tube\ side} = 834.4 + (40.34 \cdot 18) = 1560$ Pa

Air-side pressure drop, $\Delta P_{air\ side}$

The fin parameter is given by equation 48,

$$a = \frac{0.095 - 0.0889}{0.0381} = 0.16$$

Effective Reynold's number, Re_{eff} is given by equation 49,

$$Re_{eff} = 14{,}397\left(\frac{0.00191}{0.0254}\right) = 1082.6$$

Fin spacing, l is obtained from the number of fins per unit length which is given by equation 50,

$$l = \frac{1}{433} - 0.0004 = 0.00191$$

Average face velocity is derived from actual face velocity based on the ratio between the air density at the ambient temperature and at the average temperature.

$$V_{face\ av} = V_{face\ act}\frac{\rho_{air\ std}}{\rho_{air\ av}} = 2.95 \cdot \frac{1.19}{1.125} = 3.12\ m/s$$

Here, the standards air density, $\rho_{air\ std}$ = 1.19 kg/m^3

Air density, ρ_{air} at an inlet temperature of 36 ^{o}C and 1 atm. = 1.143 kg/m^3

Air density, ρ_{air} at an outlet temperature of 46.08 ^{o}C and 1 atm. = 1.106 kg/m^3

Therefore average air density, $\rho_{air\ av}$= 1.125 kg/m^3

The maximum air velocity in the tube bundles, V_{max} is given by equation 53,

$$V_{max} = \frac{0.095 \cdot\ 3.12}{0.095 - 0.0381 - (2 \cdot 433 \cdot 0.0254 \cdot 0.0004)} = 6.16\frac{m}{s}$$

Friction factor, f_{fr} is given by equation 47,

$$f_{fr} = \left(1 + \frac{2e^{-\left(\frac{0.16}{4}\right)}}{1 + 0.16}\right)\left(0.021 + \frac{27.2}{1082.6} + \frac{0.29}{1082.2^{0.2}}\right) = 0.313$$

Air mass flux, G is given by,

$$G = \rho_{air\ av}\, V_{max} = 1.125 \cdot\ 6.16 = 6.93 \frac{kg}{s\ m^2}$$

Air-side pressure drop due to friction with the tube bundles, $\Delta P_{f-air\ side}$ given by equation 46,

$$\Delta P_{f-air\ side} = \frac{2 \cdot 0.313 \cdot 4 \cdot 6.93^2}{1.125} = 107\ Pa$$

Factor 10% for other losses,

$\Delta P_{f-air\ side}$ = 1.1 ·107 = 117.7 Pa

Fan sizing

Since, the tube length, L is 10.25 m, the maximum permissible fan diameter, D_{fan} is 10 m after keeping for the side clearances.

Number of fans, N_{fan} = 3

Volumetric flow rate per fan, $\dot{V}_{fan}$ is given by,

$$\dot{V}_{fan} = \frac{\dot{m}_{air}}{N_{fan}\, \rho_{air}} = \frac{8{,}285{,}908}{3 \cdot\ 1.143}$$

$$= 2{,}416{,}421 \frac{\mathrm{m}^3}{\mathrm{hr}}\ @\ 117.7\ Pa\ static\ pressure$$

Motor sizing

The velocity of air leaving the fan V_{fan}, is given by equation 55,

$$V_{fan} = \frac{2416421}{\frac{\pi}{4} \cdot 10^2} = 30{,}766 \frac{m}{h} or\ 8.54 \frac{m}{s}$$

The velocity pressure, P_v is given by equation 54,

$$P_v = \frac{\alpha_{fan}\, \rho_{fan} V_{fan}^2}{2\, g_c} = \frac{1 \cdot 1.143 \cdot 8.54^2}{2 \cdot 1} = 41.68 \frac{N}{m^2}$$

Therefore the total pressure difference across the fan, $\Delta P_{total-fan}$ is given by equation 54,

$$\Delta P_{total-fan} = 117.7 + 41.69 = 159.38 \frac{N}{m^2}$$

The break down fan power, $\dot{W}_{fan}$ is given by equation 56,

$$\dot{W}_{fan} = \frac{159.38 \cdot \frac{2{,}416{,}421}{3600}}{0.7} = 152.8\ KW\ per\ fan$$

The power supplied to each motor, $\dot{W}_{motor}$ is given by,

$$\dot{W}_{motor} = \frac{\dot{W}_{fan}}{\eta_{sr}} = \frac{152.8}{0.95} \cong 160\ KW$$

Here,

η_{sr} is the efficiency of the speed reducer